A Thesis for the Degree of Doctor of Philosophy

Molecular Study on the Mode of Action of *Rhus javanica* and *Curcuma zedoaria* Extracts against Skin Aging and Skin Cancer

오배자 및 봉출 추출물의 피부 노화와 피부암에 대한 작용 메커니즘의 분자적 연구

August, 2021

Su Jeong Ha

Department of Agricultural Biotechnology

College of Agriculture and Life Sciences

Seoul National University

Molecular Study on the Mode of Action of *Rhus javanica* and *Curcuma zedoaria* Extracts against Skin Aging and Skin Cancer

오배자 및 봉출 추출물의 피부 노화와 피부암에 대한 작용 메커니즘의 분자적 연구

지도교수 장 판 식

이 논문을 농학박사학위논문으로 제출함

2021년 8월

서울대학교 대학원

농생명공학부

하 수 정

하수정의 박사학위논문을 인준함

2021년 8월

위 원 장 이 도 엽

부위원장 장 판 식

위 원 이 주 훈

위 원 정 성 근

위 원 변 상 균

Abstract

Ha, Su Jeong

Department of Agricultural Biotechnology

The Graduate School

Seoul National University

Excessive ultraviolet (UV) exposure can cause acute skin inflammation and chronic exposure has been linked to skin cancer. While dependent on genetic factors and lifestyle choices, repeated exposure to UV irradiation generally results in the appearance of irregular brown spots and wrinkle formation, collectively referred to as photoaging. The transcription factor AP-1 plays a critical role in these processes via regulation of *mmp-1* and *cox-2* gene expression, respectively. Due to the fact that AP-1 is a central mediator of UV-induced photoaging and inflammation, the development of analytical tools that efficiently screen compounds that can inhibit AP-1 activity represents a potential strategy to develop new anti-photoaging and anti-inflammatory agents.

To screen effective anti-photoaging and anti-inflammatory agents, I generated immortalized human keratinocyte HaCaT cells stably transfected with an MMP-1 promoter and after selection with puromycin, I confirmed that HaCaT cells were successfully transfected with the pGF1 vector containing the MMP-1 promoter. To determine the optimal conditions needed to assess MMP-1 promoter activity, I investigated different doses of UV and incubation times. The reporter gene assay revealed that 0.04 J/cm^2 and 5 h were the optimal conditions for activating the MMP-1 promoter. Using these cells, I screened 99

botanical extracts of interest. 9 botanical extracts showed UVB-induced MMP-1 promoter binding activity inhibition. *Rhus javanica* extract (RJE) and *Curcuma zedoaria* extract (CZE) were identified as the most potent anti-photoaging material, suppressing UVB-induced MMP-1 promoter binding activity by 80.9% and 75.8%, respectively. Furthermore, the viability of HaCaT cells did not show signs of cytotoxicity at 25-100 μg/mL concentrations.

Evaluation of varying RJE concentrations on UVB-induced MMP-1 promoter binding activity and cell cytotoxicity revealed that RJE inhibits UVB-induced MMP-1 promoter binding activity in a dose-dependent manner. I further observed that RJE suppressed UVB-induced MAPKs and AP-1 signaling cascades in HaCaT cells. Experiments using the SKH-1 hairless mouse model revealed that oral administration of RJE significantly suppresses UVB-induced wrinkle formation, as well as COX-2 and MMP-13 expression in mouse skin. These findings suggest that RJE is a potent anti-inflammatory and anti-photoaging agent that inhibits COX-2 and MMP-1 expression.

Several experiments confirmed that CZE significantly suppressed UVB-induced COX-2 and MMP-13 expression in HaCaT cells. My Western blot results showed that phosphorylation of all three MPAKK/MAPKs were suppressed by CZE. Additionally, CZE strongly suppressed UVB-induced Akt phosphorylation as well as EGFR and Src phosphorylation in HaCaT cells. Using an SKH-1 hairless mice model, I determined that CZE prevented chronic UVB-induced wrinkle formation. Immunohistochemistry and Western blot assay results showed that CZE significantly suppressed UVB-induced COX-2 and MMP-13 expression *in vivo*. Among the specific compounds present in CZE, curcumin was found to exhibit the strongest inhibitory effect on UVB-induced MMP-1 promoter activity.

Among the RJE compounds, syringic acid exhibited the most potent inhibitory effect

on MMP-1 promoter activity. I sought to investigate the inhibitory effects of syringic acid on UVB-induced skin carcinogenesis. *In vitro* experiment, I treated human epidermal keratinocytes (HaCaT cells) with syringic acid and measured the gene and protein expression levels. Accordingly, I detected the change in ROS due to syringic acid treatment, which was compared to the effects of the FDA-approved antioxidant drug N-acetyl-L-cysteine (NAC), which is commonly used to identify and test ROS inducers and to inhibit ROS. Since NADPH oxidases of the Nox family are important enzymatic sources of ROS, I further measured the effect of syringic acid on NADPH oxidase activity to determine the potential targets mediating its inhibitory effects. To evaluate the therapeutic potential of syringic acid, I conducted an *in vivo* experiment using the SKH-1 hairless mouse model that received topical treatment of syringic acid prior to UVB exposure, and compared the tumor incidence and expression of relevant molecules in the mouse skin.

Key words: *Rhus javanica* extract (RJE), *Curcuma zedoaria* extract (CZE), syringic acid, photoaging, skin cancer, cyclooxygenase-2 (COX-2), matrix metalloproteinase-1 (MMP-1), epidermal growth factor receptor (EGFR), reactive oxygen species (ROS)

Student number: 2017-33697

Contents

List of Figures

List of Tables

Chapter I.

General Introduction

I-1. Introduction

Based on the recent statistics for cancer, 9.6 million of people are died with skin cancer (9.5 million excluding NMSC) (Bray et al., 2018). The most frequently diagnosed two types of skin cancers, collectively known as non-melanoma skin cancers (NMSCs), are basal cell carcinoma (BCC) and squamous cell carcinoma (SCC) (Fontanillas et al., 2021). Thus, NMSC is the most frequently detected skin malignancy, which is 40% of all cancers diagnosed in the US (Lomas et al., 2012), whereas malignant melanomas were detected only 4% of all skin cancers (Didona et al., 2018). BCCs and SCCs are developed from the basal layer of the epidermis. Although BCCs are slow grown and rarely metastasized, SCCs are more invasive, and 10% of SCCs metastasize (Bowden, 2004; Matsumura & Ananthaswamy, 2002).

Among the various factors that threaten the skin's health, ultraviolet light is the one that I inevitably encounter in our living environment and has the greatest effect on skin homeostasis. Epidemiological studies have proven that solar ultraviolet (UV) irradiation is the most important environmental carcinogen in skin cancer development (Armstrong & Kricker, 2001). Although UVC is blocked by stratospheric ozone, UVB (1-10%) and UVA (90-99%) reach the surface of the earth and cause DNA damage, erythema, sunburn, immunosuppression, and eventually, skin cancer (Fisher et al., 1998). UVA irradiation to which I am exposed appears to be weakly carcinogenic and causes photoaging and wrinkling of the skin. UVB is recognized as a complete carcinogen relevant to human skin cancer (Wlaschek et al., 2001).

Prolonged exposure to UV impairs skin homeostasis and response to environmental changes, including ROS production, causing the activation of multiple signaling cascades, which serve to switch on the oncogenic and tumor suppressor gene expression. Although multiple lines of study proved that antioxidants contribute to the prevention of skin carcinogenesis, certain phytochemicals with low antioxidant capacity have relatively high chemopreventive effects and several materials, including vitamin D and lycopene, can act as a prooxidant. I reported through various studies that phytochemicals can prevent cancer by acting as inhibitors of oncogenic molecules, Fyn, Src, aryl hydrocarbon receptor (AhR), PI3K (phosphoinositide 3-kinase), Raf, and extracellular signal-regulated kinase (ERK)2 *in vitro* and *in vivo*. In this study, as molecular targets that can complement the antioxidant activity and effectively inhibit skin cancer, I selected nicotinamide adenine dinucleotide phosphate (NADPH) oxidase and epidermal growth factor receptor (EGFR), introducing their role in skin cancer and various signaling networks.

The sentence “Prevention is better than cure” expresses the importance of prevention. Therefore, many scientists and laboratories are still trying to develop chemopreventive materials. However, the effective materials for preventing diseases such as cancer are still required. By summarizing the results of our research and the results of other scientists, I would like to introduce materials that can prevent or control skin cancer and skin diseases through Nox and EGFR regulation.

I-2. Skin carcinogenesis and chemoprevention

Skin carcinogenesis is divided into three stages, including initiation, promotion, and progression. Skin cancer develops in multiple stages like other cancers. It takes over a decade for cancer to develop (Blagodatski et al., 2020; Stratton et al., 2000). Chemoprevention refers to delaying the onset of cancer or returning it to normal through drugs and appropriate treatment (Savoia et al., 2018). Initiation is caused by acute UV exposure and is characterized by DNA mutations, abnormal gene activation, or suppression. Promotion is the clonal expansion of damaged cells through aberrant signaling pathways, which takes a decade. It involves uncontrolled growth of the tumor and can invade and metastasize to secondary organs (K. W. Lee et al., 2011; Singh et al., 2014; Surh, 2003). Since initiation is an irreversible and short-time step (a second or minutes), prevention of initiation using chemopreventive agents is complicated. Promotion, however, has attracted a great deal of interest because of its characteristic of a reversible and long period (a decade) (K. W. Lee et al., 2011; Surh, 2003). In the promotion stage, mutation of the tumor-suppressor gene, including p53 and hyperactivation of inflammatory transcription factors, such as Activator protein 1 (AP-1) and nuclear factor kappa-light-chain-enhancer of activated B cells (NF-κB), and sub-sequent abnormal production of the inflammatory enzyme, cyclooxygenase-2 (COX-2), and inflammatory cytokines, interleukin (IL)-1β, IL-6, and transforming growth factor β (TGFβ). Therefore, multiple lines of study resulting in the development of chemopreventive phytochemicals have focused on targeting oncogenic signaling molecules.

I-3. Role of Noxs and its down-stream signaling pathways in UV-induced skin carcinogenesis

Excessive cellular reactive oxygen species (ROS) has a critical role in skin carcinogenesis via genotoxicity with DNA damages, causing inactivation of the tumor-suppressor gene and activation of the proto-oncogene and nongenotoxicity through hyperactivation of oncogenic signaling pathways (Xian, Lai, Song, Xiong, & Zhong, 2019). Noxs respond to UVB and are essential in cellular ROS production (Sedeek et al., 2013). Nox is a membrane-bound enzyme, consisting of a catalytic subunit (Nox1 through Nox5, Duox1, and Duox2), $p22^{phox}$, $p47^{phox}$, $p67^{phox}$, and the small guanosine triphosphatase, Rac1. For Nox to be activated, Nox1–Nox3 need to bind with subunits, but Nox4 is constitutively active, and Nox5 binds with the Duox enzyme (Geiszt et al., 2000; Helmcke et al., 2009). Nox1, 2, 4, and 5 mRNA and Nox1, 2, and 4 protein expression were detected, and those are the main producers of ROS in immortalized human keratinocyte HaCaT cells (Chamulitrat et al., 2004; T. M. Lee et al., 2011).

Generally, UVB irradiation causes a DNA damage response network that includes cell apoptosis through excessive cell cycle progression and damage to DNA repair machinery (Raad et al., 2017). Since cyclobutane pyrimidine dimers (CPDs) are well known for a type of UVB-mediated DNA damages (Berton et al., 1997; Huang et al., 2017; Pollet et al., 2018), Noxs-mediated malfunction of nucleotide excision repair, a major proofreading system to repair the UVB-induced DNA damages, plays a major role in UVB-induced skin carcinogenesis (Nijhof et al., 2007; Pollet et al., 2018). In a clinical study, it was proposed that patients taking N-acetyl cysteine (NAC), an NADPH oxidase inhibitor, had the

feasibility to prevent pro-oncogenic oxidative stress in nevi and could alleviate long-term melanoma risk (Cassidy et al., 2017; Goodson et al., 2009). Chronic UVB exposure to SKH-1 hairless-mice skin led to the development of skin cancer, and topical treatment with NAC prevented two stages of UVB-induced skin carcinogenesis (Byun et al., 2016). Additionally, direct inhibition of Nox1 with a specific peptide inhibitor of Nox1 (lnhNox1) suppressed UVB-induced bursts of ROS production, increased nucleotide excision-repair efficiency, apoptosis in HaCaT cells, and skin carcinogenesis in Xpc wild-type mice (Raad et al., 2017). These results showed that Nox has a critical role in UV-induced skin carcinogenesis, and it could be a promising target for chemopreventive materials (Figure I-1).

UV irradiation and excessive ROS result in mutation of membrane receptor, PTCH gene, which turn on the activation of hedgehog signaling pathway involved in the pathogenesis of BCC (Pellegrini et al., 2017). Mutation of p53, tumor suppressor gene, is often observed in UV-induced oxidized skin cell and tissue (Benjamin & Ananthaswamy, 2007; Herbert et al., 2014). Once DNA is damaged by acute UV irradiation, p53 makes the DNA repair protein for DNA replication, repair and regulates cell cycle, and activate the apoptosis-signaling pathways if the DNA damage is irreversible (Benjamin & Ananthaswamy, 2007). Additionally, PTEN, a tumor suppressor gene, regulates PI3K/Akt signaling pathway through its phosphatase capacity but accumulate UV results in PTEN gene mutation and subsequent low levels in SCC (Kitagishi & Matsuda, 2013; Ming et al., 2011). Therefore, damage to the p53 and PTEN caused by ROS makes it difficult to repair DNA damage caused by UV, leading to skin cancer. Based on the use of a pharmaceutical inhibitor for NADPH oxidase. Therefore, in addition to directly scavenging ROS using antioxidants, modulating EGFR, PI3K, Src, and MAPKs protein activity, such as phosphorylation, will be a significant strategy to prevent UV-induced skin damage and skin cancer.

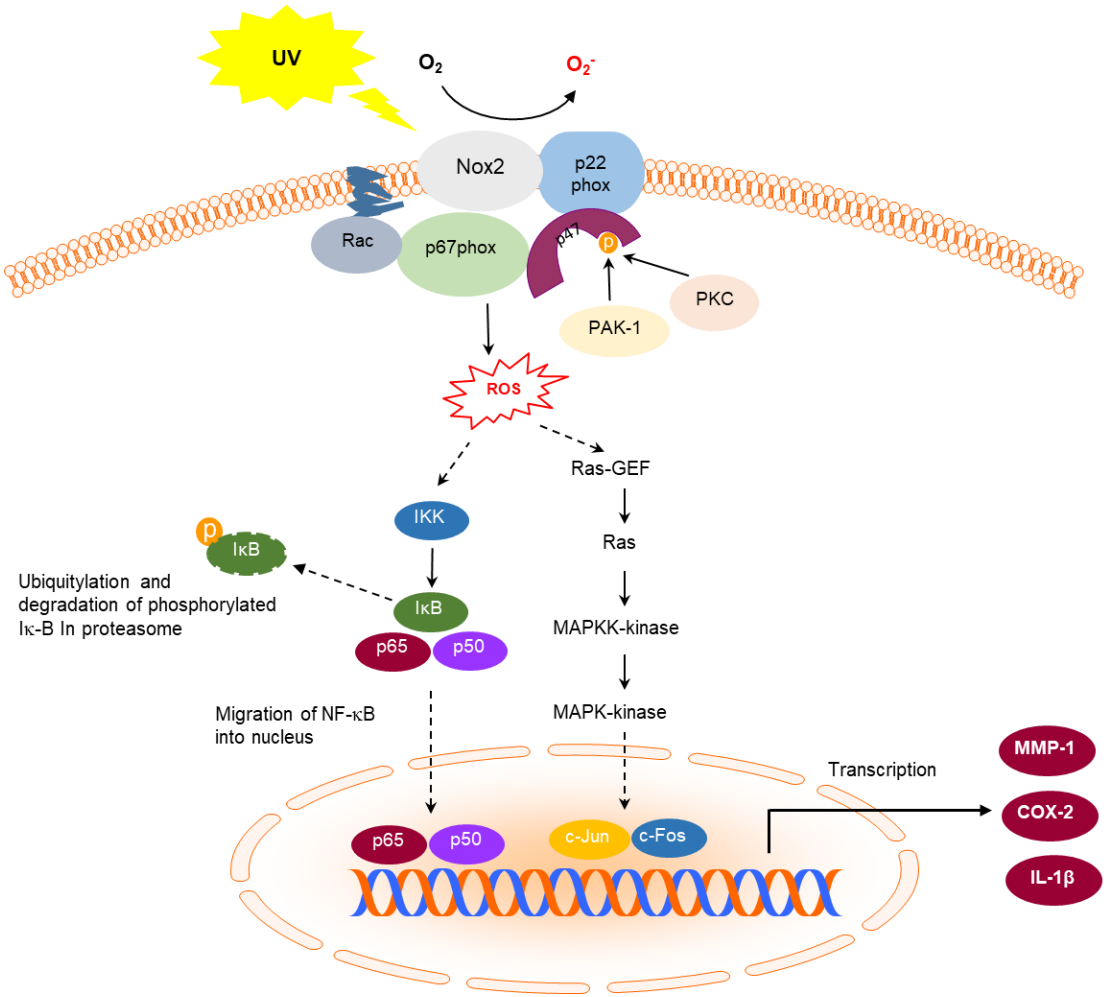

Figure I-1. Noxs and its downstream signaling pathways in UV-induced skin carcinogenesis.

I-4. Role of EGFR and its down-stream signaling pathways in UV-induced skin carcinogenesis

The epidermal growth factor (EGF) receptor (EGFR, ErbB-1, HER1) and ErbB-2, ErbB-2 (HER2), ErbB3 (HER3) and ErbB4 (HER4) (Wieduwilt & Moasser, 2008). These receptors are composed of extracellular ligand-binding, transmembrane, and intracellular tyrosine kinase domains (Ono & Kuwano, 2006; Seike & Gemma, 2012). Because hyperactivity and various mutations of EGFR contribute to the development of cancer and drug resistance, many anticancer drugs are being studied to target EGFR (Albanell et al., 2002; Herbst & Hong, 2002; Li et al., 2019; Sajadimajd et al., 2020). After the soluble ligand binds to the ectodomain of the receptor, homodimer and heterodimer formation is provoked. This step is essential to activate tyrosine kinase receptors, such as EGFR via phosphorylation of the C-terminal tail.

As a principle of UV-mediated EGFR activation, abnormal ROS production respond to UV activates a disintegrin and metalloproteinase (ADAM), and cleaves to proamphiregulin, EGFR ligand, in the cell membrane (Nakayama et al., 2012). Additionally, free amphiregulain bind to the ligand domain of EGFR and subsequent conformational change of EGFR and activates itself through dimerization (Figure I-2). Activated EGFR regulates multiple signaling pathways, including p38, c-Jun NH2-terminal kinase (JNK), ERK, phosphatidylinositol-3 kinase (PI3K)/Akt, and protein kinases C. PI3K/Akt, all of which are phosphorylated by UV irradiation in HaCaT cells. Contrarily, UV irradiation results in the dissociation of AhR and Src complex and Src phosphorylates EGFR at Tyr845, which consequently increases cyp1a1 mRNA and COX-2 protein expression in HaCaT cells (Lee et

al., 2017). Therefore, UV-induced EGFR activation accelerates multiple signaling pathways involved in skin carcinogenesis, and once the material can modulate these signaling cascade, it could serve as a promising chemopreventive material.

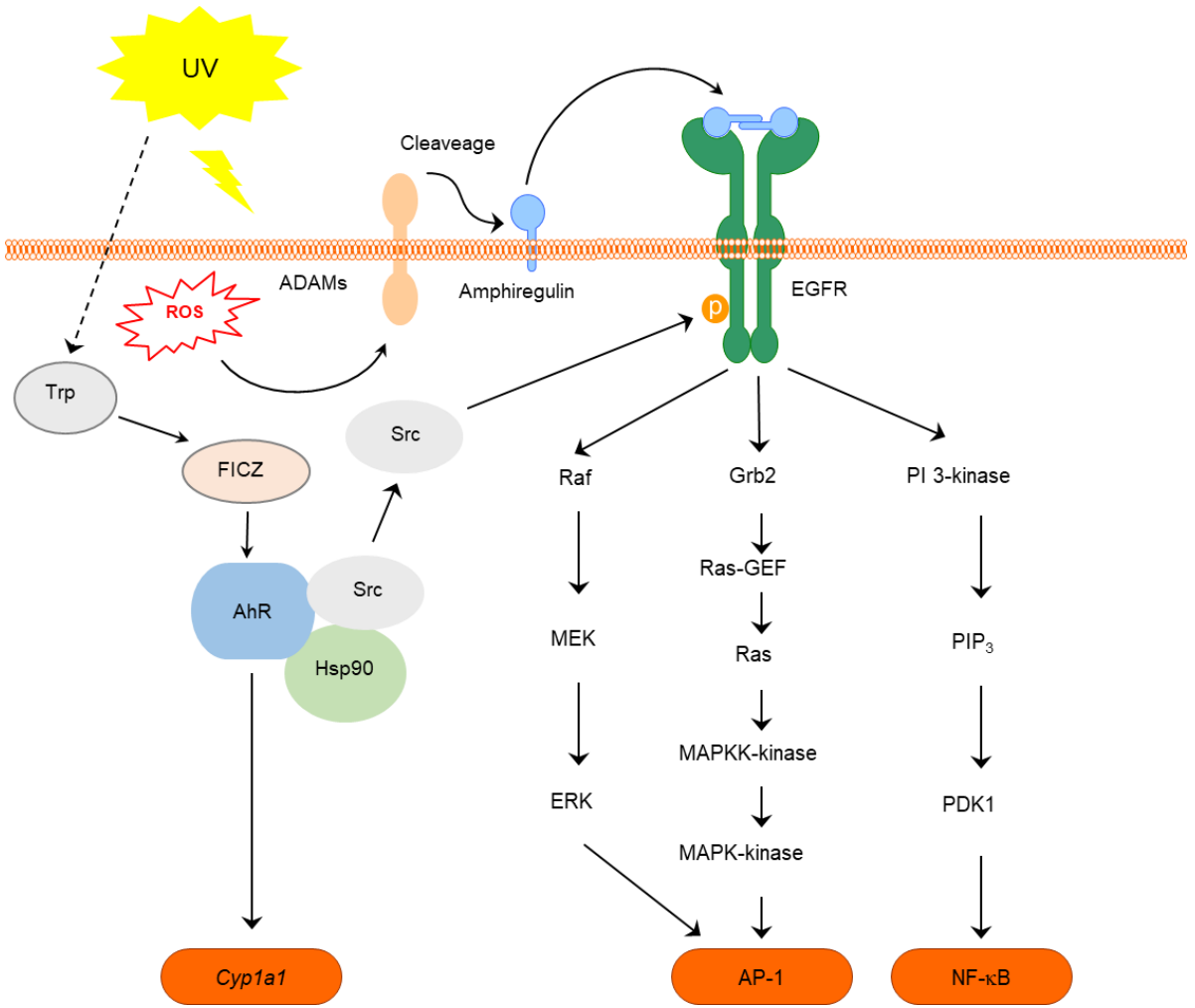

Figure I-2. EGFR and its downstream signaling pathways in UV-induced skin carcinogenesis.

I-5. Role of PTP-κ as Nox and EGFR signal transmitters in skin cancer

An early study suggested that hydrogen peroxide causes EGFR activity by inhibition of protein tyrosine phosphatases (PTPs) because the addition of catalase inhibits EGF-induced tyrosine phosphorylation of phospholipase Cγ1 (PLCγ1), a physiological substrate of the EGFR substrate (Bae et al., 1997). Further, several studies proved that ROS produced by Nox regulates EGFR. Nox4 mediated the oxidation and inactivation of PTP1B in the ER and switched the EGFR signaling pathways (Chen et al., 2008). Additionally, activation of Nox by active mutation of TRA4 induced oxidative damage of focal contact phosphatase PTP-PEST (Wu et al., 2005). Additionally, David et al., described the relationship between PTP and EGFR by Nox, the signaling network of EGFR, and the interrelationship of the redox system (Heppner et al., 2016; Heppner & van der Vliet, 2016). Therefore, the interaction of Nox, EGFR, and PTP-κ is a major factor in skin carcinogenesis, and controlling it is a major approach in preventing UV-induced skin cancer (Figure I-3).

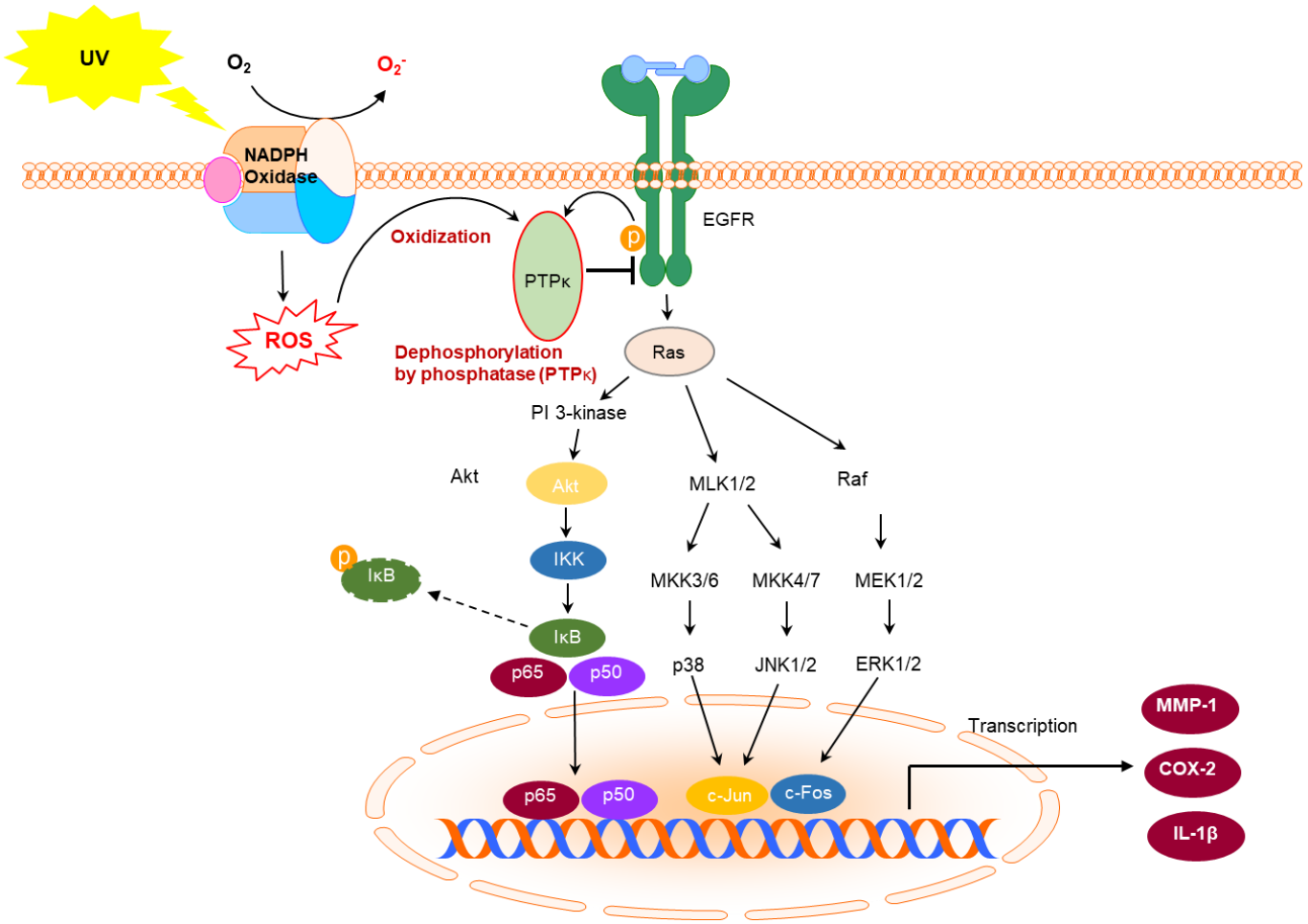

Figure I-3. Possible mechanisms of UV-induced skin carcinogenesis.

I-6. Preventive botanical extracts and phytochemicals in UV-induced skin damages by NADPH oxidase regulation

UVB induces Nox expression in the skin tissue, thereby increasing oxidant production. NADPH oxidase can be assessed directly through NADPH oxidase activity and can also be evaluated indirectly by measuring catalase (CAT), superoxide dismutase (SOD) activities, and glutathione (GSH) depletion (Table I-1). To assess whether or not Nox activity is altered by botanical extract or phytochemicals, the authors measured NADPH oxidase activity, Nox gp91^{phox} mRNA expression, and p47^{phox} translocation in previous studies.

Eupafolin, 6-methoxy 5,7,3′,4′-tetrahydroxyflavone, is a major component in methanol extract of *phyla nodiflora* Greene (Tsai et al., 2014). Human dermal fibroblasts (Hs68) treated with eupafolin *in vitro* had reduced LPS-induced ROS generation via deterioration of p47^{phox} activity and translocation of p47^{phox} from the cytosol to the plasma membrane. The authors have demonstrated that inhibition of LPS-induced COX-2 expression is mediated by transfection with scrambled siRNAs, targeting cytosolic regulatory subunit p47^{phox} and membrane catalytic subunit Nox2 (gp91^{phox}). COX-2 gene promoter contains consensus binding sites for AP-1 and NF-κB; however, only LPS-induced increase of AP-1 activity with phosphorylation of MAPK was reduced by eupafolin. Furthermore, eight-week-old male C57BL6 mice were intraperitoneally administered with eupafolin for 30 min, after which LPS was subcutaneously injected for 24 h. *In vivo* study demonstrated that eupafolin led to lower COX-2 expression in the mouse dermis than the LPS-only group. Overall, LPS-induced inflammatory response in the skin can be attenuated via inhibition of Nox2/p47^{phox}/ROS/JNK/AP-1-dependent pathway.

trans-Chalcone (Martinez et al., 2017), 1,3-diphenyl-2-propen-1-one, is the biphenolic precursor of flavonoids in plants, and Lipoxin A_4 (LXA_4) (Martinez et al., 2018), a metabolic product of arachidonic acid, is an endogenous lipoxygenase-derived eicosanoid mediator. *In vivo* experiments were performed using male hairless mice (HRS/J) treated intraperitoneally with *trans*-Chalcone or LXA_4 for 1 h, after which they were UVB irradiated. *trans*-Chalcone and LXA_4 can reduce UVB-induced excessive generation of superoxide anion and $gp91^{phox}$ mRNA overexpression. The authors described the relationship between acute inflammation and oxidative stress via the crucial role of Nox2 and ROS on proinflammatory signaling cascade as secondary messengers. *trans*-Chalcone has been shown to reduce proinflammatory Th2 and Th17 cytokines. LXA_4 also inhibited proinflammatory cytokine production and induced anti-inflammatory production. Additionally, the reduction of epidermal thickness and sunburn cells by *trans*-Chalcone and LXA_4 were shown in the skin of hairless mice exposed to UV radiation. *P. pseudocaryophyllus* belongs to the Myrtaceae family and contains flavonoids and other polyphenolic compounds (Campanini et al., 2013). *P. pseudocaryophyllus* ethanolic extract (PPE) inhibited UVB-mediated increase of skin edema, $gp91^{phox}$ mRNA overexpression, and IL-1β production, and increased IL-10 levels in the same model experiment against *trans*-Chalcone and Lipoxin A_4. These compounds and extracts were suggested to prevent skin diseases, such as oxidative stress and skin inflammation.

Apocynin, a known NADPH oxidase inhibitor, is an active compound derived from the roots of the medicinal plant *Picrorhiza kurroa* (Byun et al., 2016). *In vitro,* UVB-irradiated mouse skin epidermal JB6 P^+ cells were used for the experiment of skin carcinogenesis. Pretreatment of apocynin suppressed NADPH oxidase activity, phosphorylation of MAPK and Akt signaling, and COX-2 activity compared to UVB-induced JB6 P^+ cells. Skin tumors were developed by exposure to UVB within 21 weeks,

whereas apocynin attenuated UVB-induced tumors per female SKH-1 hairless mice. It has been reported that apocynin lowered NADPH oxidase activity and reduced AP-1 or nuclear factor-κB (NF-κB) promoter activity, thereby preventing skin carcinogenesis. Thus, the activation of transcription factors, including NF-κB and activator protein-1 (AP-1), according to UV radiation can be targeted by botanical and phytochemicals in skin carcinogenesis.

Table I-1. Phytochemicals and their effects on NADPH oxidase inactivation, enzyme activity, and transcription

Names	Stimuli	Measurement of Nox activity	Enzyme activity or transcription factor	Target disease	Reference
Eupafolin	LPS	NADPH oxidase activity $p47^{phox}$ translocation COX-2 expression using knockdown of Nox2 ($gp91^{phox}$) and $p47^{phox}$	Phosphorylation of c-Fos and c-Jun AP-1 DNA binding activity	Skin inflammation	Tsai et al., 2014
trans-Chalcone	UV source	Nox2 $gp91^{phox}$ *mRNA* expression	Myeloperoxidase (MPO) activity Metalloproteinase-9 (MMP-9) activity GSH depletion Catalase (CAT) activity	Skin inflammation Oxidative stress	Martinez et al., 2017
Lipoxin A_4	UV	Nox $gp91^{phox}$ *mRNA* expression	Myeloperoxidase (MPO) activity Metalloproteinase-9 (MMP-9) activity GSH depletion	Skin inflammation Oxidative stress	Martinez et al., 2018
Apocynin	UVB	NADPH oxidase activity	AP-1 promoter activity NF-κB promoter activity	Skin carcinogenesis	Byun et al., 2016
Tannic acid	UVB	NADPH oxidase activity	Catalase (CAT) activity Superoxide dismutase (SOD) activity GSH depletion Metalloproteinase-1, 9 (MMP-1, 9) expression	Photoaging	Daré et al., 2020
Metformin	UVB	NADPH oxidase-dependent superoxide		Photoaging	Ribeiro et al., 2020
Protocatechuic acid	UVB	NADPH oxidase activity	Catalase (CAT) activity Superoxide dismutase (SOD) activity GSH depletion Lipid peroxidation Metalloproteinase-1, 9 (MMP-1, 9) expression	Oxidative injuries Photoaging	Daré, Oliveira, et al., 2020
Rosmarinic Acid in *Lycopus europaeus*		Nox2 and Nox4 activity		Photoaging	Revoltella et al., 2018
Pimenta pseudocaryophyllus	UVB	Nox2 $gp91^{phox}$ mRNA expression	Glutathione reductase *mRNA* expression Myeloperoxidase (MPO) activity Metalloproteinase-9 (MMP-9) activity GSH depletion Superoxide anion production Lipid peroxidation	Skin inflammation Oxidative stress	Campanini et al., 2013

I-7. Preventive botanical extracts and phytochemicals in UV-induced skin damages via regulation of EGFR

Since EGFR has a central role in cancer cell growth and survival, many materials were developed to target EGFR directly. For example, gefitinib and erlotinib are well-known pharmaceutical inhibitors for EGFR. However, long-term use of these drugs was accompanied by adverse drug reactions, particularly dermatological, and finally failed in Asian female patients bearing non-small cell lung cancer. Therefore, rather than direct regulation of EGFR, we focused on investigating the effects of extracts or phytochemicals regulating the upstream or downstream signaling of EGFR.

When UV stimulated the skin *in vitro* and *in vivo*, the effect of nutraceuticals in several studies was conducted with EGFR phosphorylation. However, ERBB activation, dysregulation of amphiregulin and AhR, and excessive phosphorylation of Src can also be targeted for preventing skin diseases, excluding phosphorylation of EGFR. Therefore, various materials can inhibit inflammation or cancer occurring in the skin by inhibition of factors related to EGFR activation (Table I- 2).

The AhR signaling pathway is one of the major UVB-induced signaling pathways, and AhR mediates COX-2 overexpression. In a study, we demonstrated that 1,8-cineole, a monoterpene cyclic ether, inhibits c-Src-dependent EGFR activation induced by UVB, thereby suppressing RAF-MEK1/2-ERK1/2 signaling pathway and cyp1a1, a target gene of the AhR, mRNA expression induced by AhR activation (Lee et al., 2017). It was demonstrated by knockdown of AhR, which suppresses COX-2 expression in HaCaT cells. 1,8-cineole also reduced UVB-induced epidermal thickness and skin tumorigenesis in

hairless SKH-1 mice. Overall, UVB-induced skin carcinogenesis could be suppressed by directly targeting AhR.

Oi et al. demonstrated that taxifolin as an ATP-competitive inhibitor can bind the ATP-binding pocket of EGFR (Lys721. Met 769, and Asp 831) and suppress UVB and solar UV-induced carcinogenesis by targeting EGFR through *in silico* modeling (Oi et al., 2012). They have also shown that taxifolin regulates COX-2 through EGFR inhibition. Additionally, TGa cellulose nanocrystal (Park et al., 2013), carnosic acid (Potapovich et al., 2011), and cyanidin-3-*O*-glucoside (He et al., 2017) decreased the downstream kinases and Akt or MAPK signaling pathways, by reducing UVB-induced phosphorylation of EGFR.

Curcumin, a dietary polyphenol, is the main component of turmeric and is extracted from the East India plant Curcuma longa. The mechanism by which curcumin interacts with EGFR has not been fully elucidated. However, Starok et al reported that female BALB/c mice treated with 2, 4, 6-trinitrochlorobenzene (TNCB), dermatitis model, which increased ear swelling, ERK phosphorylation, and inflammatory cytokine, were inhibited by the application of curcumin (Starok et al., 2015). Furthermore, amphiregulin gene overexpression was also attenuated in the TNCB-challenged ear with curcumin treatment. Additionally, Capalbo et al reported through preclinical evidence that while conventional EGFR-targeted treatments, such as cetuximab have resistance, oral curcumin phospholipid supplements can overcome anti-EGFR treatment resistance (Capalbo et al., 2018).

Table I-2. Phytochemicals and their effect on EGFR activation and phosphorylation of various factors

Names	Stimuli	Measurement of EGFR activity	Phosphorylation factor	Target disease	Reference
Taxifolin	UVB and solar-UV	Phosphorylation (T1068) *in vitro* EGFR kinase assay	P38, JNK, ERK Akt, $p70^{s6k}$, p90RSK, MSK	Skin carcinogenesis	Oi et al., 2012
TGa Cellulose nanocrystal (CNC)	UVB	Phosphorylation (T1068, T1045)	P38, JNK1/2, ERK1/2 MEK1/2, MKK4/7, B-Raf	Skin inflammation	Park et al., 2013
Carnosic acid	UVB	Phosphorylation	ERK, MEK	Photoaging	Potapovich et al., 2011
Plant polyphenols: Verbascoside, Resveratrol, Polydatin, Rutin, Quercetin	TGFα TNFα+IFNγ UVA+UVB LPS	Phosphorylation nuclear translocation	ERK, p65, Akt	Skin inflammation Skin cancer	He et al., 2017
Cyanidin-3-O-glucoside	UVB	Phosphorylation	P38, JNK, ERK, Akt	Epidermal cell apoptosis Skin cancer	Ha et al., 2016
1,8-cineole	UVB	Phosphorylation (Y845)	P38, JNK1/2, ERK1/2 MEK1/2, B-Raf, C-Raf	Skin carcinogenesis	Lee et al., 2017
Curcumin	EGF	Phosphorylation (T1068) Surface plasmon resonance competition analysis			Starok et al., 2015
Silymarin	EGF	EGFR activity EGFR kinase activity			Ahmad et al., 1998
Epigallocatechin 3-Gallate	EGF	Phosphorylation of erbB1	ERK1/2		Bhatia et al., 2001

I-8. References

Ahmad, N., Gali, H., Javed, S., & Agarwal, R. (1998). Skin cancer chemopreventive effects of a flavonoid antioxidant silymarin are mediated via impairment of receptor tyrosine kinase signaling and perturbation in cell cycle progression. *Biochemical and Biophysical Research Communications*, *247*(2), 294-301.

Albanell, J., Rojo, F., Averbuch, S., Feyereislova, A., Mascaro, J. M., Herbst, R., LoRusso, P., Rischin, D., Sauleda, S., & Gee, J. (2002). Pharmacodynamic studies of the epidermal growth factor receptor inhibitor ZD1839 in skin from cancer patients: histopathologic and molecular consequences of receptor inhibition. *Journal of Clinical Oncology*, *20*(1), 110-124.

Bae, Y. S., Kang, S. W., Seo, M. S., Baines, I. C., Tekle, E., Chock, P. B., & Rhee, S. G. (1997). Epidermal growth factor (EGF)-induced generation of hydrogen peroxide. Role in EGF receptor-mediated tyrosine phosphorylation. *Journal of Biological Chemistry*, *272*(1), 217-221.

Benjamin, C. L., & Ananthaswamy, H. N. (2007). p53 and the pathogenesis of skin cancer. *Toxicology and Applied Pharmacology*, *224*(3), 241-248.

Berton, T. R., Mitchell, D. L., Fischer, S. M., & Locniskar, M. F. (1997). Epidermal proliferation but not the quantity of DNA photodamage is correlated with UV-induced mouse skin carcinogenesis. *Journal of Investigative Dermatology*, *109*(3), 340-347.

Bhatia, N., Agarwal, C., & Agarwal, R. (2001). Differential responses of skin cancer-chemopreventive agents silibinin, quercetin, and epigallocatechin 3-gallate on

mitogenic signaling and cell cycle regulators in human epidermoid carcinoma A431 cells. *Nutrition and Cancer*, *39*(2), 292-299.

Blagodatski, A., Klimenko, A., Jia, L., & Katanaev, V. L. (2020). Small Molecule Wnt Pathway Modulators from Natural Sources: History, State of the Art and Perspectives. *Cells*, *9*(3). 589.

Bowden, G. T. (2004). Prevention of non-melanoma skin cancer by targeting ultraviolet-B-light signalling. *Nature Reviews Cancer*, *4*(1), 23-35.

Byun, S., Lee, E., Jang, Y. J., Kim, Y., & Lee, K. W. (2016). The NADPH oxidase inhibitor apocynin inhibits UVB-induced skin carcinogenesis. *Experimental Dermatology*, *25*(6), 489-491.

Campanini, M. Z., Pinho-Ribeiro, F. A., Ivan, A. L., Ferreira, V. S., Vilela, F. M., Vicentini, F. T., Martinez, R. M., Zarpelon, A. C., Fonseca, M. J., & Faria, T. J. (2013). Efficacy of topical formulations containing Pimenta pseudocaryophyllus extract against UVB-induced oxidative stress and inflammation in hairless mice. *Journal of Photochemistry and Photobiology B: Biology*, *127*, 153-160.

Cassidy, P. B., Liu, T., Florell, S. R., Honeggar, M., Leachman, S. A., Boucher, K. M., & Grossman, D. (2017). A phase II randomized placebo-controlled trial of oral N-acetylcysteine for protection of melanocytic nevi against UV-induced oxidative stress in vivo. *Cancer Prevention Research*, *10*(1), 36-44.

Capalbo, C., Belardinilli, F., Filetti, M., Parisi, C., Petroni, M., Colicchia, V., Tessitore, A., Santoni, M., Coppa, A., & Giannini, G. (2018). Effective treatment of a platinum-resistant cutaneous squamous cell carcinoma case by EGFR pathway inhibition. *Molecular and Clinical Oncology*, *9*(1), 30-34.

Chamulitrat, W., Stremmel, W., Kawahara, T., Rokutan, K., Fujii, H., Wingler, K., Schmidt, H. H., & Schmidt, R. (2004). A constitutive NADPH oxidase-like system containing gp91phox homologs in human keratinocytes. *Journal of Investigative Dermatology*, *122*(4), 1000-1009.

Chen, K., Kirber, M. T., Xiao, H., Yang, Y., & Keaney Jr, J. F. (2008). Regulation of ROS signal transduction by NADPH oxidase 4 localization. *The Journal of cell biology*, *181*(7), 1129-1139.

Daré, R. G., Nakamura, C. V., Ximenes, V. F., & Lautenschlager, S. O. (2020). Tannic acid, a promising anti-photoaging agent: Evidences of its antioxidant and anti-wrinkle potentials, and its ability to prevent photodamage and MMP-1 expression in L929 fibroblasts exposed to UVB. *Free Radical Biology and Medicine*, *160*, 342-355.

Daré, R. G., Oliveira, M. M., Truiti, M. C., Nakamura, C. V., Ximenes, V. F., & Lautenschlager, S. O. (2020). Abilities of protocatechuic acid and its alkyl esters, ethyl and heptyl protocatechuates, to counteract UVB-induced oxidative injuries and photoaging in fibroblasts L929 cell line. *Journal of Photochemistry and Photobiology B: Biology*, *203*, 111771.

Didona, D., Paolino, G., Bottoni, U., & Cantisani, C. (2018). Non melanoma skin cancer pathogenesis overview. *Biomedicines*, *6*(1), 6.

Geiszt, M., Kopp, J. B., Várnai, P., & Leto, T. L. (2000). Identification of renox, an NAD (P) H oxidase in kidney. *Proceedings of the National Academy of Sciences*, *97*(14), 8010-8014.

Goodson, A. G., Cotter, M. A., Cassidy, P., Wade, M., Florell, S. R., Liu, T., Boucher, K. M., & Grossman, D. (2009). Use of oral N-acetylcysteine for protection of melanocytic nevi

against UV-induced oxidative stress: towards a novel paradigm for melanoma chemoprevention. *Clinical Cancer Research*, *15*(23), 7434-7440.

He, Y., Hu, Y., Jiang, X., Chen, T., Ma, Y., Wu, S., Sun, J., Jiao, R., Li, X., & Deng, L. (2017). Cyanidin-3-O-glucoside inhibits the UVB-induced ROS/COX-2 pathway in HaCaT cells. *Journal of Photochemistry and Photobiology B: Biology*, *177*, 24-31.

Helmcke, I., Heumüller, S., Tikkanen, R., Schröder, K., & Brandes, R. P. (2009). Identification of structural elements in Nox1 and Nox4 controlling localization and activity. *Antioxidants & Redox Signaling*, *11*(6), 1279-1287.

Heppner, D. E., Hristova, M., Dustin, C. M., Danyal, K., Habibovic, A., & van der Vliet, A. (2016). The NADPH Oxidases DUOX1 and Nox2 Play Distinct Roles in Redox Regulation of Epidermal Growth Factor Receptor Signaling. *Journal of Biological Chemistry*, *291*(44), 23282-23293.

Heppner, D. E., & van der Vliet, A. (2016). Redox-dependent regulation of epidermal growth factor receptor signaling. *Redox Biology*, *8*, 24-27.

Herbert, K. J., Cook, A. L., & Snow, E. T. (2014). SIRT1 inhibition restores apoptotic sensitivity in p53-mutated human keratinocytes. *Toxicology and Applied Pharmacology*, *277*(3), 288-297.

Herbst, R. S., Kim, E. S., & Harari, P. M. (2001). IMC-C225, an anti-epidermal growth factor receptor monoclonal antibody, for treatment of head and neck cancer. *Expert Opinion on Biological Therapy, 1*(4), 719-732.

Hordijk, P. L. (2006). Regulation of NADPH oxidases: the role of Rac proteins. *Circulation Research, 98*(4), 453-462.

Huang, K. M., Liang, S., Yeung, S., Oiyemhonlan, E., Cleveland, K. H., Parsa, C., Orlando, R., Meyskens, F. L., Andresen, B. T., & Huang, Y. (2017). Topically applied carvedilol attenuates solar ultraviolet radiation induced skin carcinogenesis. *Cancer Prevention Research*, *10*(10), 598-606.

Kitagishi, Y., & Matsuda, S. (2013). Redox regulation of tumor suppressor PTEN in cancer and aging. *International Journal of Molecular Medicine*, *31*(3), 511-515.

Lee, J., Ha, S. J., Park, J., Kim, Y. H., Lee, N. H., Kim, Y. E., Kim, Y., Song, K. M., & Jung, S. K. (2017). 1,8-cineole prevents UVB-induced skin carcinogenesis by targeting the aryl hydrocarbon receptor. *Oncotarget*, *8*(62), 105995-106008.

Lee, K. W., Bode, A. M., & Dong, Z. (2011). Molecular targets of phytochemicals for cancer prevention. *Nature Reviews Cancer*, *11*(3), 211-218.

Lee, T. M., Chen, C. C., & Hsu, Y. J. (2011). Differential effects of NADPH oxidase and xanthine oxidase inhibition on sympathetic reinnervation in postinfarct rat hearts. *Free Radical Biology and Medicine*, *50*(11), 1461-1470.

Li, L., Fan, P., Chou, H., Li, J., Wang, K., & Li, H. (2019). Herbacetin suppressed MMP9 mediated angiogenesis of malignant melanoma through blocking EGFR-ERK/AKT signaling pathway. *Biochimie*, *162*, 198-207.

Matsumura, Y., & Ananthaswamy, H. N. (2002). Short-term and long-term cellular and molecular events following UV irradiation of skin: implications for molecular medicine. *Expert Reviews in Molecular Medicine*, *4*(26), 1-22.

Martinez, R., Fattori, V., Saito, P., Melo, C., Borghi, S., Pinto, I., Bussmann, A., Baracat, M., Georgetti, S., & Verri Jr, W. (2018). Lipoxin A4 inhibits UV radiation-induced skin inflammation and oxidative stress in mice. *Journal of Dermatological Science*, *91*(2),

164-174.

Martinez, R. M., Pinho-Ribeiro, F. A., Steffen, V. S., Caviglione, C. V., Fattori, V., Bussmann, A. J., Bottura, C., Fonseca, M. J., Vignoli, J. A., & Baracat, M. M. (2017). trans-Chalcone, a flavonoid precursor, inhibits UV-induced skin inflammation and oxidative stress in mice by targeting NADPH oxidase and cytokine production. *Photochemical & Photobiological Sciences, 16*(7), 1162-1173.

Ming, M., Feng, L., Shea, C. R., Soltani, K., Zhao, B., Han, W., Smart, R. C., Trempus, C. S., & He, Y.-Y. (2011). PTEN positively regulates UVB-induced DNA damage repair. *Cancer Research, 71*(15), 5287-5295

Nakayama, H., Fukuda, S., Inoue, H., Nishida-Fukuda, H., Shirakata, Y., Hashimoto, K., & Higashiyama, S. (2012). Cell surface annexins regulate ADAM-mediated ectodomain shedding of proamphiregulin. *Molecular Biology of the Cell*, *23*(10), 1964-1975.

Nijhof, J. G., van Pelt, C., Mulder, A. A., Mitchell, D. L., Mullenders, L. H., & de Gruijl, F. R. (2007). Epidermal stem and progenitor cells in murine epidermis accumulate UV damage despite NER proficiency. *Carcinogenesis*, *28*(4), 792-800.

Oi, N., Chen, H., Kim, M. O., Lubet, R. A., Bode, A. M., & Dong, Z. (2012). Taxifolin suppresses UV-induced skin carcinogenesis by targeting EGFR and PI3K. *Cancer Prevention Research*, *5*(9), 1103-1114.

Ono, M., & Kuwano, M. (2006). Molecular mechanisms of epidermal growth factor receptor (EGFR) activation and response to gefitinib and other EGFR-targeting drugs. *Clinical Cancer Research*, *12*(24), 7242-7251.

Park, M., Han, J., Lee, C. S., Heung Soo, B., Lim, K. M., & Ha, H. (2013). Carnosic acid, a phenolic diterpene from rosemary, prevents UV-induced expression of matrix

metalloproteinases in human skin fibroblasts and keratinocytes. *Experimental Dermatology*, *22*(5), 336-341.

Pellegrini, C., Maturo, M. G., Di Nardo, L., Ciciarelli, V., Garcia-Rodrigo, C. G., & Fargnoli, M. C. (2017). Understanding the Molecular Genetics of Basal Cell Carcinoma. *International Journal of Molecular Sciences*, *18*(11). 2485

Pollet, M., Shaik, S., Mescher, M., Frauenstein, K., Tigges, J., Braun, S. A., Sondenheimer, K., Kaveh, M., Bruhs, A., & Meller, S. (2018). The AHR represses nucleotide excision repair and apoptosis and contributes to UV-induced skin carcinogenesis. *Cell Death & Differentiation*, *25*(10), 1823-1836.

Potapovich, A. I., Lulli, D., Fidanza, P., Kostyuk, V. A., De Luca, C., Pastore, S., & Korkina, L. G. (2011). Plant polyphenols differentially modulate inflammatory responses of human keratinocytes by interfering with activation of transcription factors NFκB and AhR and EGFR–ERK pathway. *Toxicology and Applied Pharmacology*, *255*(2), 138-149.

Raad, H., Serrano-Sanchez, M., Harfouche, G., Mahfouf, W., Bortolotto, D., Bergeron, V., Kasraian, Z., Dousset, L., Hosseini, M., & Taieb, A. (2017). NADPH oxidase-1 plays a key role in keratinocyte responses to UV radiation and UVB-induced skin carcinogenesis. *Journal of Investigative Dermatology*, *137*(6), 1311-1321.

Revoltella, S., Baraldo, G., Waltenberger, B., Schwaiger, S., Kofler, P., Moesslacher, J., Huber-Seidel, A., Pagitz, K., Kohl, R., & Jansen-Duerr, P. (2018). Identification of the NADPH Oxidase 4 inhibiting principle of lycopus europaeus. *Molecules*, *23*(3), 653.

Ribeiro, F. M., Ratti, B. A., dos Santos Rando, F., Fernandez, M. A., Ueda-Nakamura, T., Lautenschlager, S. d. O. S., & Nakamura, C. V. (2020). Metformin effect on driving cell survival pathway through inhibition of UVB-induced ROS formation in human

keratinocytes. *Mechanisms of Ageing and Development*, *192*, 111387.

Sajadimajd, S., Bahramsoltani, R., Iranpanah, A., Patra, J. K., Das, G., Gouda, S., Rahimi, R., Rezaeiamiri, E., Cao, H., & Giampieri, F. (2020). Advances on natural polyphenols as anticancer agents for skin cancer. *Pharmacological Research*, *151*, 104584.

Savoia, P., Zavattaro, E., & Cremona, O. (2018). Chemoprevention of Skin Carcinomas in High-Risk Transplant Recipients. *Current Medicinal Chemistry*, *25*(6), 687-697.

Sedeek, M., Nasrallah, R., Touyz, R. M., & Hébert, R. L. (2013). NADPH oxidases, reactive oxygen species, and the kidney: friend and foe. *Journal of the American Society of Nephrology*, *24*(10), 1512-1518.

Seike, M., & Gemma, A. (2012). Therapeutic biomarkers of EGFR-TKI. Gan to kagaku ryoho. *Cancer & Chemotherapy*, *39*(11), 1613-1617.

Singh, S., Singh, P. P., Roberts, L. R., & Sanchez, W. (2014). Chemopreventive strategies in hepatocellular carcinoma. *Nature reviews Gastroenterology & Hepatology*, *11*(1), 45-54.

Starok, M., Preira, P., Vayssade, M., Haupt, K., Salome, L., & Rossi, C. (2015). EGFR inhibition by curcumin in cancer cells: a dual mode of action. *Biomacromolecules*, *16*(5), 1634-1642.

Stratton, S. P., Dorr, R. T., & Alberts, D. S. (2000). The state-of-the-art in chemoprevention of skin cancer. *European Journal of Cancer*, *36*(10), 1292-1297.

Surh, Y. J. (2003). Cancer chemoprevention with dietary phytochemicals. *Nature Reviews Cancer*, *3*(10), 768-780.

Tsai, M.-H., Lin, Z.-C., Liang, C.-J., Yen, F.-L., Chiang, Y.-C., & Lee, C.-W. (2014). Eupafolin inhibits PGE2 production and COX2 expression in LPS-stimulated human dermal

fibroblasts by blocking JNK/AP-1 and Nox2/p47phox pathway. *Toxicology and Applied Pharmacology*, *279*(2), 240-251.

Wieduwilt, M. J., & Moasser, M. (2008). The epidermal growth factor receptor family: biology driving targeted therapeutics. *Cellular and Molecular Life Sciences*, *65*(10), 1566-1584.

Wu, R. F., Xu, Y. C., Ma, Z., Nwariaku, F. E., Sarosi Jr, G. A., & Terada, L. S. (2005). Subcellular targeting of oxidants during endothelial cell migration. *The Journal of Cell Biology*, *171*(5), 893-904.

Xian, D., Lai, R., Song, J., Xiong, X., & Zhong, J. (2019). Emerging perspective: role of increased ROS and redox imbalance in skin carcinogenesis. *Oxidative Medicine and Cellular Longevity*, *2019*.

Chapter II.

Preventive Effect of *Rhus javanica* Extract on UVB-induced Skin Inflammation and Photoaging

Abstract

Rhus javanica has long been used in traditional medicines, and found to possess bioactive properties. In this study, I sought to investigate whether *Rhus javanica* extract (RJE) has preventive effects against UVB-induced inflammation and photoaging. RJE was identified as a promising candidate based on an MMP-1 promoter assay, and I confirmed suppressive effects on UVB-induced COX-2 and MMP-1 expression (67.6% and 80.9%, respectively) in immortalized human keratinocyte HaCaT cells. RJE suppressed both UVB-induced mitogen activated protein kinase (MAPK) and Akt signalling pathways as well as EGFR activity. RJE significantly suppressed repetitive UVB-induced wrinkle formation and COX-2 and MMP-13 expression *in vivo*. Among the compounds identified, syringic acid was found to exhibit the strongest inhibitory effect on UVB-induced MMP-1 promoter activity (45.2%). These results demonstrate that RJE has potent preventive activity for skin inflammation and photoaging which occurs via suppression of pathways related to EGFR.

II-1. Introduction

The skin is the largest organ of the integumentary system and protects the human body against pathogens and irritants as a primary defence system. Although ultraviolet (UV) radiation is required for the biosynthesis of vitamin D3, stimulates the production of photoprotective melanin, and can help treat psoriasis and vitiligo (Almutawa et al., 2015; Bansal, Sahoo, & Garg, 2013; Fett, 2013), excessive UV exposure is a major risk factor for skin inflammation and cancer (Jung et al., 2008). While also dependent on genetic factors and lifestyle choices, repeated exposure to UV irradiation generally results in the appearance of irregular brown spots and wrinkle formation, collectively referred to as photogaing.

Among the UV wavelengths, UVB (290–320 nm) is considered to be a complete carcinogen because repetitive treatment with UVB can induce skin cancer (Goswami & Haldar, 2014). Additionally, chronic irradiation of the skin by UV induces wrinkle formation and irregular pigmentation, referred to as photoaging (Fisher, 2005). Skin inflammation and photoaging are sometimes clinically considered as minor skin problems, however, these conditions can cause pain and distress related to appearance (Peharda et al., 2007).

COX-2 and MMP-1 are two major enzymes involved in skin inflammation and photoaging, respectively, and are responsive to UV irradiation (Oh et al., 2014). Both acute and chronic UV irradiation up-regulates COX-2 expression in keratinocytes and skin in SKH-1 hairless mice and humans (Bermudez et al., 2015; Jung et al., 2008). The genetic deletion of one *cox-2* allele is strongly associated with a higher risk of UV-induced skin carcinogenesis (Fischer, Pavone, Mikulec, Langenbach, & Rundhaug, 2007). MMP-1, the so-called interstitial collagenase, plays a major role in the process of photoaging because it

specifically cleaves type 1 collagen, a major constituent of the dermis (Wolfle et al., 2012). Transcription of COX-2 and MMP-1 is regulated by AP-1, which is a key transcriptional factor in skin inflammation and photoaging (Eferl & Wagner, 2003). Increased AP-1 activity stimulates skin inflammation via an abnormal increase in prostaglandin $(PGE)_2$ production (Jung et al., 2008) and photoaging via the degradation of collagen, a major extracellular matrix protein (Quan et al., 2010). Major signalling pathways known to mediate UVB-induced biological responses involve mitogen-activated protein kinases (MAPKs) and signal transduction associated with these pathways is known to play central role in the upregulation of COX-2 and MMP-1 expression by UV (Bode & Dong, 2003). Therefore, regulation of the MAPKs/AP-1 signalling cascade represents a promising strategy for the prevention of UV-induced skin inflammation and photoaging.

Multiple lines of evidence suggest that high consumption of food phytochemicals from vegetables and fruits can help to prevent inflammation and cancer (Bulla et al., 2015). Some plant phytochemicals exhibit potent bioactive properties that mitigate the adverse effects of UV radiation on the skin (Korac & Khambholja, 2011). *Rhus javanica* (Galla rhois) is a member of the Anacardiaceae family and is a type of nutgall sumac (Lee et al., 2012). This plant is widely used in herbal medicines to treat diarrhoea, inflammation, dysentery and coughs. Furthermore, *Rhus javanica* compounds have been shown to possess strong antiviral, antibacterial, anticancer, hepatoprotective, antidiarrhoeal and antioxidant activities (Ahn, Lee, Oh, Kim, & Lee, 2005; Choi et al., 2009). Although published evidence suggests that *Rhus javanica* may have promising biological effects on various diseases mechanisms, its effect on UVB-induced skin inflammation and photoaging and the mechanisms of action responsible remain unclear. I screened several botanical extracts of interest and identified RJE as the most potent anti-inflammatory and anti-photoaging material. In the present study, I sought to investigate the inhibitory effects of RJE on UVB-induced inflammation and photoaging, and

observed that RJE inhibits UVB-induced COX-2 and MMP-1 expression via suppression of the MAPKKs/MAPKs/ AP-1 pathways. Experiments using the SKH-1 hairless mouse model revealed that oral administration of RJE significantly suppresses UVB-induced wrinkle formation, as well as COX-2 and MMP-13 expression in mouse skin. Among the RJE compounds, syringic acid exhibited the most potent inhibitory effect on MMP-1 promoter activity. These findings suggest that RJE is a potent anti-inflammatory and anti-photoaging agent that inhibits COX-2 and MMP-1 expression.

II-2. Materials and Methods

II-2.1. Materials

Chemical reagents were purchased from Sigma-Aldrich (St Louis, MO, USA). Dulbecco's Modified Eagle's Medium (DMEM), gentamicin, L-glutamine, penicillin–streptomycin and foetal bovine serum (FBS) were obtained from Thermo Scientific HyClone (Logan, UT, USA). The antibodies against c-Jun, MMP-1, MMP-13 and β-actin were purchased from Santa Cruz Biotech (Santa Cruz, CA, USA). The antibodies against COX-2, p44/42 MAP Kinase, SAPK/JNK, p38 MAPK, phospho-p44/42 MAPK (Erk 1/2) (Thr202/Tyr204), phospho-SAPK/JNK (Thr183/Tyr185), MKK3b, phospho-MKK3 (Ser189)/MKK6 (Ser 207), SEK1/MKK4, phospho-SEK1/MKK4 (Ser257/Thr261), MEK1/2, phospho-MEK1/2 (Ser217/ 221), phospho-c-Jun (Ser73), Akt, phospho-Akt (Thr308), PKD/PKCμ, phospho- PKD/PKCμ (Ser916), Src and phospho-Src (Tyr527) were purchased from Cell Signaling Biotechnology (Beverly, MA, USA). The antibody against phosphorylated p38 MAPK (pT180/pY182) was purchased from BD Biosciences (Franklin Lakes, NJ, USA).

II-2-2. Sample preparation and extraction procedure

Rhus javanica specimens were purchased from Kyungdong Market (Seoul, Korea). The specimen was deposited in the Plant Resources and Environment Department, Cheju National University, Korea and identified by a botanist, Dr. Ji-Hun Kim (Department of Plant Resources and Environment, Cheju National University). The samples were ground with a blender (Wonder Blender, OSAKA CHEMICAL Co., Osaka, Japan) to obtain a fine powder. Powdered materials were stored in plastic bags at room temperature for use in the extraction

experiments. Dried powder (100 g) was extracted with an Ultrasonic Processor VCX 750 (Sonics & Materials, Inc., Newtown, USA) with 1,000 mL of 95% ethanol, and incubated at room temperature for 24 h. After precipitate removal, the extracts were concentrated to 100 mL with an IKA RV 10 Rotary Evaporator (IKA® Works, Guangzhou, China), then freeze-dried.

II-2-3. Cell culture, UVB exposure and viability assay

Human epidermal keratinocyte HaCaT and 293T cells were maintained in DMEM containing 10% FBS, 100 units/mL of penicillin and 100 mg/mL of streptomycin at 37℃ in a 5% CO_2 humidified incubator. UVB irradiation was conducted using a bank of four Westinghouse F520 lamps (National Biological, Twinsburg, OH) at 6 J/s/m light in the UVB range. Approximately 10% of the additional radiation from the F520 lamp is in the UVA spectrum (320 nm). A UVB exposure chamber was fitted with a Kodak Kodacel K6808 filter to eliminates all wavelengths below 290 nm. UVB radiation was measured using a UVX radiometer (UVX-31). To assess cell viability, HaCaT cells were seeded (1×10^3 cells/well) in 96-well plates and incubated at 37℃ in a 5% CO_2 incubator. After the cells were treated with RJE, 20 μL of MTS reagent (Promega, Madison, WI, USA) was added to each well. After 1 h of incubation, absorbance levels for formazan at 490 and 690 nm were measured using a microplate reader (Bio-Rad Inc., Hercules, CA, USA).

II-2-4. Animal experiments

Six-week-old male SKH-1 hairless mice, weighing approximately 20–22 g, were purchased from OrientBio Inc. (Gyeonggi-do, Korea). The mice were housed in an air-

conditioned room (23 ± 2℃) with a 12 h light/dark cycle. They were allowed free access to food and tap water. All animals received humane care, and the study protocol (KFRI-M-14013) was approved and performed in accordance with guidelines for animal use and care at Korea Food Research Institute. Twenty mice were randomly allocated to each group (five mice per group, four groups in total): (i) control group (normal), (ii) UVB-irradiated group (UVB), (iii) UVB-irradiated and 40 mg/kg/day RJE-treated group and (iv) UVB-irradiated and 200 mg/kg/day RJE-treated group. The mice in the RJE-treated groups (40 or 200 mg/kg/day) were administered oral doses of RJE for 13 weeks with exposure to UVB irradiation three times per week on their dorsal region. UVB irradiation doses were increased each week by 1 MED (1 MED = 130 mJ/cm^2) to 4 MED, and then maintained at 4 MED until 13 weeks had passed.

II-2-5. MMP-1 promoter assay

To evaluate the MMP-1 promoter activity of various botanical extracts, I constructed a pGreenFire (pGF1) vector containing an MMP-1 promoter plasmid (Kim, Shin, Eun, & Chung, 2009) . For stable expression of pGF1 with the MMP-1 promoter, 293T cells were transfected with the pGF1 plasmid using Lipofectamine (ThermoFisher Scientific, MA, USA), following the manufacturer's instructions. The transfection medium was changed at 4 h after transfection, and the cells were then cultured for 36 h. Virus particles were harvested by filtration using a 0.45 mm syringe filter, then combined with 8 mg/mL of polybrene (Millipore) and infected into HaCaT cells for 24 h. The cell culture media was replaced with fresh culture medium and the cells were further cultured for 24 h, prior to selection with puromycin (1 mg/mL) for 36 h. Selected HaCaT cells (8×10^3 cells/well) were seeded into 96-well plates, which were incubated at 37℃ in a 5% CO_2 incubator. When the cells reached

80–90% confluence, they were starved by culturing in serum-free DMEM for a further 24 h. Cells were then treated with RJE for 1 h prior to UVB (0.04 J/cm^2) exposure and then incubated for 5 h. Cells were disrupted with 100 μL of lysis buffer [0.1 M potassium phosphate buffer (pH 7.8), 1% Triton X-100, 1 mM dithiothreitol (DTT), and 2 mM EDTA], after which luciferase activity was measured using a luminometer (SpectraMax L, Molecular Devices, Sunnyvale, CA).

II-2-6. Western blot assay

For *in vitro* Western blot assays, cells (1.5×10^6 cells/mL) were cultured in 10 cm dishes for 24 h, followed by starvation in serum-free DMEM for 24 h. Cells were then treated with RJE for 1 h and irradiated with UVB (0.04 J/cm^2). After incubation, the cells were collected and washed twice with cold PBS, before lysis in Cell Lysis Buffer (Cell Signaling Biotechnology, Beverly, MA, USA) and maintained on ice for 30 min. The lysated protein was washed via centrifugation and the concentration determined using a DC Protein Assay kit (Bio-Rad Laboratories) following manufacturer's instructions. The lysate was subjected to 10% sodium dodecyl sulfate–polyacrylamide gel electrophoresis (SDS-PAGE) and transferred to a polyvinylidene difluoride (PVDF) membrane (Millipore, Immobilon® -P transfer membrane). After transferring, the membranes were incubated with the specific primary antibodies at 4℃ overnight. Protein bands were visualized using a chemiluminescence detection kit (ATTO, Tokyo, Japan) after hybridization with a horseradish peroxidase (HRP)-conjugated secondary antibody.

For *in vivo* Western blots, mouse skin tissue was added to 2 mL microcentrifuge tubes containing lysis buffer and stainless steel bead, and subsequently homogenized twice for 2 min at 20 Hz in a TissueLyser II (Qiagen, Valencia, CA, USA). Skin lysates were

centrifuged at 12,000 rpm for 20 min. After the protein content was determined, the skin tissue extract was subjected to 10% SDS-PAGE and transferred to a PVDF membrane. Membranes were processed, and proteins were analyzed as described above for *in vitro* Western blot assay.

II-2-7. EGFR kinase assay

EGFR kinase activity was assayed in accordance with instructions provided by Abcam (Cambridge, UK). Active EGFR protein (100 ng) was added to a mixture containing basic protein, 5X assay buffer, and diluted ATP solution in the presence or absence of RJE. Reactions were carried out at 30℃ for 30 min, and incorporated activity was determined using the Western blot assay. The resultant kinase activity data represent the mean of three independent experiments.

II-2-8. Immunohistochemical analysis

Sections (5 μm thick) of 10% neutral formalin solution-fixed, paraffin-embedded skin tissues were cut on silane-coated glass slides. Deparaffinized sections were heated for 15 min in 10 mM citrate buffer (pH 6.0) in a microwave oven for antigen retrieval. For the detection of target proteins, slides were incubated with affinity-purified primary antibody in a refrigerator overnight in 1% BSA solution and then developed using the SignalStain® Boost IHC Detection Reagent (HPR, rabbit) antibodies (Cell Signaling Biotechnology). Peroxidase-binding sites were detected by staining with SignalStain® DAB Substrate Kit (Cell Signaling Biotechnology). Finally, counterstaining was performed using Harris hematoxylin solution (Sigma–Aldrich). The MMP-13 and COX-2 were visualized using a fluorescent microscope

(Nikon Eclipse Ti-S, Tokyo, Japan) and images were analyzed using Metamorph (Molecular Devices, Danville, PA) software.

II-2-9. Metabolite extraction

Metabolites were extracted using the Bligh-Dyer protocol. Powder sample were dissolved in methanol and vortexed for 30 sec followed sonication for 2 min. Cold chloroform was then added, followed by further vortexing for 30 sec. After sonication for 2 min, cold HPLC-graded water was added and vortexed for 30 sec resulting in a ratio of 1:2:0.72 (methanol:chloroform:water). The samples were centrifuged at 12,000 rpm for 10 min after incubation for 10 min at room temperature.

II-2-10. Chromatograph

Dried extracts were dissolved in mobile phase buffer and injected into UPLC-ESI-QQQ (Agilent Technologies, CA, USA) with Hypersil gold C18 (Thermo, 2.1 × 100 mm, 1.9 μm) or with ZORBAX-RRHD C18 (Agilent, 2.1 × 100 mm, 1.8 μm). The mobile phase buffers were Buffer A (100% H_2O, and 0.1% formic acid (v/v)) and Buffer B (90% acetonitrile, 10% H_2O, and 0.1% formic acid (v/v/v). The column was equilibrated and eluted according to gradient conditions with a flow rate of 0.2 mL/min at 40℃. The gradient was started at 5% B, changing to a linear gradient of 100% over 5 min, followed by washing time for 2 min, and re-equilibration at 5% B for 3 min.

II-2-11. Statistical analysis

Where appropriate, data are expressed as the means ± S.E.M., and significant differences were determined using one-way ANOVA (Analysis Of Variance). A probability value of $p < 0.05$ was used as the criterion for statistical significance.

II-3. Results

II-3-1. RJE inhibits UVB-induced MMP-1 promoter activity in HaCaT cells

COX-2 and MMP-1 play critical roles in UV-mediated skin inflammation and photoaging, respectively and the AP-1 transcription factor is a major regulator of their expression (Eferl & Wagner, 2003; Fisher et al., 1996; Jung, Ha, et al., 2015). To develop anti-inflammatory and -photoaging treatments, I previously developed immortalized human keratinocyte HaCaT cells stably transfected with an MMP-1 promoter. Using these cells, I screened several botanical extracts of interest and identified RJE as the most potent anti-inflammatory and anti-photoaging material (data not shown). RJE significantly inhibited UVB-induced MMP-1 promoter activity in a dose-dependent manner (Figure II-1A). The tested concentrations of RJE did not affect the viability of immortalized human keratinocyte HaCaT cells (Figure II-1B). Next, I evaluated the inhibitory effect of RJE on UVB-induced COX-2 and MMP-1 expression. Western blot results showed that RJE significantly inhibited UVB-induced COX-2 and MMP-1 expression in HaCaT cells (Figure II-1C and D).

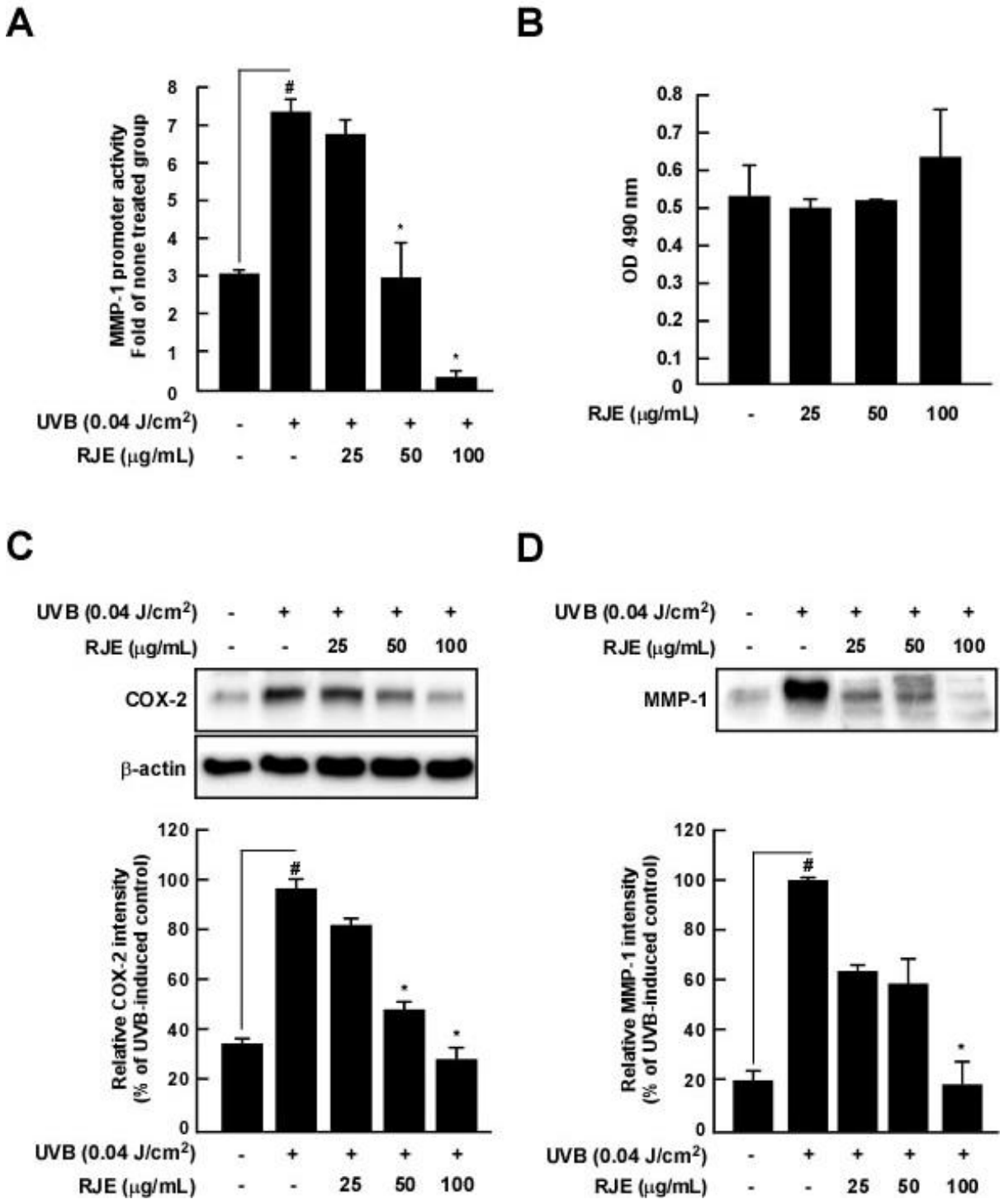

Figure II-1. Effect of RJE on UVB-induced MMP-1 promoter activity, cell viability, and COX-2 and MMP-1 expression in HaCaT cells. (A) RJE suppresses UVB-induced MMP-1 promoter activity in HaCaT cells. For the luciferase assay, HaCaT cells were stably transfected with an MMP-1-luciferase reporter plasmid and cultured as described in the

Materials and Methods. MMP-1 luciferase activity is presented as the mean ± SD of three independent experiments. (B) RJE exhibits no detectable cell cytotoxicity up to 100 μg/mL in HaCaT cells. Cell viability was measured by MTS assay as described in the Materials and Methods. (C) RJE inhibits UVB-induced COX-2 expression in HaCaT cells. (D) RJE inhibits UVB-induced MMP-1 expression in HaCaT cells. Expression levels of COX-2, MMP-1 and β-actin were determined by Western blot assay. Hash symbols (#) indicate a significant difference ($p < 0.05$) between the control group and the group exposed to UVB alone; asterisks (*) indicate significant differences ($p < 0.05$) between groups irradiated with UVB and RJE and the group exposed to UVB alone. Data are presented as the mean ± SD of three independent experiments.

II-3-2. RJE inhibits UVB-induced phosphorylation of MAPKKs/MAPKs, Akt, EGFR, Src and PKD/PKCμ in HaCaT cells

Because MAPKs are the primary mediators of UV-induced COX-2 and MMP-1 expression via regulation of AP-1 activity (Roberts & Der, 2007), I further sought to determine which signaling pathway were modulated by RJE treatment. The results showed that RJE inhibited UVB-induced phosphorylation of MKK4/7/JNK1/2/c-Jun, MKK3/6/p38, and Raf/MEK1/2/ERK1/2 in HaCaT cells (Figure II-2A, B and C). Furthermore, treatment of UVB-irradiated with RJE markedly decreased Akt phosphorylation in HaCaT cells (Figure II-2D). To identify the upstream signaling molecules regulating MAPKKs/MAPKs and Akt, I examined the phosphorylation status of EGFR, Src, and PKC. RJE inhibited UVB-induced phosphorylation of EGFR, Src and PKD/ PKCμ in HaCaT cells (Figure II-2E and F). Because RJE suppressed UVB-induced EGFR phosphorylation, I hypothesized that RJE could be acting on UVB-induced EGFR activity. *In vitro* kinase assays using active EGFR confirmed that RJE strongly inhibits EGFR kinase activity in a dose-dependent manner (Figure II-2G). Butein was used as positive control (Jung, Lee, et al., 2015).

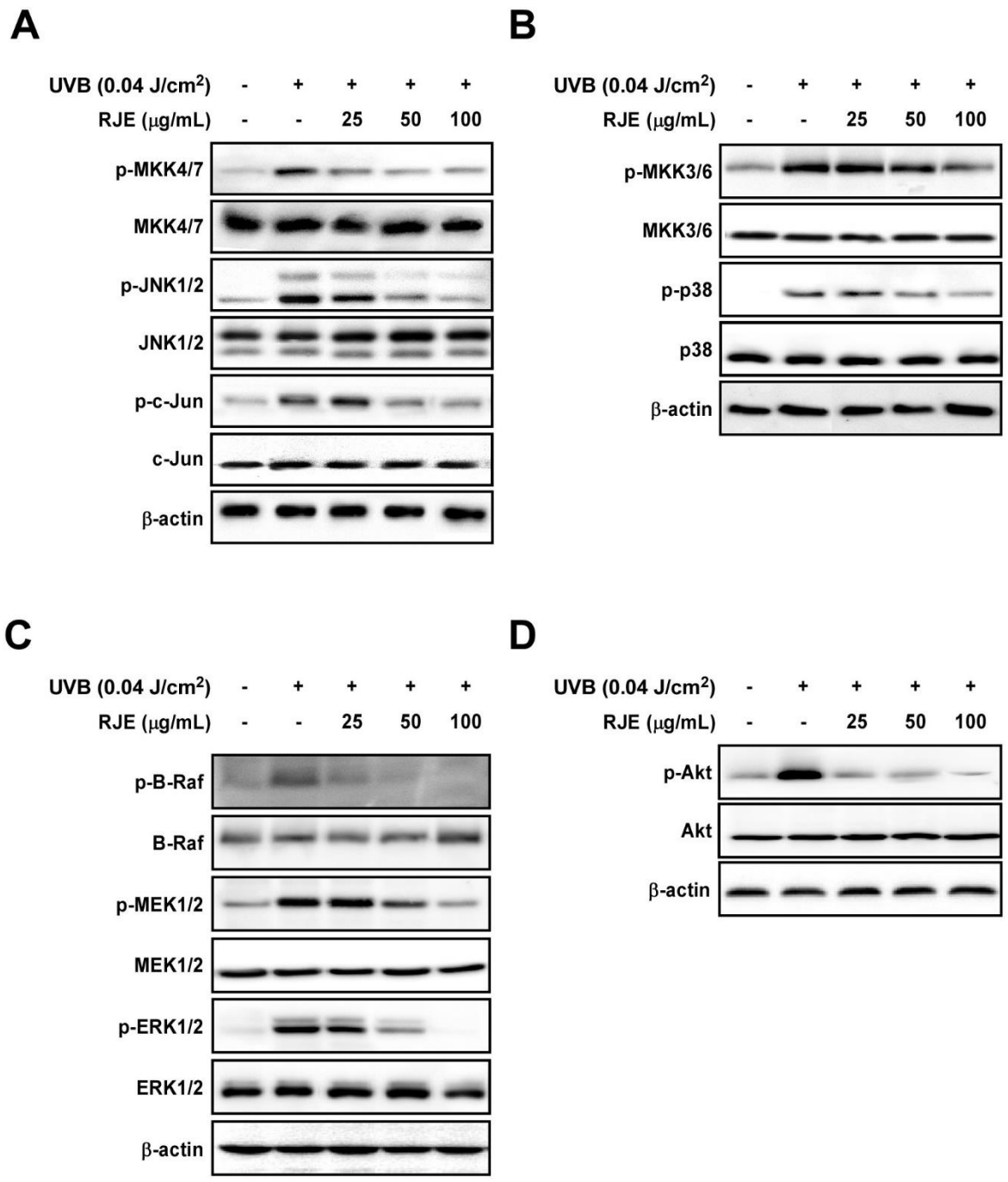
A
UVB (0.04 J/cm2) - + + + +
RJE (μg/mL) - - 25 50 100
p-MKK4/7
MKK4/7
p-JNK1/2
JNK1/2
p-c-Jun
c-Jun
β-actin
B
UVB (0.04 J/cm2) - + + + +
RJE (μg/mL) - - 25 50 100
p-MKK3/6
MKK3/6
p-p38
p38
β-actin
C
UVB (0.04 J/cm2) - + + + +
RJE (μg/mL) - - 25 50 100
p-B-Raf
B-Raf
p-MEK1/2
MEK1/2
p-ERK1/2
ERK1/2
β-actin
D
UVB (0.04 J/cm2) - + + + +
RJE (μg/mL) - - 25 50 100
p-Akt
Akt
β-actin

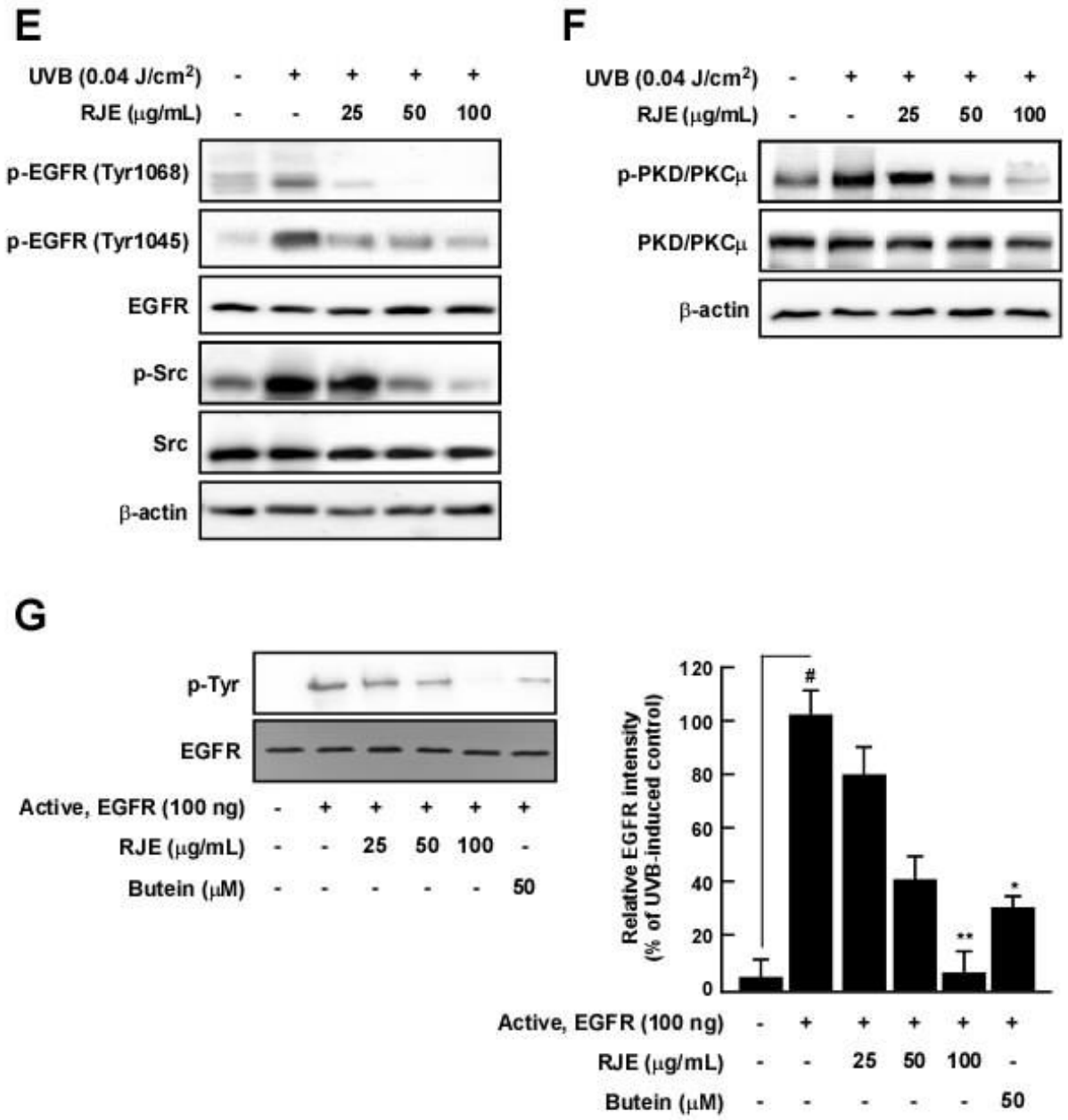

Figure II-2. Effect of RJE on UVB-induced phosphorylation of MAPKs, MAPKKs, Akt, EGFR, Src and PKD/PKCμ in HaCaT cells. (A) RJE inhibits UVB-induced phosphorylation of MKK4/7, JNK1/2, and c-Jun in HaCaT cells. (B) RJE inhibits UVB-induced phosphorylation of MKK3/6 and p38 in HaCaT cells. (C) RJE inhibits UVB-induced phosphorylation of MEK1/2 and ERK1/2 in HaCaT cells. (D) RJE inhibits UVB-induced

phosphorylation of Akt in HaCaT cells. (E) EGFR and Src, and (F) PKD/PKCμ in HaCaT cells. (G) RJE inhibits EGFR activity. Phosphorylation and expression were detected by Western blotting assay with specific antibodies. Data are presented as the mean ± SD of three independent experiments.

II-3-3. RJE inhibits UVB-induced wrinkle formation and COX-2 and MMP-13 expression in the SKH-1 hairless mouse

To further confirming the *in vivo* anti-inflammatory and -photoaging properties of RJE, I used a UVB and SKH-1 hairless mice model. Repetitive irradiation of the dorsal skin with UVB abnormally increased wrinkle formation in these mice (Figure II-3). Conversely, the oral administration of RJE significantly reduced UVB-induced wrinkle formation in comparison to the UVB control group (Figure II-3). Western blot assay results using mouse skin extract also showed that RJE significantly inhibited UVB-induced COX-2 and MMP-13 expression in this model (Figure II-4A). This immunohistochemical analyzes revealed showed that RJE inhibited UVB-induced COX-2 and MMP-13 expression (Figure II-4B).

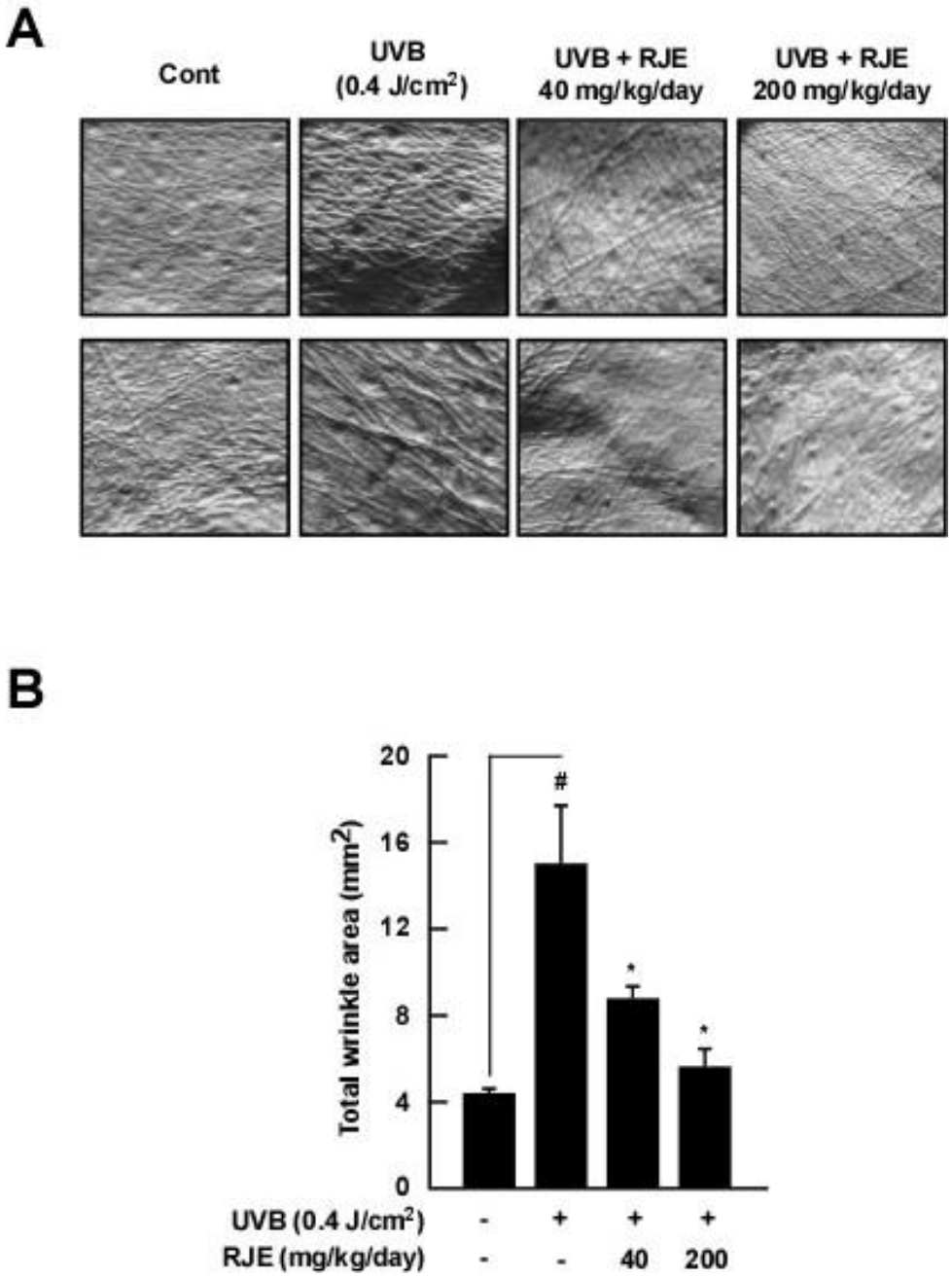

Figure II-3. Effect of RJE on UVB-induced wrinkle formation in SKH-1 hairless mice. (A) External appearance of wrinkles. (B) RJE significantly inhibits UVB-induced wrinkle formation in SKH-1 hairless mice. The dorsal skin surface of the animals was exposed to UVB irradiation three times per week for 13 weeks. Prior to sacrifice, skin replica samples of the dorsal areas were taken. Wrinkle values were obtained based on skin replica analysis. Data are presented as the mean ± SD of five mice in each group.

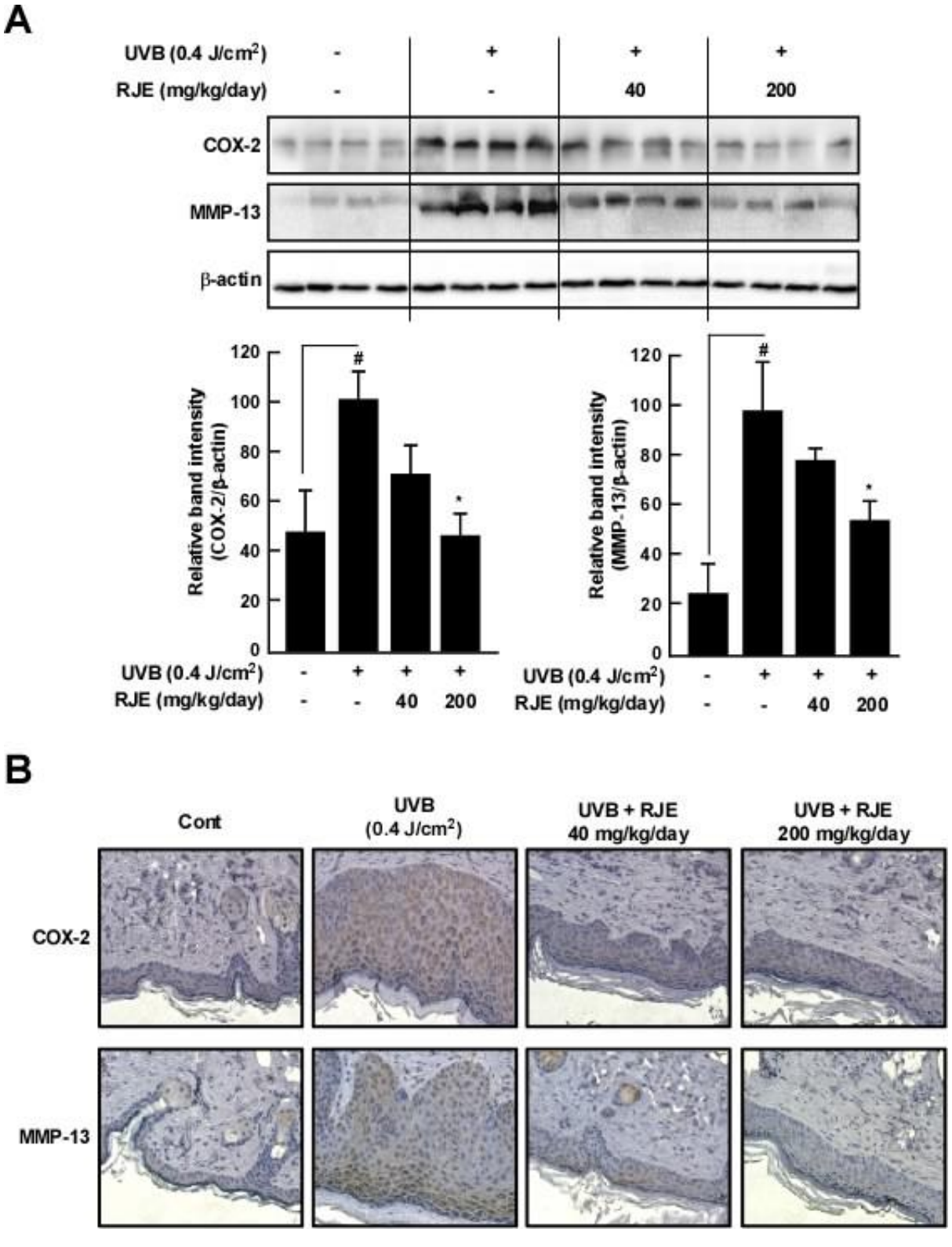

Figure II-4. Effect of RJE on UVB-induced COX-2 and MMP-13 expression in SKH-1 hairless mice. (A) RJE inhibits UVB-induced COX-2 and MMP-13 expression in SKH-1 hairless mice. Expression levels of COX-2 and MMP-13 were determined by Western blot

assay with specific antibodies. Each band was densitometrically quantified by image analysis. Results are shown as the means SEM (n = 5). The hash symbol (#) indicates a significant difference ($p < 0.05$) between the control group and the group exposed to UVB alone; asterisks (*) indicate a significant difference ($p < 0.05$) between groups irradiated with UVB and RJE and the group exposed to UVB alone. (B) Immunohistochemical staining for COX-2 and MMP-13 expression in the skin. COX-2 and MMP-13 are stained brown. Representative photographs of overall immunohistochemical staining patterns from each group are shown.

II-3-4. Identification and quantification of phenolic compounds by LC-MS/MS and effect of RJE compounds on UVB-induced MMP-1 promoter activity

I next investigated the presence of phenolic compounds in RJE. The major phenolic compounds were listed by comparison of their mass spectra with the standards (Figure II-5A, B, C, D and E). Gallic acid, 5-O-galloyly-β-D-glucose, methyl gallate, syringic acid and protocatechuic acid were identified as the major phenolic compounds in RJE. The concentrations present were calculated to be 3.30 ± 0.31, 8.78 ± 0.10, 1.55 ± 0.10, 0.04 ± 0.01 and 0.05 ± 0.02 μg/g of gallic acid, 5-O-galloyly-β-D-glucose, methyl gallate, syringic acid, and protocatechuic acid, respectively (Table II-1). MMP-1 promoter assay results showed that among the identified compounds in RJE, syringic acid had strongest inhibitory effect on UVB-induced MMP-1 promoter activity (Figure II-5F).

Table II-1. Levels of 5 major phenolic compounds identified in RJE

Compound	RT (min) [a]	Content (μg/g) [b]	MRM Transition (*m/z*) [c]
Gallic acid	2.85	3.30±0.31	169 → 125
5-O-galloyl-β-D-glucose	3.73	8.78±0.10	939 → 769
Methyl gallate	3.54	1.55±0.10	183.1 → 124
Syringic acid	3.77	0.04±0.01	197 → 182
Protocatechuic acid	3.27	0.05±0.02	153 → 109

[a] Retention time; [b] Contents based on the dry weight (n = 3); [c] Multiple reaction monitoring.

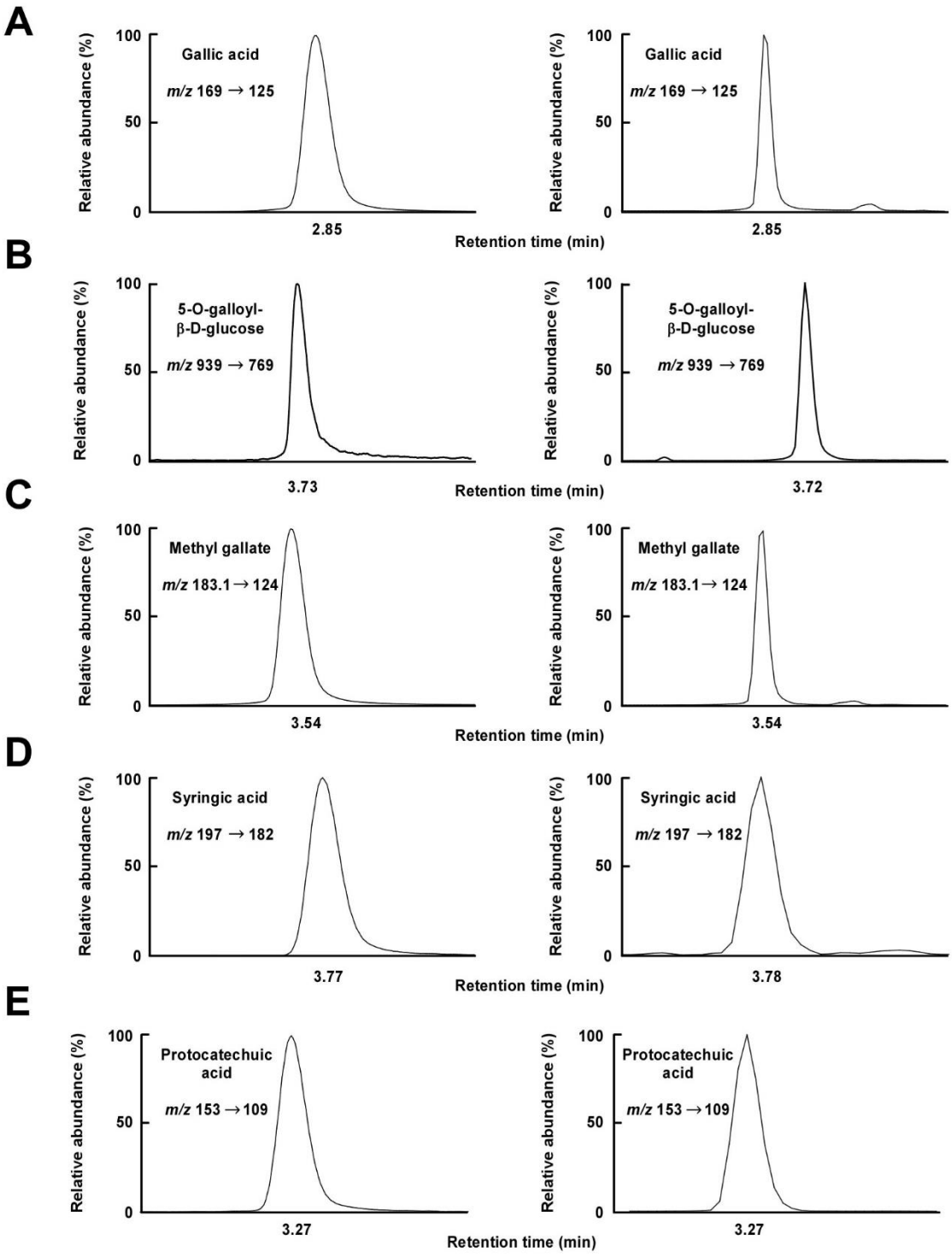
A
Gallic acid
m/z 169 → 125
Relative abundance (%)
100
50
0
2.85
Gallic acid
m/z 169 → 125
2.85
Retention time (min)
B
5-O-galloyl-
β-D-glucose
m/z 939 → 769
3.73
5-O-galloyl-
β-D-glucose
m/z 939 → 769
3.72
Retention time (min)
C
Methyl gallate
m/z 183.1→ 124
3.54
Methyl gallate
m/z 183.1→ 124
3.54
Retention time (min)
D
Syringic acid
m/z 197 → 182
3.77
Syringic acid
m/z 197 → 182
3.78
Retention time (min)
E
Protocatechuic
acid
m/z 153 →109
3.27
Protocatechuic
acid
m/z 153 →109
3.27
Retention time (min)

F

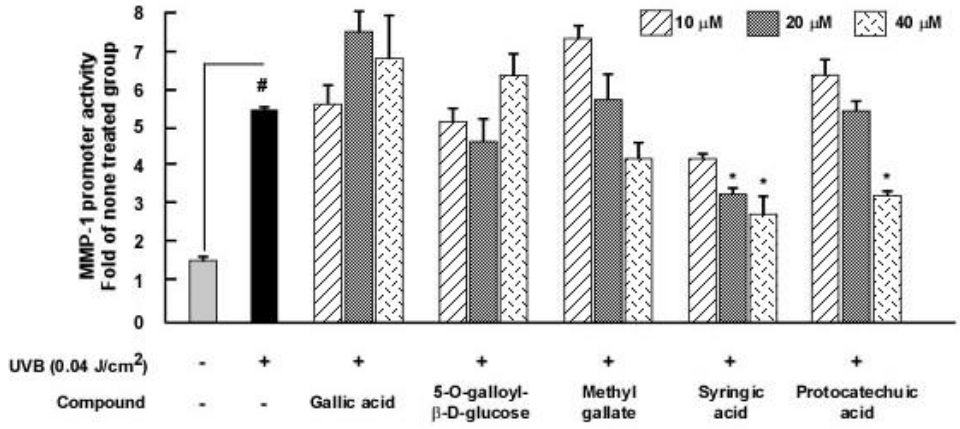

Figure II-5. LC-MS/MS chromatograms of (A) gallic acid, (B) 5-O-galloyl-β-D-glucose, (C) methyl gallate, (D) syringic acid and (E) protocatechuic acid in 50 mg/L standard solution (left) and RJE (right). (F) Effect of RJE compounds on UVB-induced MMP-1 promoter activity. For the luciferase assay, HaCaT cells were stably transfected with an MMP-1-luciferase reporter plasmid and cultured as described in the Materials and Methods. MMP-1 luciferase activity is presented as the mean ± SD of three independent experiments.

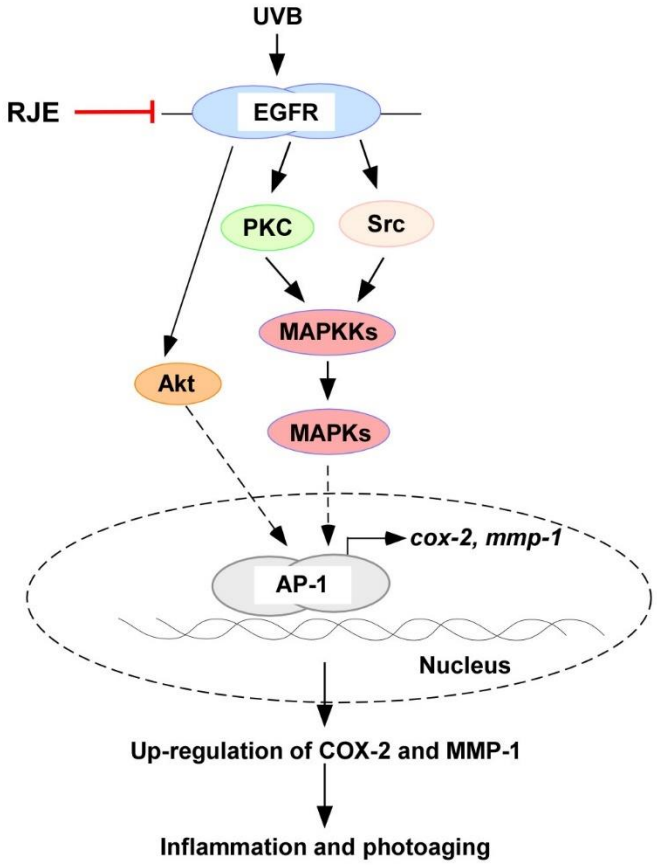

Figure II-6. Mechanism of *Rhus javanica* extract on UVB-induced skin inflammation and photoaging.

II-4. Discussion

Of the UV wavelengths generated by the Sun: UVC (200-280 nm) is blocked by stratospheric ozone, while UVB (280-320 nm) and UVA (320-400 nm) penetrate through to the surface of the earth and can cause DNA damage, erythema, sunburn, photoaging, and skin cancer (Melnikova & Ananthaswamy, 2005). The cosmetics and healthcare industries have invested significantly in the development of effective anti-inflammatory and -photoaging agents. However, currently available therapies and agents for the treatment of UV-induced skin damage remain inadequate. All-trans retinoic acid, an FDA approved drug, is widely used for the treatment of skin diseases including acne vulgaris and keratosis pilaris and has denemostrated benefits for skin inflammation and photoaging (Griffiths & Voorhees, 1993). However, unintended side effects remain a significant issue for this agent.

In order to develop effective anti-inflammatory and -photoaging agents, I created immortalized human keratinocyte HaCaT cells containing an MMP-1 promoter plasmid (M. K. Kim, Shin, Eun, & Chung, 2009). Because the transcription of MMP-1 is primarily regulated by AP-1 activity, and COX-2 is a major target gene of AP-1, I concluded that this construct could be used to evaluate *cox-2* gene expression. I thus established optimal conditions for induction with various UV exposure conditions and incubation times following UV exposure (data not shown) and screened hundreds of botanical extracts of interest. After further examination of cell cytotoxicity and dose dependency, I identified RJE as the most effective anti-inflammatory and anti-photoaging agent tested. Although several studies have reported that the gall of *Rhus javanica* exerts biological effects including histamine and inflammatory cytokine secretion (S. H. Kim et al., 2005) and tyrosinase activity (Kubo et al., 2003), the protective effect of RJE against UV damage and the mechanism of action

responsible has not previously been investigated. I therefore examined whether RJE affects UV-induced AP-1 activity, as well as and COX-2 and MMP-1 expression in the immortalized human keratinocyte HaCaT cells. An MMP-1 promoter assay and Western blot assay of COX-2 and MMP-1 expression clearly showed that RJE strongly suppresses UVB-induced COX-2 and MMP-1 expression by suppressing AP-1 activity.

MAPKs mediate a wide range of intracellular signaling molecules that are involved in skin inflammation and photoaging (Bode & Dong, 2003) and play a critical roles in the regulation of AP-1 activity (Eferl & Wagner, 2003). I observed that RJE suppressed UVB-induced MAPKKs/MAPKs and Akt phosphorylation. Based on these results, I sought to identify which signaling molecule was modulated by RJE to regulate the MAPKs signaling pathway. Previous studies have reported that c-Src regulates EGFR/Akt and MAPKs, consequently upregulating COX-2 expression in brain microvascular endothelial cells (Hsieh, Lin, Chan, & Yang, 2012). Another study reported that EGFR regulates Src activity by recruiting pyk (Schauwienold, Sastre, Genzel, Schaefer, & Reusch, 2008). My observations revealed that RJE strongly suppresses EGFR, Src, and PKC phosphorylation. Based on the accumulated evidence, I hypothesized that RJE may affect EGFR activity. Using a kinase assay, I found that RJE completely blocked EGFR phosphorylation, with butein used as positive control (Jung, Lee, et al., 2015).

Clinical observations and epidemiologic data strongly suggest that wrinkle formation is a hall mark of photoaging in response to UV exposure (Fisher, 2005; Fisher et al., 1996; Fisher et al., 1997; Griffiths & Voorhees, 1993). I further confirmed that oral administration of RJE suppresses chronic UV-irradiation induced wrinkle formation in the skin of SKH-1 hairless mice. As expected, RJE prevented chronic UV-induced up-regulation of COX-2 and MMP-13 expression in the mouse skin. MMP-1 is substituted by mouse interstitial

collagenase MMP-13, a close structural homologue of human MMP-13 (collagenase-3) in mice skin. The tissue specific expression pattern of mouse MMP-13 indicates functional homology between mouse MMP-13 and both human MMP-1 and MMP-13 (Toriseva et al., 2012; Vaalamo et al., 1997).

A verification of the chemical constituents present in RJE, showed the presence of gallic acid, 5-O-galloyly-β-D-glucose, methyl gallate, syringic acid, and protocatechuic acid. Although the constituent profile was dependents on the property of solvent used, 5-O-galloyly-β-D-glucose and gallic acid were the major components. To verify which compound exhibited the most potential anti-inflammatory and –photoaging effects, I compared their effects on MMP-1 promoter activity in HaCaT cells. Interestingly, syringic acid exhibited the strongest inhibitory effect on MMP-1 promoter activity.

II-5. Conclusions

Taken together, the results show that RJE significantly inhibits UVB-induced wrinkle and COX-2 and MMP-1 expression *in vivo*. This inhibition occurs primarily via the targeting of EGFR activity, leading to the suppression of COX-2 and MMP-1 expression via reduced MAPK and AP-1 activity. Of the phenolic acids present, syringic acid is likely to be the most active compound in RJE. This represents the first report elucidating the anti-inflammatory and –photoaging factors present in RJE and sheds light on the mechanisms of action responsible.

II-6. References

Ahn, Y.-J., Lee, H.-S., Oh, H.-S., Kim, H.-T., & Lee, Y.-H. (2005). Antifungal activity and mode of action of Galla rhois-derived phenolics against phytopathogenic fungi. *Pesticide Biochemistry and Physiology, 81*(2), 105-112.

Almutawa, F., Thalib, L., Hekman, D., Sun, Q., Hamzavi, I., & Lim, H. W. (2015). Efficacy of localized phototherapy and photodynamic therapy for psoriasis: a systematic review and meta-analysis. *Photodermatology, Photoimmunology & Photomedicine, 31*(1), 5-14.

Bansal, S., Sahoo, B., & Garg, V. (2013). Psoralen–narrowband UVB phototherapy for the treatment of vitiligo in comparison to narrowband UVB alone. *Photodermatology, Photoimmunology & Photomedicine, 29*(6), 311-317.

Bermudez, Y., Stratton, S. P., Curiel-Lewandrowski, C., Warneke, J., Hu, C., Bowden, G. T., Dickinson, S. E., Dong, Z., Bode, A. M., & Saboda, K. (2015). Activation of the PI3K/Akt/mTOR and MAPK signaling pathways in response to acute solar-simulated light exposure of human skin. *Cancer Prevention Research, 8*(8), 720-728.

Bode, A. M., & Dong, Z. (2003). Mitogen-activated protein kinase activation in UV-induced signal transduction. *Science Signaling, 2003*(167), re2-re2.

Bulla, M. K., Hernandes, L., Baesso, M. L., Nogueira, A. C., Bento, A. C., Bortoluzzi, B. B., Serra, L. Z., & Cortez, D. A. (2015). Evaluation of photoprotective potential and percutaneous penetration by photoacoustic spectroscopy of the Schinus terebinthifolius Raddi extract. *Photochemistry and Photobiology, 91*(3), 558-566.

Choi, J.-G., Kang, O.-H., Lee, Y.-S., Oh, Y.-C., Chae, H.-S., Jang, H.-J., Shin, D.-W., & Kwon, D.-Y. (2009). Antibacterial activity of methyl gallate isolated from Galla Rhois

or carvacrol combined with nalidixic acid against nalidixic acid resistant bacteria. *Molecules, 14*(5), 1773-1780.

Eferl, R., & Wagner, E. F. (2003). AP-1: a double-edged sword in tumorigenesis. *Nature Reviews Cancer, 3*(11), 859-868.

Fett, N. (2013). Scleroderma: nomenclature, etiology, pathogenesis, prognosis, and treatments: facts and controversies. *Clinics in Dermatology, 31*(4), 432-437.

Fischer, S. M., Pavone, A., Mikulec, C., Langenbach, R., & Rundhaug, J. E. (2007). Cyclooxygenase-2 expression is critical for chronic UV-induced murine skin carcinogenesis. *Molecular Carcinogenesis: Published in cooperation with the University of Texas MD Anderson Cancer Center, 46*(5), 363-371.

Fisher, G. J. (2005). The pathophysiology of photoaging of the skin. *Cutis, 75*(2 Suppl), 5-8; discussion 8.

Fisher, G. J., Datta, S. C., Talwar, H. S., Wang, Z.-Q., Varani, J., Kang, S., & Voorhees, J. J. (1996). Molecular basis of sun-induced premature skin ageing and retinoid antagonism. *Nature, 379*(6563), 335-339.

Fisher, G. J., Wang, Z., Datta, S. C., Varani, J., Kang, S., & Voorhees, J. J. (1997). Pathophysiology of premature skin aging induced by ultraviolet light. *New England Journal of Medicine, 337*(20), 1419-1429.

Goswami, S., & Haldar, C. (2014). Melatonin improves ultraviolet B-induced oxidative damage and inflammatory conditions in cutaneous tissue of a diurnal I ndian palm squirrel F unambulus pennanti. *British Journal of Dermatology, 171*(5), 1147-1155.

Griffiths, C. E., & Voorhees, J. J. (1993). Topical retinoic acid for photoaging: clinical response and underlying mechanisms. *Skin Pharmacology and Physiology, 6*(Suppl. 1), 70-77.

Hsieh, H.-L., Lin, C.-C., Chan, H.-J., Yang, C. M., & Yang, C.-M. (2012). c-Src-dependent

EGF receptor transactivation contributes to ET-1-induced COX-2 expression in brain microvascular endothelial cells. *Journal of Neuroinflammation, 9*(1), 1-15.

Jung, S. K., Ha, S. J., Kim, Y. A., Lee, J., Lim, T. G., Kim, Y. T., Lee, N. H., Park, J. S., Yeom, M. H., & Lee, H. J. (2015). MLK 3 is a novel target of dehydroglyasperin D for the reduction in UVB-induced COX-2 expression in vitro and in vivo. *Journal of Cellular and Molecular Medicine, 19*(1), 135-142.

Jung, S. K., Ha, S. J., Kim, Y. A., Lee, J., Lim, T. G., Kim, Y. T., Lee, N. H., Park, J. S., Yeom, M. H., & Lee, H. J. (2008). Myricetin suppresses UVB-induced skin cancer by targeting Fyn. *Cancer Research, 68*(14), 6021-6029.

Jung, S. K., Lee, M. H., Lim, D. Y., Lee, S. Y., Jeong, C. H., Kim, J. E., Lim, T. G., Chen, H., Bode, A. M., & Lee, H. J. (2015). Butein, a novel dual inhibitor of MET and EGFR, overcomes gefitinib-resistant lung cancer growth. *Molecular Carcinogenesis, 54*(4), 322-331.

Kim, M.-K., Shin, J.-M., Eun, H. C., & Chung, J. H. (2009). The role of p300 histone acetyltransferase in UV-induced histone modifications and MMP-1 gene transcription. *PloS one, 4*(3), e4864.

Kim, S.-H., Park, H.-H., Lee, S., Jun, C.-D., Choi, B.-J., Kim, S.-Y., Kim, S.-H., Kim, D.-K., Park, J.-S., & Chae, B.-S. (2005). The anti-anaphylactic effect of the gall of Rhus javanica is mediated through inhibition of histamine release and inflammatory cytokine secretion. *International Immunopharmacology, 5*(13-14), 1820-1829.

Korać, R. R., & Khambholja, K. M. (2011). Potential of herbs in skin protection from ultraviolet radiation. *Pharmacognosy Reviews, 5*(10), 164.

Kubo, I., Kinst-Hori, I., Nihei, K.-I., Soria, F., Takasaki, M., Calderón, J. S., & Céspedes, C. L. (2003). Tyrosinase inhibitors from galls of Rhus javanica leaves and their effects on insects. *Zeitschrift für Naturforschung C, 58*(9-10), 719-725.

Lee, K., Kim, J., Lee, B.-j., Park, J.-W., Leem, K.-H., & Bu, Y. (2012). Protective effects of Galla Rhois, the excrescence produced by the sumac aphid, Schlechtendalia chinensis, on transient focal cerebral ischemia in the rat. *Journal of Insect Science, 12*(1).

Melnikova, V. O., & Ananthaswamy, H. N. (2005). Cellular and molecular events leading to the development of skin cancer. *Mutation Research/Fundamental and Molecular Mechanisms of Mutagenesis, 571*(1-2), 91-106.

Oh, J. E., Kim, M. S., Jeon, W.-K., Seo, Y. K., Kim, B.-C., Hahn, J. H., & Park, C. S. (2014). A nuclear factor kappa B-derived inhibitor tripeptide inhibits UVB-induced photoaging process. *Journal of Dermatological Science, 76*(3), 196-205.

Peharda, V., Gruber, F., Kaštelan, M., Prpić Massari, L., Saftić, M., Čabrijan, L., & Zamolo, G. (2007). Occupational skin diseases caused by solar radiation. *Collegium Antropologicum, 31*(1), 87-90.

Quan, T., Qin, Z., Xu, Y., He, T., Kang, S., Voorhees, J. J., & Fisher, G. J. (2010). Ultraviolet irradiation induces CYR61/CCN1, a mediator of collagen homeostasis, through activation of transcription factor AP-1 in human skin fibroblasts. *Journal of Investigative Dermatology, 130*(6), 1697-1706.

Roberts, P. J., & Der, C. J. (2007). Targeting the Raf-MEK-ERK mitogen-activated protein kinase cascade for the treatment of cancer. *Oncogene, 26*(22), 3291-3310.

Schauwienold, D., Sastre, A. P., Genzel, N., Schaefer, M., & Reusch, H. P. (2008). The transactivated epidermal growth factor receptor recruits Pyk2 to regulate Src kinase activity. *Journal of Biological Chemistry, 283*(41), 27748-27756.

Wölfle, U., Heinemann, A., Esser, P. R., Haarhaus, B., Martin, S. F., & Schempp, C. M. (2012). Luteolin prevents solar radiation-induced matrix metalloproteinase-1 activation in human fibroblasts: a role for p38 mitogen-activated protein kinase and interleukin-20 released from keratinocytes. *Rejuvenation Research, 15*(5), 466-475.

Chapter III.

Preventive Effect of *Curcuma zedoaria* Extract on UVB-induced Skin Inflammation and Photoaging

Abstract

I sought to investigate whether *Curcuma zedoaria* extract (CZE) has preventive effects against UVB-induced skin inflammation and photoaging. CZE was identified as a promising anti-inflammatory and photoaging candidate based on a matrix metalloproteinase (MMP)-1 promoter assay and the suppressive effects of CZE on UVB-induced cyclooxygenases (COX)-2 and MMP-13 expression were confirmed in immortalized skin human keratinocytes. CZE suppressed UVB-induced phosphorylation of c-Jun N-terminal kinases, mitogen-activated protein kinase kinases 3/6/p38, B-Raf/ERK kinase (MEK)1/2/extracellular signal-regulated kinases (ERK)1/2, and Akt as well as phosphorylation of epidermal growth factor receptor (EGFR) and Src. Using a chronic skin inflammation and photoaging model, I observed that CZE significantly suppressed repetitive UVB-induced wrinkle formation and COX-2 and MMP-13 expression *in vivo*. Among the compounds investigated, curcumin was found to exhibit the strongest inhibitory effect on UVB-induced MMP-1 promoter activity. These results demonstrate that CZE has a potent preventive activity for UVB-induced skin inflammation and photoaging, which occurs via the suppression of EGFR, Src, MAPKKs/MAPKs, and Akt phosphorylation.

III-1. Introduction

Our skin is the primary barrier that regulates homeostasis and protects our body from environmental damage. The most important environmental factor that causes inflammation of the skin and accelerated aging is UV radiation present within sunlight (Fisher, Kang, Varani, & et al., 2002). Chronic UV radiation can generate DNA damage, leading to genetic mutations and skin cancer (Reuter, Gupta, Chaturvedi, & Aggarwal, 2010). Of the UV wavelengths present in the electromagnetic spectrum (UVA; 320-400 nm, UVB; 280-320 nm, UVC; 100-280 nm), UVB is the major cause of skin reddening and sunburn and is considered a complete carcinogen because UVB treatment alone can induce skin cancer (Jung et al., 2008). The expression of several genes important for the maintenance of healthy skin is highly correlated with levels of inflammation and photoaging (Quigley et al., 2009). COX-2 and matrix metalloproteinases including MMP-1 and -13 are representative enzymes that mediate skin inflammation and photoaging, respectively, as a result of exposure to UV irradiation. COX-2 is an inducible protein and its expression is highly elevated in various types of cells when exposed to inflammatory cytokines, mitogenic factors, and tumor promoters (Hla, Ristimäki, Appleby, & Barriocanal, 1993). Multiple lines of evidence suggest that genetic depletion of COX-2 decreases skin inflammation and cancer in response to UV irradiation (Seibert & Masferrer, 1993). The collagenases including MMP-1 and MMP-13, can also be induced by UV, and degrade collagen, resulting in collagen deficiency and wrinkling of the dermis (J. Y. Seo et al., 2003).

UV irradiation of human skin results in the simultaneous activation of multiple receptor-coupled signal transduction pathways (Buckman et al., 1998; Fisher, 2005). EGFR is a multifunctional growth factor receptor that regulates a variety of fundamental cell

properties including growth, differentiation, invasion and apoptosis in numerous cell types (LaMarca et al., 2008). Activation of the PI3K/Akt and the MAPK1/2 pathways has also been linked to activation of members of the EGFR family, either by direct interaction with the activated receptor or via adaptor molecules (Huang, Zhang, Ding, & Chen, 2009). Similarly, activation of the MAPK and Akt pathways is linked with activation of the EGFR family (Singh, Schneider, Knyazev, & Ullrich, 2009).

Botanical extracts have long been used as a source of traditional medicine for thousands of years. *Curcuma zedoaria* has been popular for cultivation as a vegetable, spice, traditional medicine, and perfume in Western and Asian countries (W. G. Seo et al., 2005). Additionally, *C. zedoaria* exerts multiple biological functions including soothing effects for ulcers, wounds, tumor, skin ailments, and inflammation (Morikawa, Matsuda, Ninomiya, & Yoshikawa, 2002). A previous study reported that a number of volatile and essential oils including terpenoids, flavonoids, and sesquiterpenes have anti-inflammatory properties (Lai et al., 2004). Curdione isolated from CZE has been found to inhibit prostaglandin E_2 production and cyclooxygenase-2 expression, both of which are implicated in the inflammatory and carcinogenic processes (Oh, Min, & Lee, 2007). However, the inhibitory effect of *C. zedoaria* on UVB-induced skin inflammation and photoaging and its impact on the signaling network remains unclear.

I screened several botanical extracts of interest and identified CZE as the most potent anti-inflammatory and anti-photoaging material. In the present study, I sought to investigate the inhibitory effects of CZE on UVB-induced inflammation and photoaging and observed that CZE inhibits UVB-induced COX-2 and MMP-1 expression via suppression of the EGFR, Src, and Akt and MAPKKs/MAPKs/AP-1 pathways. Experiments using the SKH-1 hairless mouse model revealed that topical application of CZE significantly suppresses UVB-induced wrinkle formation, as well as COX-2 and MMP-13 expression in mouse skin. Among the

CZE compounds, curcumin showed the strongest inhibitory effect on UVB-induced MMP-1 promoter activity.

III-2. Materials and Methods

III-2-1. Materials

Chemical reagents were purchased from Sigma–Aldrich (St Louis, MO, USA). Dulbecco's Modified Eagle's Medium (DMEM), gentamicin, L-glutamine, penicillin–streptomycin, and fetal bovine serum (FBS) were obtained from Thermo Scientific HyClone (Logan, UT, USA). The antibodies against c-Jun, MMP-1, MMP-13, and β-actin were purchased from Santa Cruz Biotech (Santa Cruz, CA, USA). The antibodies against COX-2, p44/42 MAP Kinase, SAPK/JNK, p38 MAPK, phospho-p44/42 MAPK (Erk 1/2) (Thr202/Tyr204), phospho-SAPK/JNK (Thr183/Tyr185), MKK3b, phospho-MKK3 (Ser189)/MKK6 (Ser 207), SEK1/MKK4, phospho-SEK1/MKK4 (Ser257/Thr261), MEK1/2, phospho-MEK1/2 (Ser217/221), phospho-c-Jun (Ser73), Akt, phospho-Akt (Thr308), Src, and phospho-Src (Tyr527) were purchased from Cell Signaling Biotechnology (Beverly, MA, USA). The antibody against phosphorylated p38 MAPK (pT180/pY182) was purchased from BD Biosciences (Franklin Lakes, NJ, USA).

III-2-2. Sample preparation and extraction procedure

Curcuma zedoaria specimens were purchased from Kyungdong Market (Seoul, Korea). The specimen was deposited in the Plant Resources and Environment Department, Cheju National University, Korea and identified by a botanist, Dr. Ji-Hun Kim (Department of Plant Resources and Environment, Cheju National University). The samples were ground with a blender (Wonder Blender, OSAKA CHEMICAL Co., Osaka, Japan) to obtain a fine powder. Powdered materials were stored in plastic bags at room temperature for use in the

extraction experiments. Dried powder (100 g) was extracted with an Ultrasonic Processor VCX 750 (Sonics & Materials, Inc., Newtown, USA) with 1,000 mL of 95% ethanol, and incubated at room temperature for 24 h (Table II-1). After precipitate removal, the extracts were concentrated to 100 mL with an IKA RV 10 Rotary Evaporator (IKA® Works, Guangzhou, China), then freeze-dried.

Table III-1. Conditions of ultrasonic treatment

Ultrasonic treatment	Conditions
Power output	750 W
Frequency	20 kHz
Pulse on/off	20/20 s
Time	24 h
Temperature	Room temperature

III-2-3. Cell culture, UVB exposure, and viability assay

Human epidermal keratinocyte HaCaT and 293T cells were maintained in DMEM containing 10% FBS, 100 units/mL of penicillin and 100 mg/mL of streptomycin at 37℃ in a 5% CO_2 humidified incubator. UVB irradiation was conducted using a bank of four Westinghouse F520 lamps (National Biological, Twinsburg, OH) at 6 J/s/m light in the UVB range. Approximately 10% of the additional radiation from the F520 lamp is in the UVA spectrum (320 nm). A UVB exposure chamber was fitted with a Kodak Kodacel K6808 filter to eliminate all wavelengths below 290 nm. UVB radiation was measured using a UVX radiometer (UVX-31). To assess cell viability, HaCaT cells were seeded (1×10^3 cells/well) in 96-well plates and incubated at 37℃ in a 5% CO_2 incubator. After the cells were treated with CZE, 20 μL of MTS reagent (Promega, Madison, WI, USA) was added to each well. After 1 h of incubation, absorbance levels for formazan at 490 and 690 nm were measured using a microplate reader (Bio-Rad Inc., Hercules, CA, USA).

III-2-4. Animal experiments

Six-week-old male SKH-1 hairless mice, weighing approximately 20–22 g, were purchased from OrientBio Inc. (Gyeonggi-do, Korea). The mice were housed in an air-conditioned room (23 ± 2℃) with a 12 h light/dark cycle. They were allowed free access to food and tap water. All animals received humane care, and the study protocol (KFRI-M-14013) was approved and performed in accordance with guidelines for animal use and care at Korea Food Research Institute. Twenty mice were randomly allocated to each group (five mice per group, four groups in total): (i) control group (normal), (ii) UVB-irradiated group (UVB), (iii) UVB-irradiated and 20 mg/kg/day CZE-treated group and (iv) UVB-irradiated and 100 mg/kg/day CZE-treated group. The mice were topically treated with 200 μL acetone

before UVB exposure 3 day/week for 13 weeks. UVB irradiation doses were increased each week by 1 MED (1 MED = 100 mJ/cm^2) to 4 MED and then maintained at 4 MED until 13 weeks had passed.

III-2-5. MMP-1 promoter assay

To evaluate the MMP-1 promoter activity elicited by various botanical extracts, I constructed a pGreenFire (pGF1) vector containing an MMP-1 promoter plasmid (Kim, Shin, Eun, & Chung, 2009). For stable expression of pGF1 with the MMP-1 promoter, 293T cells were transfected with the pGF1 plasmid using Lipofectamine (ThermoFisher Scientific, MA, USA), following the manufacturer's instructions. The transfection medium was changed at 4 h after transfection, and the cells were then cultured for 36 h. Virus particles were harvested by filtration using a 0.45 mm syringe filter, then combined with 8 mg/ml of polybrene (Millipore) and infected into HaCaT cells for 24 h. The cell culture media was replaced with fresh culture medium and the cells were further cultured for 24 h, prior to selection with puromycin (1 mg/mL) for 36 h. Selected HaCaT cells (8×10^3 cells/well) were seeded into 96-well plates, which were incubated at 37℃ in a 5% CO_2 incubator. When the cells reached 80–90% confluence, they were starved by culturing in serum-free DMEM for a further 24 h. Cells were then treated with CZE for 1 h prior to UVB (0.04 J/cm^2) exposure and then incubated for 5 h. Cells were disrupted with 100 μL of lysis buffer [0.1 M potassium phosphate buffer (pH 7.8), 1% Triton X-100, 1 mM dithiothreitol (DTT), and 2 mM EDTA], after which luciferase activity was measured using a luminometer (SpectraMax L, Molecular Devices, Sunnyvale, CA).

III-2-6. Western blot assay

For *in vitro* Western blot assays, cells (1.5×10^6 cells/mL) were cultured in 10 cm dishes for 24 h, followed by starvation in serum-free DMEM for 24 h. Cells were then treated with CZE for 1 h and irradiated with UVB (0.04 J/cm^2). After incubation, the cells were collected and washed twice with cold PBS, before lysis in Cell Lysis Buffer (Cell Signaling Biotechnology, Beverly, MA, USA) and maintained on ice for 30 min. The lysate protein was washed via centrifugation and the concentration determined using a DC Protein Assay kit (Bio-Rad Laboratories) following manufacturer's instructions. The lysate was subjected to 10% sodium dodecyl sulfate–polyacrylamide gel electrophoresis (SDS-PAGE) and transferred to a polyvinylidene difluoride (PVDF) membrane (Millipore, Immobilon® -P transfer membrane). After transferring, the membranes were incubated with the specific primary antibodies at 4℃ overnight. Protein bands were visualized using a chemiluminescence detection kit (ATTO, Tokyo, Japan) after hybridization with a horseradish peroxidase (HRP)-conjugated secondary antibody.

For *in vivo* Western blots, mouse skin tissue was added to 2 mL microcentrifuge tubes containing lysis buffer and stainless steel bead and subsequently homogenized twice for 2 min at 20 Hz in a TissueLyser II (Qiagen, Valencia, CA, USA). Skin lysates were centrifuged at 12,000 rpm for 20 min. After the protein content was determined, the skin tissue extract was subjected to 10% SDS-PAGE and transferred to a PVDF membrane. Membranes were processed, and proteins were analyzed as described above for *in vitro* Western blot assay.

III-2-7. Immunohistochemical analysis

Sections (5-μm thick) of 10% neutral formalin solution-fixed, paraffin-embedded skin tissue samples were cut on silane-coated glass slides. Deparaffinized sections were heated for 15 min in 10 mM citrate buffer (pH 6.0) in a microwave oven for antigen retrieval. For the detection of target proteins, slides were incubated with affinity-purified primary antibody in a refrigerator overnight in 1% BSA solution and then developed using the SignalStain® Boost IHC Detection Reagent (HPR, rabbit) antibodies (Cell Signaling Biotechnology). Peroxidase-binding sites were detected by staining with SignalStain® DAB Substrate Kit (Cell Signaling Biotechnology). Finally, counterstaining was performed using Harris hematoxylin solution (Sigma–Aldrich). MMP-13 and COX-2 expression were visualized using a fluorescent microscope (Nikon Eclipse Ti-S, Tokyo, Japan) and images were analyzed using Metamorph (Molecular Devices, Danville, PA) software.

III-2-8. Metabolite extraction

Metabolites were extracted using the Bligh-Dyer protocol. Powder sample was dissolved in methanol and vortexed for 30 sec followed sonication for 2 min. Cold chloroform was then added, followed by further vortexing for 30 sec. After sonication for 2 min, cold HPLC-graded water was added and vortexed for 30 sec resulting in a ratio of 1:2:0.72 (methanol:chloroform:water). The samples were centrifuged at 12,000 g for 10 min after incubation for 10 min at room temperature.

III-2-9. Chromatograph

Dried extracts were dissolved in mobile phase buffer and injected into UPLC-ESI-QQQ (Agilent Technologies, CA, USA) with Hypersil gold C18 (Thermo, 2.1 x 100 mm, 1.9

μm) or with ZORBAX-RRHD C18 (Agilent, 2.1 x 100 mm, 1.8 μm). The mobile phase buffers were Buffer A (100% H_2O, and 0.1% formic acid (v/v)) and Buffer B (90% acetonitrile, 10% H_2O, and 0.1% formic acid (v/v/v). The column was equilibrated and eluted according to gradient conditions with a flow rate of 0.2 mL/min at 40℃. The gradient was started at 5% B, changing to a linear gradient of 100% over 5 min, followed by washing time for 2 min, and re-equilibration at 5% B for 3 min.

III-2-10. Statistical analysis

Where appropriate, data are expressed as the means ± S.E.M. and significant differences were determined using one-way ANOVA (Analysis Of Variance). A probability value of $p < 0.05$ was used as the criterion for statistical significance.

III-3. Results

III-3-1. CZE inhibits UVB-induced MMP-1 promoter activity, as well as COX-2 and MMP-13 expression in HaCaT cells

UV-irradiation results in the upregulation of AP-1 activity and subsequently induces skin inflammation and photoaging by increasing *cox-2* and *mmp-1* gene expression, respectively (C. Kim, Ryu, & Kim, 2010; Kuo, Chen, Chu, Lin, & Chiang, 2015; Vincenti & Brinckerhoff, 2001). Using previously developed immortalized human keratinocyte HaCaT cells stably transfected with the MMP-1 promoter, I observed that CZE significantly inhibited UVB-induced MMP-1 promoter activity in a dose-dependent manner (Figure III-1A). The viability of HaCaT cells was slightly increased at 25 μg/mL and did not show signs of cytotoxicity at 50 and 100 μg/mL concentrations (Figure III-1B). Evaluation of the inhibitory effect of CZE on UVB-induced COX-2 and MMP-13 expression in immortalized human keratinocyte HaCaT cells showed that CZE significantly inhibited UVB-induced COX-2 and MMP-13 expression (Figure III-1C and D).

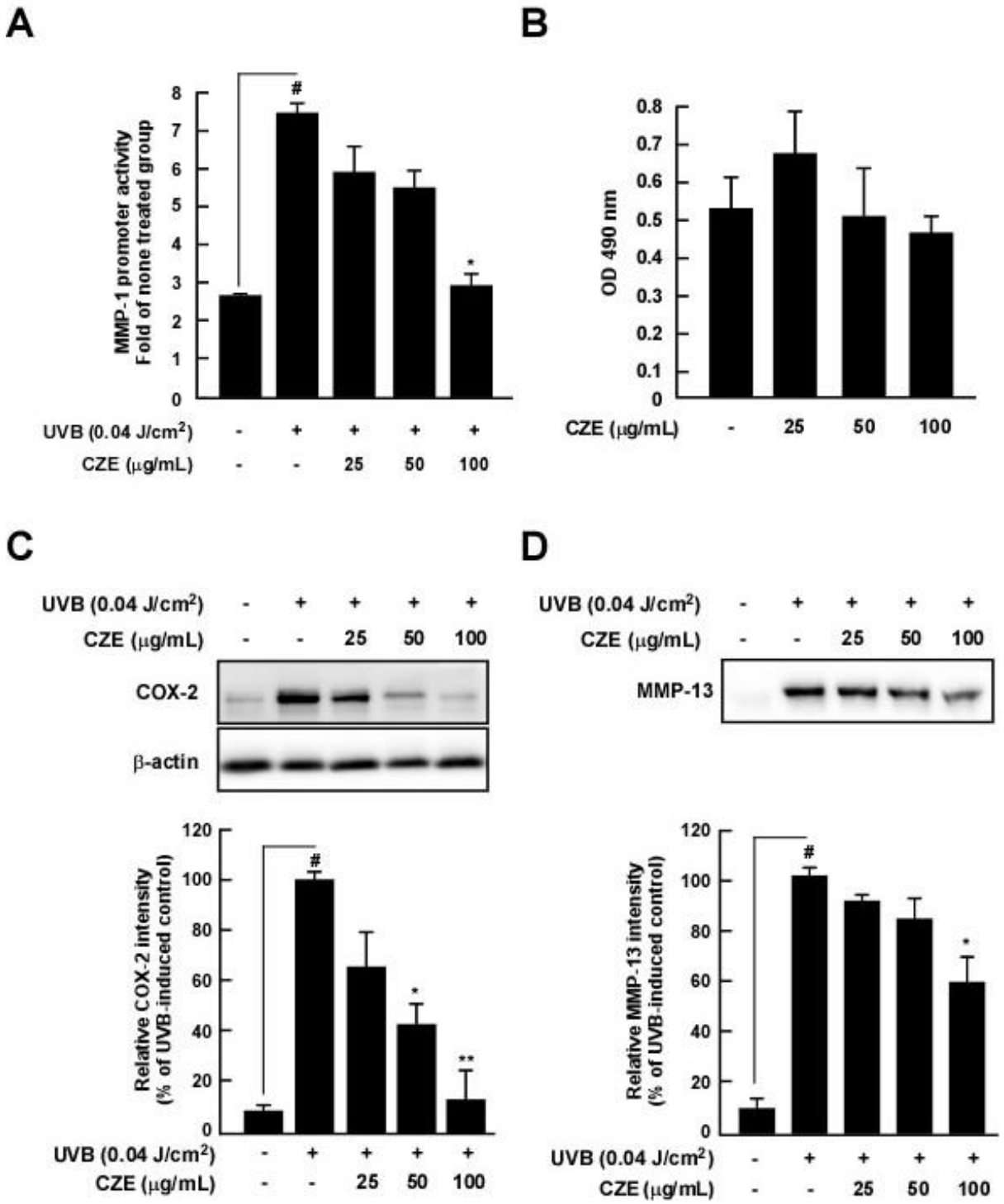

Figure III-1. Effects of CZE on UVB-induced MMP-1 promoter activity, cell viability, and COX-2 and MMP-13 expression in HaCaT cells. (A) CZE inhibits UVB-induced MMP-1 promoter activity in HaCaT cells. HaCaT cells were stably transfected with an MMP-1-luciferase plasmid in the presence or absence of stimulation with UVB (0.04 J/cm^2) for 1 h.

(B) CZE exhibits no detectable cell cytotoxicity up to 100 μg/mL in HaCaT cells. Cell viability was measured by MTS assay as described in the Materials and Methods. (C) CZE inhibits UVB-induced COX-2 expression in HaCaT cells. (D) CZE inhibits UVB-induced MMP-13 expression in HaCaT cells. Expression levels of COX-2, MMP-13, and β-actin were determined by Western blot assay. The data are represented as the mean ± SD of three independent experiments. Hash symbols (#) indicate a significant difference ($p < 0.05$) between the control group and the group exposed to UVB alone; asterisks (* and **) indicate significant differences [($p < 0.05$) and ($p < 0.01$), respectively] between groups irradiated with UVB and CZE and the group exposed to UVB alone.

III-3-2. CZE inhibits UVB-induced phosphorylation of MAPKK/MAPK, Akt, EGFR, and Src in HaCaT cells

Because the MAPK family plays an important role in regulating COX-2 and MMP expression (S. H. Kim et al., 2005), I next examined the effects of CZE on UVB-induced phosphorylation of MAPKs. The results showed that CZE inhibited UVB-induced phosphorylation of c-Jun N-terminal kinases (JNK1/2), mitogen-activated protein kinase kinases (MKK) 3/6/p38, and B-Raf/MEK1/2/ERK1/2 in HaCaT cells (Figure III-2A–C). Furthermore, treatment with CZE markedly decreased UVB-induced Akt phosphorylation (Figure III-2B). In contrast, CZE treatment had no impact on phosphorylation of MKK4/7. The activation of EGFR in response to either ligand or UV irradiation arises from increased phosphorylation of specific tyrosine residues in the cytoplasmic domain of EGFR (Xu, Shao, Zhou, Voorhees, & Fisher, 2009). Because CZE suppressed UVB-induced phosphorylation of MAPKs, MEK1/2, MKK3/6, and Akt (Figure III-2), I sought to evaluate the effect of CZE on UVB-induced upstream signaling intermediates including EGFR and Src. The results showed that CZE inhibited UVB-induced phosphorylation of EGFR (tyrosine residues 1068 and 1045) and Src (Figure III-2E).

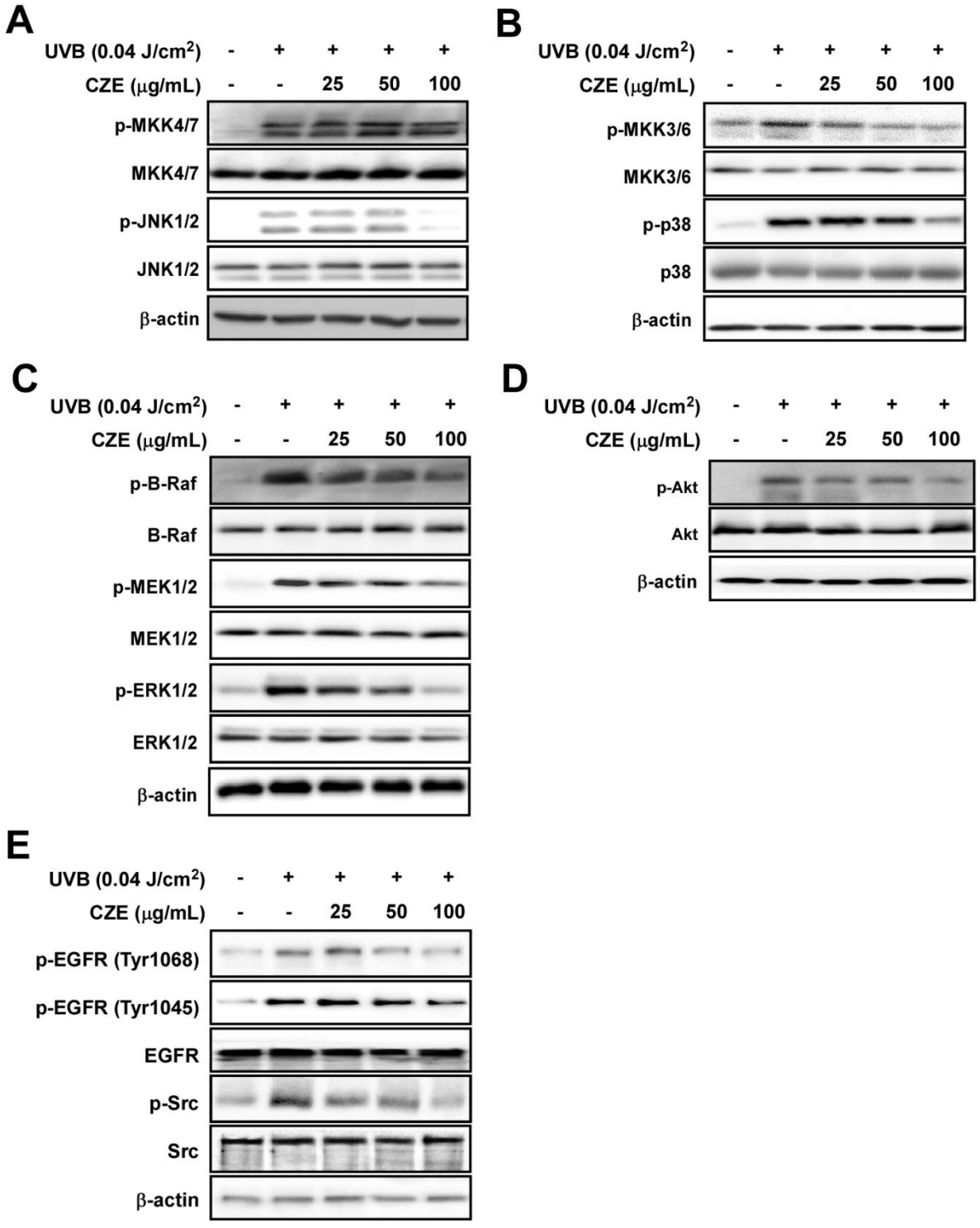

Figure III-2. Effects of CZE on UVB-induced phosphorylation of MAPKs, MAPKKs, and Akt in HaCaT cells. CZE inhibits UVB-induced phosphorylation of JNK1/2 (A), MKK3/6/p38 (B), B-Raf/MEK1/2/ERK1/2 (C), Akt (D), and (E) EGFR and Src in HaCaT cells. Phosphorylation and expression were detected by Western blotting assay with specific

antibodies. The data are represented as the mean ± SD of three independent experiments.

III-3-3. CZE inhibits UVB-induced wrinkle formation and COX-2 and MMP-13 expression in SKH-1 hairless mice

To further investigate the *in vivo* anti-inflammatory and photoaging properties of CZE, I used a UVB and SKH-1 hairless mice model. Repetitive irradiation of the dorsal skin with UVB increased wrinkle formation abnormally in these mice (Figure III-3). Conversely, topically applied CZE (20 or 100 mg/kg) on the skin significantly inhibited wrinkle formation in comparison to the UVB control group (Figure III-4). Western blot assay results also showed that CZE significantly inhibited UVB-induced COX-2 and MMP-13 expression in SKH-1 hairless mice skin (Figure III-4A). Immunohistochemical analysis results confirmed a CZE-dependent inhibition of UVB-induced COX-2 and MMP-13 expression (Figure III-4B).

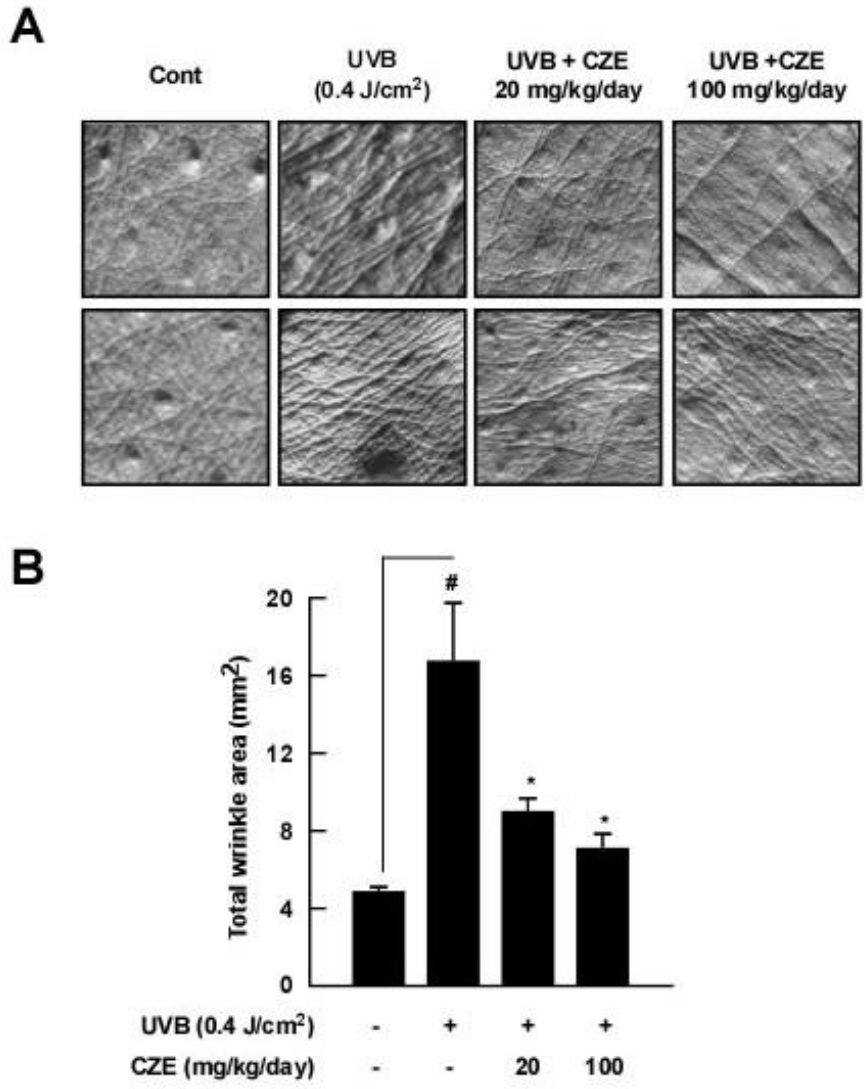

Figure III-3. Effect of CZE on UVB-induced wrinkle formation in SKH-1 hairless mice. (A) The external appearance of wrinkles. (B) CZE significantly inhibits UVB-induced wrinkle formation in SKH-1 hairless mice. The dorsal skin of the animals was exposed to UVB irradiation three times per week for 13 weeks. Prior to sacrifice, skin replica samples of the dorsal areas were taken. Wrinkle values were obtained based on the skin replica analysis. The photographs are representative images of the average results observed. Hash symbols (#) indicate a significant difference ($p < 0.05$) between the control group and the group exposed to UVB alone; asterisks (* and **) indicate significant differences [($p < 0.05$) and ($p < 0.01$),

respectively] between groups irradiated with UVB and CZE and the group exposed to UVB alone. The data are represented as the mean ± SD of five mice in each group.

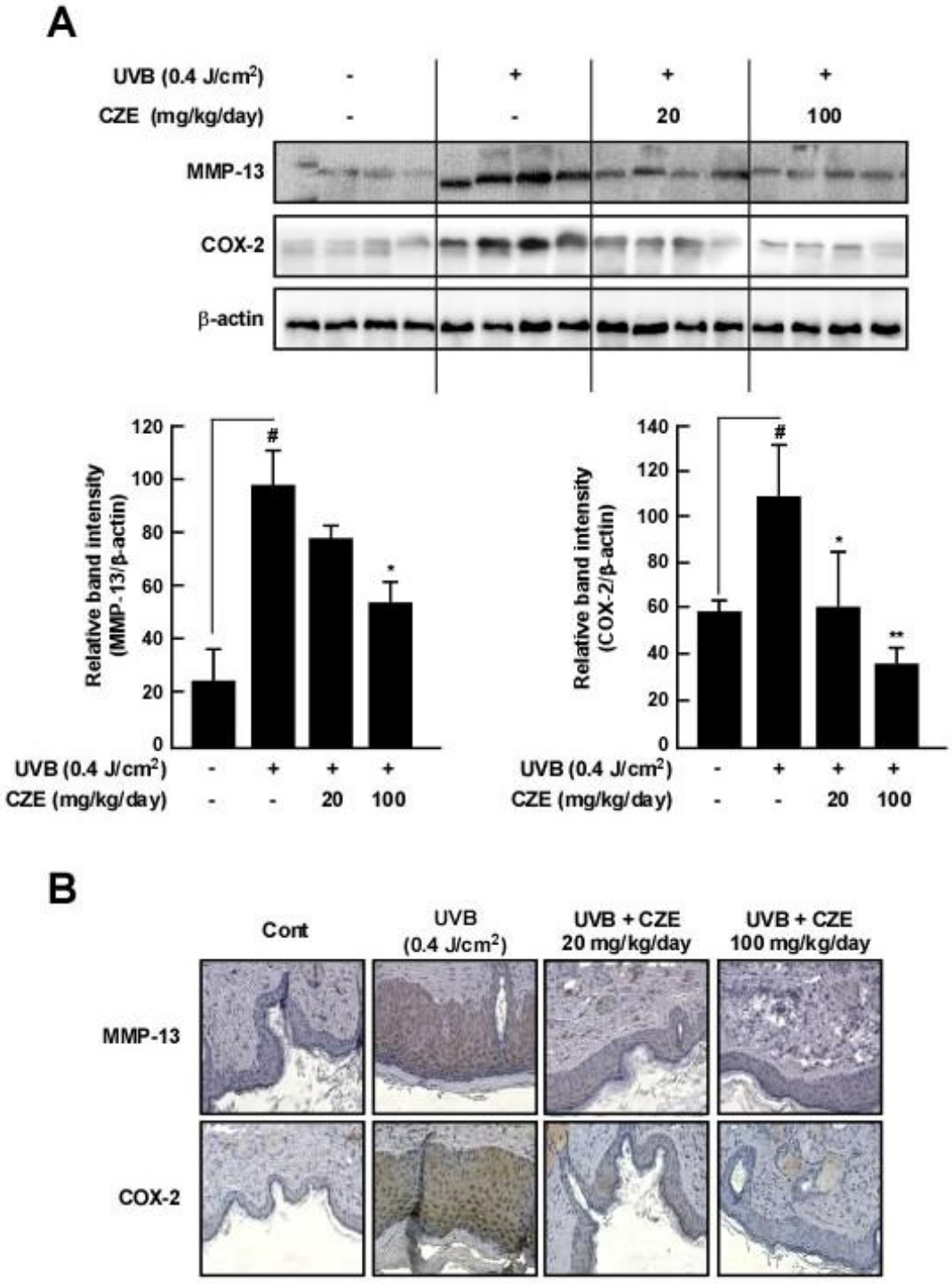

Figure III-4. Effect of CZE on UVB-induced COX-2 and MMP-13 expression in SKH-1 hairless mice. (A) CZE inhibits UVB-induced COX-2 and MMP-13 expression in SKH-1 hairless mice. Skin samples from mice were analyzed for COX-2 and MMP-13 expression by Western blot. (B) Immunohistochemical staining for COX-2 and MMP-13 expression in the

skin (magnification ×200). The methods for the animal experiments are described in the Materials and Methods. Skin samples were stained for COX-2 and MMP-13 expression with a specific polyclonal antibody and analyzed by microscopy. Hash symbols (#) indicate a significant difference ($p < 0.05$) between the control group and the group exposed to UVB alone; asterisks (* and **) indicate significant differences [($p < 0.05$) and ($p < 0.01$), respectively] between groups irradiated with UVB and CZE and the group exposed to UVB alone. The data are represented as the mean ± SD of five mice in each group.

III-3-4. Identification and quantification of phenolic compounds by LC-MS/MS and effect of CZE compounds on UVB-induced MMP-1 promoter activity

To verity which compound has a major inhibitory effect on UVB-induced skin inflammation and photoaging, I analyzed the composition of phenolic compounds in CZE. The major phenolic compounds were listed by comparison of their mass spectra with the standards (Figure III-5A and B). Curcumin and azulene were identified as the major phenolic compounds in CZE (Figure III-5A and B). The concentrations present were calculated to be 3.93 ± 0.14 and 3.36 ± 0.05 μg/g of curcumin and azulene, respectively (Table III-2). The MMP-1 promoter activity assay results showed that among the identified compounds in CZE, curcumin had a strongest inhibitory effect on UVB-induced MMP-1 promoter activity (Figure III-5C).

Table III-2. Levels of 2 major phenolic compounds identified in CZE

Compound	RT (min) [a]	Content (μg/g) [b]	MRM Transition (*m/z*) [c]
Curcumin	1.29	3.93 ± 0.14	369 → 285
Azulene	1.55	3.36 ± 0.05	129 → 78

[a] Retention time; [b] Contents based on the dry weight (n = 3); [c] Multiple reaction monitoring.

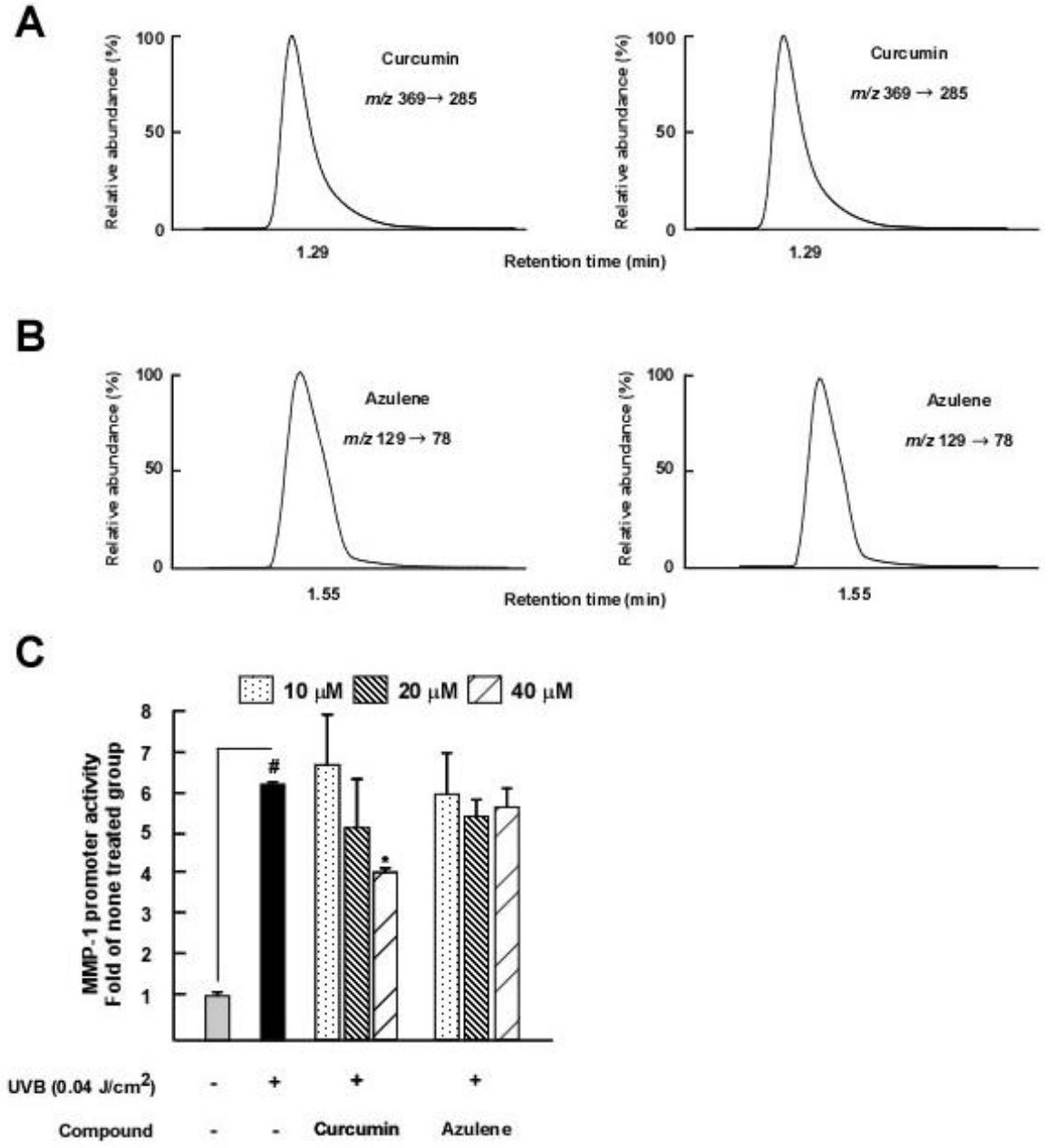

Figure III-5. LC-MS/MS chromatograms and effect of CZE compounds on UVB-induced MMP-1 promoter activity. LC-MS/MS chromatograms of (A) Curcumin and (B) Azulene in 50 mg/L standard solution (left) and CZE (right). (C) Curcumin of CZE compounds inhibits UVB-induced MMP-1 promoter activity. HaCaT cells were transfected with an MMP-1-

luciferase plasmid in the presence or absence of stimulation with UVB (0.04 J/cm^2) for 1 h. The data represent the mean ± SD values from three independent experiments. Hash symbols (#) indicate a significant difference ($p < 0.05$) between the control group and the group exposed to UVB alone; asterisks (* and **) indicate significant differences [($p < 0.05$) and ($p < 0.01$), respectively] between the groups irradiated with UVB and treated with the compound, and the group exposed to UVB alone.

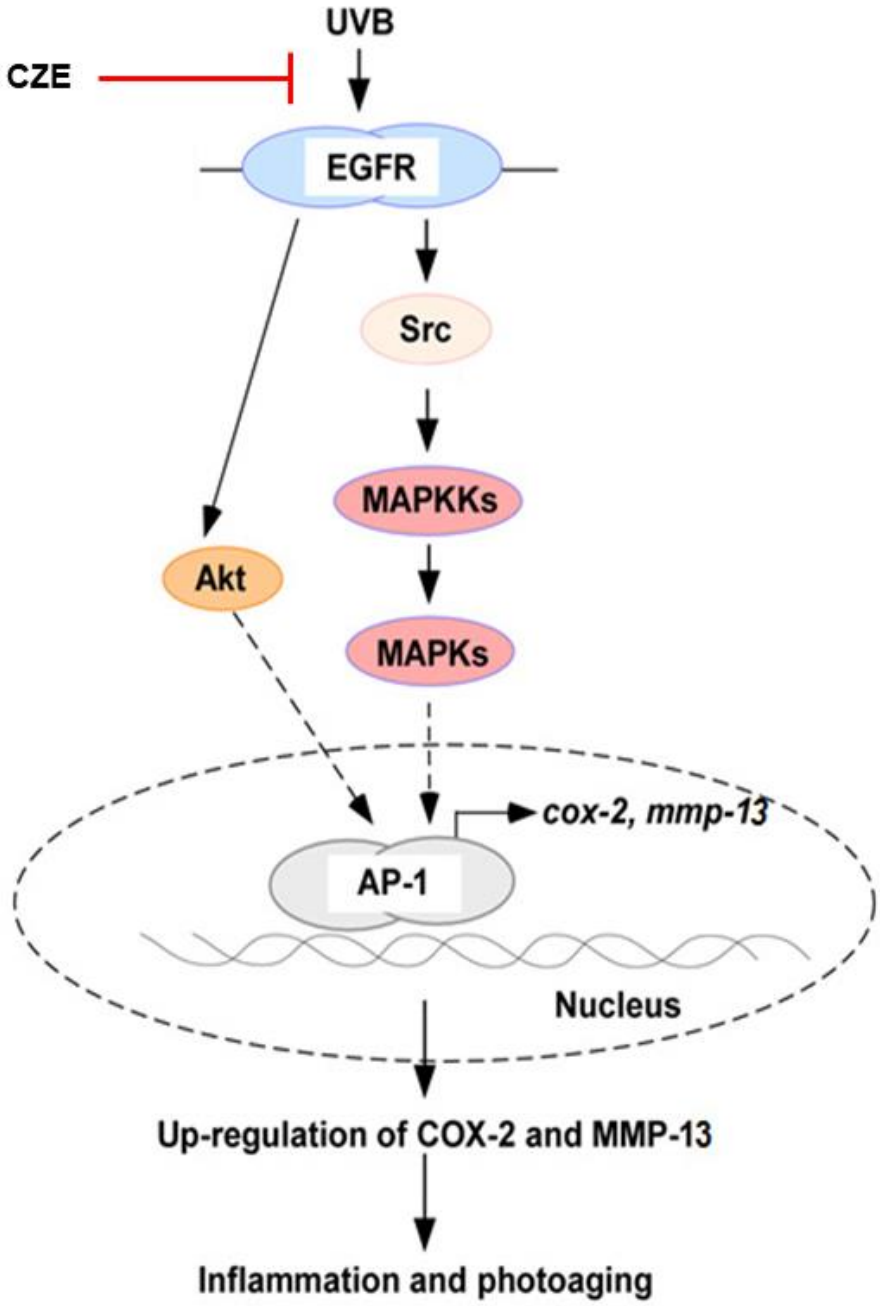

Figure III-6. Mechanism of *Curcuma zedoaria* extract on UVB-induced skin inflammation and photoaging.

III-4. Discussion

In recent years, the incidence of various diseases and disorders related to ultraviolet (UV) radiation has caused a significant burden on the healthcare system due to a high incidence and considerable cost of treatment (Katiyar, 2016). Chronic and sustained exposure of human skin to UV has been implicated in skin diseases through the generation of inflammatory responses (Byun et al., 2010). Considerable interest has arisen for the use of plant-based products for the prevention and treatment of skin diseases. Although various natural sources including *Matricaria* flower and *Aloe barbadensis* exert preventive effects on several skin diseases including skin inflammation and photoaging (Tabassum & Hamdani, 2014), more effective and safe treatments for skin inflammation and photoaging are still needed.

UV irradiation causes skin inflammation and photoaging via induction of the transcription factor AP-1, which regulates the expression of COX-2 and MMP-1 and -13, respectively (Kuo, Chen, Chu, Lin, & Chiang, 2015; Vincenti & Brinckerhoff, 2001). In order to develop effective anti-inflammatory and -photoaging agents, I created immortalized human skin keratinocyte HaCaT cells containing the MMP-1 promoter plasmid. Interestingly, although CZE exhibited an inhibitory effect on UVB-induced MMP-1 promoter activity, CZE only suppressed UVB-induced MMP-13 expression, and not MMP-1 (data not shown). Because the major transcription factor involved in regulation of the MMP-13 gene expression is AP-1, it is reasonable that CZE suppressed UVB-induced MMP-13 expression. However, why CZE only affected MMP-13 expression without impacting MMP-1 requires further investigation.

C. zedoaria exhibits a wide variety of beneficial biological properties, including antiviral, antibacterial, immune-stimulating, anti-inflammatory, and anti-carcinogenic effects (Bala Nambisan & Vimala, 2012). However, the protective effect of CZE against UV damage and the mechanism of action have not previously been investigated. Because CZE strongly suppressed AP-1 activity and COX-2 and MMP-13 expression, I analyzed the expression of major signaling molecules influenced by CZE. Western blot assay results showed that CZE suppressed UVB-induced phosphorylation of JNK1/2, MKK3/6/p38, B-Raf/MEK1/2/ERK1/2, and Akt in HaCaT cells. These accumulated experimental results indicate that CZE suppresses UVB-induced COX-2 and MMP-13 expression by regulating the MAPKKs/MAPKs/AP-1 signaling pathways.

A previous study reported that activation of Src by UV leads to the phosphorylation of epidermal growth factor receptor (EGFR) and p38/Akt and PI3K/Akt signaling pathways, resulting in an increase in MMPs expression (Devary, Gottlieb, Smeal, & Karin, 1992; Huveneers & Danen, 2009). Ultraviolet B radiation activates EGFR-MEK-ERK-dependent keratinocyte survival, migration, and proliferation, and type I collagen synthesis is known to be crucial for skin wound healing (J. Chen, Zeng, Forrester, Eguchi, Zhang, & Harris, 2016). Additionally, our results show that CZE suppressed phosphorylation of all three MAPKs including p38, ERK1/2, and JNK1/2 (with the exception of MKK4/7), as well as Akt. I, therefore, hypothesized that CZE may affect the EGFR signaling pathway to inhibit UVB-induced COX-2 and MMP-13 expression. However, our results showed that both EGFR and Src phosphorylation were suppressed by CZE.

A previous paper reported that EGFR transactivation is shown to activate the receptor indirectly, which is thought to be a major mechanism by which G-protein-coupled receptor (GPCR) agonist stimulation leads to EGFR activation (Ohtsu, Dempsey, & Eguchi,

2006). This pathway involves activation of metalloproteases belonging to the A Disintegrin and A Metalloprotease family, which in turn cleaves membrane-anchored proligands of the EGF family such as EGF, heparin-binding EGF, amphiregulin, betacellulin, epiregulin, or transforming growth factor α at the receptor's ectodomain (Schlessinger, 2002). In this study, CZE regulated EGFR and JNK and p38 phosphorylation. Interestingly, CZE did not interfere with B-Raf phosphorylation, although the Raf substrate MEK was strongly suppressed. Therefore, I hypothesized that CZE affects EGFR and Raf activity and subsequently suppressed AP-1/COX-2 and MMP-13. Further investigation is needed to support this hypothesis.

I further confirmed that topical application of CZE suppresses chronic UV-irradiation induced wrinkle formation in the skin of SKH-1 hairless mice. As expected, CZE prevented chronic UV-induced up-regulation of COX-2 and MMP-13 expression in mouse skin. Additionally, CZE prevented abnormal increase in epidermal thickness induced by UVB-irradiaiton in mice. Because hyperplasia is a general marker for inflammation, it is presumed that CZE has an anti-inflammatory effect by suppressing UVB-mediated hyperplasia of mouse keratinocytes. The identification of bioactive compounds in functional foods is necessary for a thorough investigation of the mechanisms of action. Although various phytochemical constituents of the plant extract CZE have been reported (Chaithong et al., 2006; Toshio, 2002), including β-elemene, 1,8-cineole, curcumin, isologifolene, azulene, and octahydroantheracene, our LC-MS results only detected the presence of curcumin and azulene. Several compounds including 1,8-cineole and β-elemene were detected when using GC-MS; however, further compounds could not be detected. Therefore, a deeper analysis using ESI-MS/MS is needed. To verify which compound exhibited the most potent anti-inflammatory and photoaging effects, we compared the effect of CZE compounds on MMP-1 promoter activity in HaCaT cells. Curcumin exhibited the strongest inhibitory effect on

MMP-1 promoter activity. Curcumin, a bioactive photochemical has been previously employed for the treatment of skin diseases and wound healing (Liu, Zhang, & Xu, 2018). Tsai et al demonstrated that curcumin provided protection against UVB radiation-induced skin cancer growth in a mouse model. Curcumin significantly inhibited NF-κB, COX-2, PGE_2, and nitric oxide (NO) levels while upregulation of p53 and p21/Cip1 to prevent DNA damage and facilitate DNA repair (Tsai et al., 2012).

III-5. Conclusions

In this study, my *in vitro* and *in vivo* results indicate that CZE inhibits UVB-induced COX-2 and MMP-13 expression. The results provide proof of concept for the importance of EGFR and MAPKs signal transduction pathways as a major driving force for COX-2- and MMP-13-mediated inflammation and photoaging, respectively. CZE application on the skin may exert a preventive effect on UVB-induced skin inflammation and photoaging.

III-6. References

Angel, G., Vimala, B., & Nambisan, B. (2012). Phenolic content and antioxidant activity in five underutilized starchy Curcuma species. *International Journal of Pharmacognosy and Phytochemical Research, 4*(2), 69-73.

Buckman, S., Gresham, A., Hale, P., Hruza, G., Anast, J., Masferrer, J., & Pentland, A. P. (1998). COX-2 expression is induced by UVB exposure in human skin: implications for the development of skin cancer. *Carcinogenesis, 19*(5), 723-729.

Byun, S., Lee, K. W., Jung, S. K., Lee, E. J., Hwang, M. K., Lim, S. H., Bode, A. M., Lee, H. J., & Dong, Z. (2010). Luteolin inhibits protein kinase Cε and c-Src activities and UVB-induced skin cancer. *Cancer Rsearch, 70*(6), 2415-2423.

Chaithong, U., Choochote, W., Kamsuk, K., Jitpakdi, A., Tippawangkosol, P., Chaiyasit, D., Champakaew, D., Tuetun, B., & Pitasawat, B. (2006). Larvicidal effect of pepper plants on Aedes aegypti (L.) (Diptera: Culicidae). *Journal of Vector Ecology, 31*(1), 138-144.

Chen, J., Zeng, F., Forrester, S. J., Eguchi, S., Zhang, M.-Z., & Harris, R. C. (2016). Expression and function of the epidermal growth factor receptor in physiology and disease. *Physiological Reviews, 96*(3), 1025-1069.

Chen, W., Borchers, A. H., Dong, Z., Powell, M. B., & Bowden, G. T. (1998). UVB irradiation-induced activator protein-1 activation correlates with increased c-fos gene expression in a human keratinocyte cell line. *Journal of Biological Chemistry, 273*(48), 32176-32181.

Devary, Y., Gottlieb, R. A., Smeal, T., & Karin, M. (1992). The mammalian ultraviolet

response is triggered by activation of Src tyrosine kinases. *Cell, 71*(7), 1081-1091.

Fisher, G. J., Kang, S., Varani, J., Bata-Csorgo, Z., Wan, Y., Datta, S., & Voorhees, J. J. (2002). Mechanisms of photoaging and chronological skin aging. *Archives of Drmatology, 138*(11), 1462-1470.

Hla, T., Ristimäki, A., Appleby, S., & Barriocanal, J. G. (1993). Cyclooxygenase Gene Expression in Inflammation and Angiogenesis a. *Annals of the New York Academy of Sciences, 696*(1), 197-204.

Huang, S., Zhang, A., Ding, G., & Chen, R. (2009). Aldosterone-induced mesangial cell proliferation is mediated by EGF receptor transactivation. *American Journal of Physiology-Renal Physiology, 296*(6), F1323-F1333.

Huveneers, S., & Danen, E. H. (2009). Adhesion signaling–crosstalk between integrins, Src and Rho. *Journal of Cll Sience, 122*(8), 1059-1069.

Jung, S. K., Lee, K. W., Byun, S., Kang, N. J., Lim, S. H., Heo, Y.-S., Bode, A. M., Bowden, G. T., Lee, H. J., & Dong, Z. (2008). Myricetin suppresses UVB-induced skin cancer by targeting Fyn. *Cancer Rsearch, 68*(14), 6021-6029.

Katiyar, S. K. (2016). Dietary proanthocyanidins inhibit UV radiation-induced skin tumor development through functional activation of the immune system. *Molecular Ntrition & Fod Rsearch, 60*(6), 1374-1382.

Kim, C., Ryu, H.-C., & Kim, J.-H. (2010). Low-dose UVB irradiation stimulates matrix metalloproteinase-1 expression via a BLT2-linked pathway in HaCaT cells. *Experimental & Molecular Medicine, 42*(12), 833-841.

Kim, H. H., Shin, C. M., Park, C.-H., Kim, K. H., Cho, K. H., Eun, H. C., & Chung, J. H. (2005). Eicosapentaenoic acid inhibits UV-induced MMP-1 expression in human dermal fibroblasts. *Journal of Lipid Research, 46*(8), 1712-1720.

Kuo, Y.-H., Chen, C.-W., Chu, Y., Lin, P., & Chiang, H.-M. (2015). *In vitro* and *in vivo*

studies on protective action of N-phenethyl caffeamide against photodamage of skin. *PloS one, 10*(9), e0136777.

Lai, E. Y., Chyau, C.-C., Mau, J.-L., Chen, C.-C., Lai, Y.-J., Shih, C.-F., & Lin, L.-L. (2004). Antimicrobial activity and cytotoxicity of the essential oil of Curcuma zedoaria. *The American Journal of Chinese Medicine, 32*(02), 281-290.

Lakshmi, S., Padmaja, G., & Remani, P. (2011). Antitumour effects of isocurcumenol isolated from Curcuma zedoaria rhizomes on human and murine cancer cells. *International Journal of Medicinal Chemistry, 2011*.

LaMarca, H. L., Dash, P. R., Vishnuthevan, K., Harvey, E., Sullivan, D. E., Morris, C. A., & Whitley, G. S. J. (2008). Epidermal growth factor-stimulated extravillous cytotrophoblast motility is mediated by the activation of PI3-K, Akt and both p38 and p42/44 mitogen-activated protein kinases. *Human Reproduction, 23*(8), 1733-1741.

Liu, X., Zhang, R., Shi, H., Li, X., Li, Y., Taha, A., & Xu, C. (2018). Protective effect of curcumin against ultraviolet A irradiation-induced photoaging in human dermal fibroblasts. *Molecular Medicine Reports*, *17*(5), 7227-7237.

Morikawa, T., Matsuda, H., Ninomiya, K., & Yoshikawa, M. (2002). Medicinal foodstuffs. XXIX. Potent protective effects of sesquiterpenes and curcumin from Zedoariae Rhizoma on liver injury induced by D-galactosamine/lipopolysaccharide or tumor necrosis factor-α. *Biological and Pharmaceutical Bulletin, 25*(5), 627-631.

Ohtsu, H., Dempsey, P. J., & Eguchi, S. (2006). ADAMs as mediators of EGF receptor transactivation by G protein-coupled receptors. *American Journal of Physiology-Cell Physiology, 291*(1), C1-C10.

Quigley, D. A., To, M. D., Pérez-Losada, J., Pelorosso, F. G., Mao, J.-H., Nagase, H., Ginzinger, D. G., & Balmain, A. (2009). Genetic architecture of mouse skin inflammation and tumour susceptibility. *Nature*, *458*(7237), 505-508.

Reuter, S., Gupta, S. C., Chaturvedi, M. M., & Aggarwal, B. B. (2010). Oxidative stress, inflammation, and cancer: how are they linked? *Free Radical Biology and Medicine, 49*(11), 1603-1616.

Schlessinger, J. (2002). Ligand-induced, receptor-mediated dimerization and activation of EGF receptor. *Cell, 110*(6), 669-672.

Schulze, W. X., Deng, L., & Mann, M. (2005). Phosphotyrosine interactome of the ErbB-receptor kinase family. *Molecular Systems Biology, 1*(1), 2005.0008.

Seibert, K., & Masferrer, J. (1994). Role of inducible cyclooxygenase (COX-2) in inflammation. *Receptor, 4*(1), 17-23.

Seo, J. Y., Kim, E. K., Lee, S. H., Park, K. C., Kim, K. H., Eun, H. C., & Chung, J. H. (2003). Enhanced expression of cylooxygenase-2 by UV in aged human skin in vivo. *Mechanisms of Ageing and Development, 124*(8-9), 903-910.

Seo, W.-G., Hwang, J.-C., Kang, S.-K., Jin, U.-H., Suh, S.-J., Moon, S.-K., & Kim, C.-H. (2005). Suppressive effect of Zedoariae rhizoma on pulmonary metastasis of B16 melanoma cells. *Journal of Ethnopharmacology, 101*(1-3), 249-257.

Singh, B., Schneider, M., Knyazev, P., & Ullrich, A. (2009). UV-induced EGFR signal transactivation is dependent on proligand shedding by activated metalloproteases in skin cancer cell lines. *International Journal of Cancer, 124*(3), 531-539.

Tabassum, N., & Hamdani, M. (2014). Plants used to treat skin diseases. *Pharmacognosy Reviews, 8*(15), 52.

Toshio, M. (2002). Potent protective effects of sesquiterpenesnand curcumin form zedoaiae rhizoma on liver injury induced by D-Galactosamine/lipopolys-acchaide or tumor necrosis factor-α. *Pharma Soci of Japan, 25*(5), 627.

Tsai, K. D., Lin, J. C., Yang, S. M., Tseng, M. J., Hsu, J. D., Lee, Y. J., & Cherng, J. M. (2012). Curcumin protects against UVB-induced skin cancers in SKH-1 hairless

mouse: analysis of early molecular markers in carcinogenesis. *Evidence-Based Complementary and Alternative Medicine, 2012*.

Vincenti, M. P., & Brinckerhoff, C. E. (2002). Transcriptional regulation of collagenase (MMP-1, MMP-13) genes in arthritis: integration of complex signaling pathways for the recruitment of gene-specific transcription factors. *Arthritis Research & Therapy, 4*(3), 1-8.

Xu, Y., Shao, Y., Zhou, J., Voorhees, J. J., & Fisher, G. J. (2009). Ultraviolet irradiation-induces epidermal growth factor receptor (EGFR) nuclear translocation in human keratinocytes. *Journal of Cellular Biochemistry, 107*(5), 873-880.

Chapter IV.

Syringic Acid Prevents Skin Carcinogenesis via Regulation of Nox and EGFR Signaling

Abstract

Validation of nutraceutical and pharmaceutical targets is essential for prediction of physiological and side effects. Epidemiologic evidence and molecular studies suggest that non-melanoma skin cancer is directly associated with excessive exposure to ultraviolet (UV) radiation. The aim of the present study was to evaluate the inhibitory effects of syringic acid on UVB-induced signaling and skin carcinogenesis, and determine the molecular targets. Treatment of human epidermal keratinocytes (HaCaT) cells with syringic acid resulted in the suppression of UVB-induced cyclooxygenase-2, matrix metalloproteinase-1, and prostaglandin E_2 expression as well as activator protein-1 activity. Moreover, syringic acid inhibited the UVB-induced phosphorylation of mitogen-activated protein kinases and Akt signaling pathways as well as epidermal growth factor receptor (EGFR). Syringic acid treatment further inhibited intracellular reactive oxygen species and protein-tyrosine phosphatase-κ activity, a regulator of EGFR activation. Syringic acid and the antioxidant N-acetyl-L-cysteine inhibited UVB-induced nicotinamide adenine dinucleotide phosphate (NADPH) oxidase activity. *In vivo*, pretreatment of mouse skin with syringic acid significantly suppressed UVB-induced skin tumor incidence in a dose-dependent manner. Overall, these results indicate that syringic acid exerts potent chemopreventive activity in skin carcinogenesis mainly by inhibition of the Nox/PTP-κ/EGFR axis. Syringic acid might serve as an effective chemopreventive and therapeutic agent against UVB-mediated skin cancer.

IV-1. Introduction

Skin cancer is the most common form of cancer, accounting for at least 40% of cases (Jemal, Siegel, Xu, & Ward, 2010; Rogers, Weinstock, Feldman, & Coldiron, 2015). The incidence of new cases of skin cancer was reported to be 22.3 per 100,000 men and women per year in 2010-2014, accounting for 2.7 deaths per 100,000 men and women annually (R. Siegel, Naishadham, & Jemal, 2013; R. L. Siegel, Miller, & Jemal, 2016). Approximately 90% of human skin cancers are considered to be caused by ultraviolet (UV)-induced damage through excessive generation of the reactive oxygen species (ROS) (D'Orazio, Jarrett, Amaro-Ortiz, & Scott, 2013). ROS is normally produced throughout oxygen metabolism and play a major role in physiological and pathological redox signaling (Schieber & Chandel, 2014). Oxidative stress results in overproduction of ROS to directly induce damage to cellular proteins, lipid, and DNA, resulting in an imbalance of cellular sources such as NADPH oxidases, leading to carcinogenesis in the skin (Park, 2013; Svobodova, Walterova, & Vostalova, 2006).

ROS are produced by energy transfer from UV irradiation, and thus UVB-ROS are closely related to skin carcinogenesis via stimulating oncogenic signaling pathways (Lim, Jung, Kim, Kim, Lee, Jang, et al., 2013; Sun, Park, Hwang, Zhang, Seo, Lin, et al., 2017). Multiple lines of evidence have indicated that activation of epidermal growth factor receptor (EGFR) mediated by UVB plays central roles in skin carcinogenesis. The oxidative damage of protein tyrosine phosphatase-kappa (PTP-κ) is one of the most important factors involved in UVB-mediated EGFR activation (Herrlich, Karin, & Weiss, 2008; Xu, Baker, Quan, Baldassare, Voorhees, & Fisher, 2010). Activated EGFR stimulates many intracellular signaling pathways including p38 mitogen-activated protein kinase (MAPK) and

phosphatidylinositol 3-kinase (PI3-K)/Akt pathways, leading to transcriptional activation of the cyclooxygenase-2 (COX-2) gene (Lee, Lin, Hu, Chiang, Hsu, Lin, et al., 2016; Wu, Silbajoris, Whang, Graves, Bromberg, & Samet, 2005). COXs are enzymes involved in the synthesis of prostaglandins (PGs) (Ricciotti & FitzGerald, 2011), and COX-2 specifically regulated inflammation via the production of PGE_2. COX-2 is not normally expressed in most tissues but can be induced by UVB irradiation causes inflammation, tumor promotion, and cancer development (Elmets, Ledet, & Athar, 2014). Accordingly, recent studies have demonstrated that drugs that block COX-2 expression may prevent the development of skin cancers. In addition, abnormal expression of matrix metalloproteinase-1 (MMP-1) is a marker for UVB irradiation-induced skin damage. Therefore, regulation of COX-2 and/or MMP-1 expression with a pharmaceutical inhibitor is a promising strategy to prevent cancer development.

Syringic acid is a naturally occurring *O*-methylated trihydroxybenzoic acid. Syringic acid can be found in the acai palm (*Euterpe oleracea*) and its oil, as well as in red or white wine (Pacheco-Palencia, Mertens-Talcott, & Talcott, 2008). Compared with traditional chemical agents, natural ingredients extracted from plants are known to be less toxic to normal cells but are selectively toxic to cancer cells (Ryu, & Na, 2018). In our previous study, I found that *Rhus javanica* extract (RJE) attenuates UVB-induced photo-damage and inflammation by modulating the expression of MMPs and COX-2 in SKH-1 hairless mice. In addition, syringic acid the phenolic compound of RJE, exhibited the strongest inhibitory effect on the transactivation of the transcription factor activator protein-1 (AP-1), which plays an essential role in several biological processes such as inflammation and carcinogenesis (Ha, Lee, Kim, Song, Lee, Kim, et al., 2016). Moreover, a previous study reported that syringic acid could normalize hyperglycemia via glycoprotein components in experimental diabetic rats, and showed a hepatoprotective effect of strong radical scavenging activity in liver

injured mice (Muthukumaran, Srinivasan, Venkatesan, Ramachandran, & Muruganathan, 2013). However, the mechanisms of syringic acid on oxidative stress and its chemopreventive effect on UVB-induced skin carcinogenesis remain unclear.

In the present study, I sought to investigate the inhibitory effects of syringic acid on UVB-induced skin carcinogenesis. I hypothesized that syringic acid might inhibit UVB damage through suppressing the above oncogenic signaling pathway-related molecules. In an *in vitro* experiment, I treated human epidermal keratinocytes (HaCaT cells) with syringic acid and measured the gene and protein expression levels. In addition, a previous study reported that excessive ROS impair PTP-κ activity and subsequently increase EGFR phosphorylation; therefore, I hypothesized that syringic acid may affect UVB-mediated ROS production cascades and its producers. Accordingly, I detected the change in ROS due to syringic acid treatment, which was compared to the effects of the FDA-approved antioxidant drug N-acetyl-L-cysteine (NAC), which is commonly used to identify and test ROS inducers and to inhibit ROS. Since NADPH oxidases of the Nox family are important enzymatic sources of ROS, I further measured the effect of syringic acid on NADPH oxidase activity to determine the potential targets mediating its inhibitory effects. To evaluate the therapeutic potential of syringic acid, I conducted an *in vivo* experiment using the SKH-1 hairless mouse model that received topical treatment of syringic acid prior to UVB exposure, and compared the tumor incidence and expression of relevant molecules in the mouse skin. These results should provide a foundation for the development of syringic acid as a novel, naturally derived chemopreventive agent in skin cancer.

IV-2. Materials and Methods

IV-2-1. Materials

Chemical reagents were purchased from Sigma–Aldrich (St Louis, MO, USA). Dulbecco's Modified Eagle's Medium (DMEM), gentamicin, L-glutamine, penicillin–streptomycin and fetal bovine serum (FBS) were obtained from Thermo Scientific HyClone (Logan, UT, USA). The antibodies against MMP-1, MMP-13, PTP-κ, EGFR, amphiregulin, and β-actin were purchased from Santa Cruz Biotech (Santa Cruz, CA, USA). The antibodies against COX-2, p44/42 MAP Kinase, SAPK/JNK, p38 MAPK, phospho-p44/42 MAPK (Erk 1/2) (Thr202/Tyr204), phospho-SAPK/JNK (Thr183/Tyr185), MKK3b, phospho-MKK3 (Ser189)/MKK6 (Ser 207), SEK1/MKK4, phospho-SEK1/MKK4 (Ser257/Thr261), MEK1/2, phospho-MEK1/2 (Ser217/221), phospho-c-Jun (Ser73), Akt, phospho-Akt (Thr308), Src, phospho-Src (Tyr527), EGF receptor, phosphor-EGF receptor (Tyr 1068), and phosphor-EGF receptor (Tyr 1045) were purchased from Cell Signaling Biotechnology (Beverly, MA, USA). The antibody against phosphorylated p38 MAPK (pT180/pY182) was purchased from BD Biosciences (Franklin Lakes, NJ, USA). The antibody against Oxidized PTP active site was purchased from R&D systems (Biotechne, Minneapolis, MN).

IV-2-2. Cell culture, UVB exposure and viability assay

Human epidermal keratinocyte HaCaT cells were generous obtained from Dr. Zigang Dong (The Hormel Institute, University of Minnesota, USA). HaCaT cells were maintained in DMEM containing 10% FBS, 100 units/mL of penicillin and 100 mg/mL of streptomycin at 37℃ in a 5% CO_2 humidified incubator. UVB irradiation was conducted using a bank of

four Westinghouse F520 lamps (National Biological, Twinsburg, OH) at 6 J/s/m light in the UVB range. Approximately 10% of the additional radiation from the F520 lamp is in the UVA spectrum (320 nm). A UVB exposure chamber was fitted with a Kodak Kodacel K6808 filter to eliminate all wavelengths below 290 nm. UVB radiation was measured using a UVX radiometer (UVX-31). To assess cell viability, HaCaT cells (1×10^3 cells/mL) were seeded in 96-well plates and incubated at 37℃ in a 5% CO_2 incubator. After the cells were treated with syringic acid, 20 μL of MTS reagent (Promega, Madison, WI, USA) was added to each well. After 1 h of incubation, absorbance levels for formazan at 490 and 690 nm were measured using a microplate reader (Bio-Rad Inc., Hercules, CA, USA).

IV-2-3. Animal experiments

Six-week-old male SKH-1 hairless mice, weighing approximately 20–22 g, were purchased from Central Laboratory Animal Inc. (Seoul, Korea). The mice were housed in an air-conditioned room (23 ± 2℃) with a 12-h light/dark cycle. They were allowed free access to food and tap water. All animals received humane care, and the study protocol (KFRI-M-16013) was approved and performed in accordance with guidelines for animal use and care at Korea Food Research Institute. Twenty mice were randomly allocated to each group (five mice per group, four groups in total): (i) control group (normal), (ii) UVB-irradiated group (UVB), (iii) UVB-irradiated and 0.2 mM syringic acid -treated group and (iv) UVB-irradiated and 1 mM syringic acid -treated group. The mice were topically treated with 200 μL acetone before UVB exposure 3 day/week for 22 weeks. UVB irradiation doses were increased each week by 1 MED (1 MED = 50 mJ/cm^2) to 4 MED and then maintained at 4 MED until 22 weeks had passed.

IV-2-4. MMP-1 promoter assay

To evaluate the MMP-1 promoter activity, I constructed a pGreenFire (pGF1) vector containing an MMP-1 promoter plasmid(Kim, Shin, Eun, & Chung, 2009). For stable expression of pGF1 with the MMP-1 promoter, 293T cells were transfected with the pGF1 plasmid using Lipofectamine (ThermoFisher Scientific, MA, USA), following the manufacturer's instructions. The transfection medium was changed at 4 h after transfection, and the cells were then cultured for 36 h. Virus particles were harvested by filtration using a 0.45 mm syringe filter, then combined with 8 mg/mL of polybrene (Millipore) and infected into HaCaT cells for 24 h. The cell culture media was replaced with fresh culture medium and the cells were further cultured for 24 h, prior to selection with puromycin (1 mg/mL) for 36 h. Selected HaCaT cells (8×10^3 cells/mL) were seeded into 96-well plates, which were incubated at 37℃ in a 5% CO_2 incubator. When the cells reached 80–90% confluence, they were starved by culturing in serum-free DMEM for a further 24 h. Cells were then treated with syringic acid for 1 hour prior to UVB (0.04 J/cm^2) exposure and then incubated for 5 h. Cells were disrupted with 100 μL of lysis buffer [0.1 M potassium phosphate buffer (pH 7.8), 1% Triton X-100, 1 mM dithiothreitol (DTT), and 2 mM EDTA], after which luciferase activity was measured using a luminometer (SpectraMax L, Molecular Devices, Sunnyvale, CA).

IV-2-5. PGE_2 assay

HaCaT cells (2×10^6 cells/mL) were seeded in 6-well plates and incubated at 37℃ for 24 h in a 5% CO_2 incubator. Cells were then treated with syringic acid for 1 h prior to UVB (0.04 J/cm^2) exposure and then incubated for 20 h. The quantity of PGE_2 released into the medium was measured using a PGE_2 enzyme immunoassay kit (Enzo Life Science,

Farmingdale, NY, USA).

IV-2-6. Western blot assay

For *in vitro* Western blot assays, cells (1.5×10^6 cells/mL) were cultured in 10 cm dishes for 24 h, followed by starvation in serum-free DMEM for 24 h. Cells were then treated with syringic acid for 1 h and irradiated with UVB (0.04 J/cm^2). After incubation, the cells were collected and washed twice with cold PBS, before lysis in Cell Lysis Buffer (Cell Signaling Biotechnology, Beverly, MA, USA) and maintained on ice for 30 min. The lysate protein was washed via centrifugation and the concentration determined using a DC Protein Assay kit (Bio-Rad Laboratories) following manufacturer's instructions. The lysate was subjected to 10% sodium dodecyl sulfate–polyacrylamide gel electrophoresis (SDS-PAGE) and transferred to a polyvinylidene difluoride (PVDF) membrane (Millipore, Immobilon® -P transfer membrane). After transferring, the membranes were incubated with the specific primary antibodies at 4℃ overnight. Protein bands were visualized using a chemiluminescence detection kit (ATTO, Tokyo, Japan) after hybridization with a horseradish peroxidase (HRP)-conjugated secondary antibody.

For *in vivo* Western blots, mouse skin tissue was added to 2 mL microcentrifuge tubes containing lysis buffer and stainless steel bead and subsequently homogenized twice for 2 min at 20 Hz in a TissueLyser II (Qiagen, Valencia, CA, USA). Skin lysates were centrifuged at 12,000 rpm for 20 min. After the protein content was determined, the skin tissue extract was subjected to 10% SDS-PAGE and transferred to a PVDF membrane. Membranes were processed, and proteins were analyzed as described above for *in vitro* Western blot assay.

IV-2-7. Measurement of ROS

Intracellular ROS generation was measured by fluorometric examination with H_2DCFDA. H_2DCFDA is cleaved by non-specific cellular esterases and is oxidized in the presence of H_2O_2 and peroxidases to yield fluorescent 2',7'-dichlorofluorescein (DCF). In brief, HaCaT cells (8×10^3 cells/mL) were seeded in a 96-well plate and allowed to attach overnight. When the cells reached 80–90% confluence, they were starved by culturing in serum-free DMEM for a further 24 h. The cells were treated with 0.04 J/cm^2 UVB and then syringic acid was added to the medium at increasing concentrations within 1 h. The cells were stained with 5 μM H_2DCFDA. Immediately after the addition of syringic acid, the fluorescence was measured in kinetic mode at an excitation wavelength of 485 nm and emission wavelength of 520 nm using a fluorescent microscope (Nikon Eclipse Ti-S, Tokyo, Japan). Images were analyzed using Metamorph (Molecular Devices, Danville, PA, USA) software.

IV-2-8. PTP-κ immunoprecipitation

HaCaT cell lysates were prepared in TGH buffer (50 mM Hepes, pH 7.2, 20 mM NaCl, 10% glycerol, and 1% Triton X-100), and were pre-cleared with normal rabbit IgG before incubation with PTP-κ and EGFR antibody for 3 h at 4°C. Protein A-conjugated agarose beads were then added, and incubation continued for 2 h at 4℃, followed by extensive washing. The washed immunoprecipitates were subjected to a western blot assay. For measurement of protein phosphatase activity, a tyrosine-phosphorylated peptide derived from EGFR was added. Reactions were terminated by the addition of 100 μL of BIOMOL®

Green Reagent (Enzo, Farmingdale, NY, USA) and the absorbance was measured at 620 nm.

IV-2-9. Histological analysis

Sections (5-μm thick) of 10% neutral formalin solution-fixed, paraffin-embedded skin tissues were cut on silane-coated glass slides. The fixed tissue samples were washed with distilled water, dehydrated using an ethanol gradient, cleared with xylene and embedded in paraffin wax. The tissue sections were stained with hematoxylin and eosin (H&E). Deparaffinized sections were heated for 15 min in 10 mM citrate buffer (pH 6.0) in a microwave oven for antigen retrieval. For the detection of target proteins, slides were incubated with affinity-purified primary antibody in a refrigerator overnight in 1% BSA solution and then developed using the SignalStain® Boost IHC Detection Reagent (HPR, rabbit) antibodies (Cell Signaling Biotechnology). Peroxidase-binding sites were detected by staining with SignalStain® DAB Substrate Kit (Cell Signaling Biotechnology). Finally, counterstaining was performed using Harris hematoxylin solution (Sigma–Aldrich). The thickness of the epidermis and the MMP-13 and COX-2 were visualized using a fluorescent microscope (Nikon Eclipse Ti-S, Tokyo, Japan) and images were analyzed using Metamorph (Molecular Devices, Danville, PA) software.

IV-2-10. Statistical analysis

Where appropriate, data are expressed as the means ± SD of three independent experiments and significant differences were determined using one-way ANOVA (Analysis Of Variance). A probability value of $p < 0.05$ was used as the criterion for statistical significance.

IV-3. Results

IV-3-1. Syringic acid inhibits UVB-induced COX-2 and MMP-1 expression, PGE_2 production, and MMP-1 promoter activity in HaCaT cells

Syringic acid exhibited no detectable cell cytotoxicity up to 40 μM in HaCaT cells (Figure IV-1B). Syringic acid significantly inhibited UVB-induced COX-2 and MMP-1 expression (Figure IV-1C and D), as well as PGE_2 production (Figure IV-1E). Using HaCaT cells stably transfected with the MMP-1-luciferase reporter plasmid, I observed that syringic acid significantly inhibited UVB-induced MMP-1 promoter activity (Figure IV-1F).

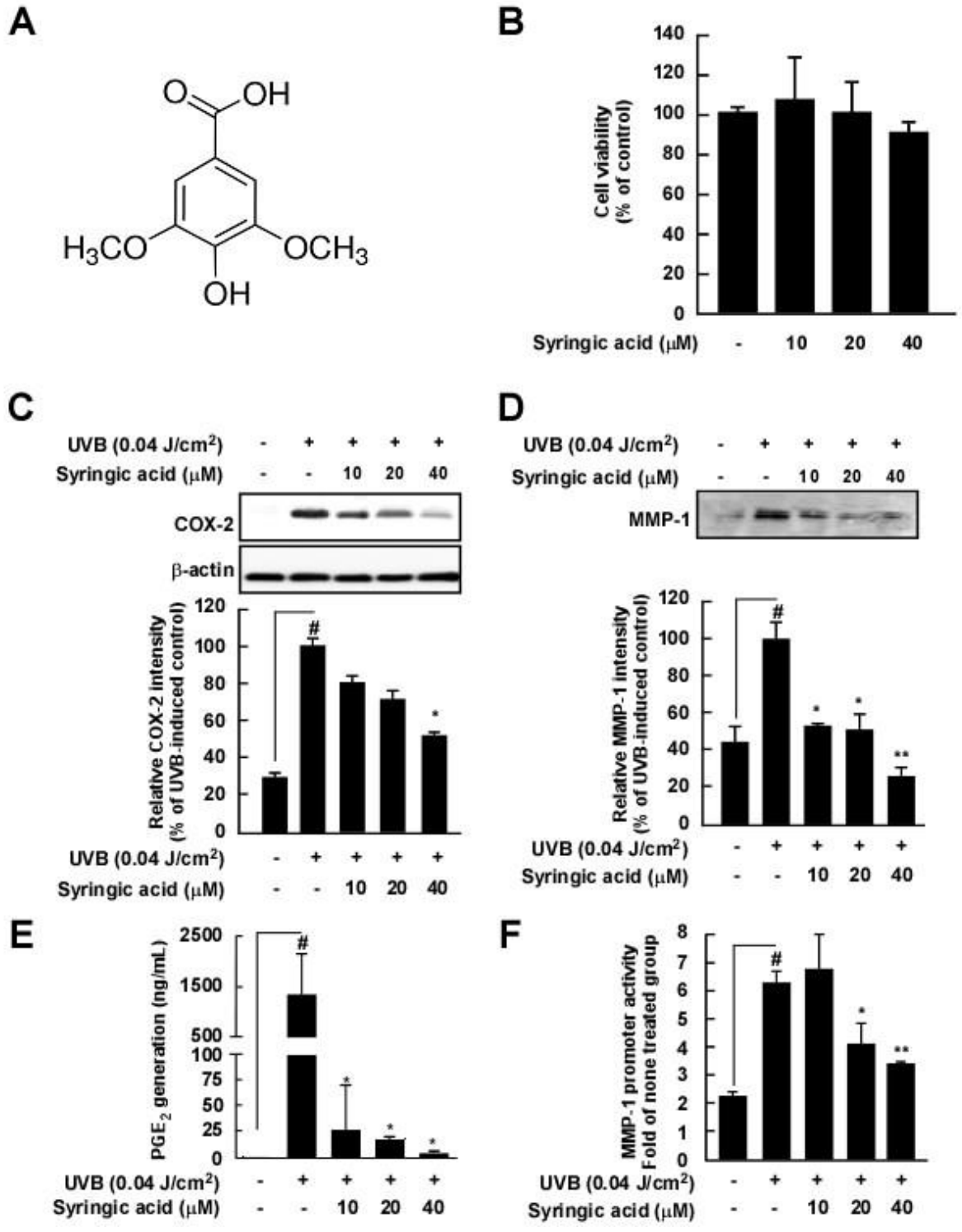

Figure IV-1. Effects of syringic acid on UVB-induced COX-2 and MMP-1 expression, PGE_2 production, and MMP-1 promoter activity in HaCaT cells. (A) Chemical structure of syringic acid. (B) Syringic acid exhibited no detectable cell cytotoxicity up to 40 μM in

HaCaT cells. Cell viability was measured by the MTS assay as described in the Methods. (C) Syringic acid inhibits UVB-induced COX-2 expression in HaCaT cells. (D) Syringic acid inhibits UVB-induced MMP-1 expression in HaCaT cells. Phosphorylation and expression were detected by western blotting assay with specific antibodies. The data represent the mean ± SD of three independent experiments. (E) Syringic acid inhibits UVB-induced PGE_2 generation in HaCaT cells. Expression levels of PGE_2 were determined using Prostaglandin E_2 Express EIA kit. (F) Syringic acid inhibits UVB-induced MMP-1 promoter activity in HaCaT cells. HaCaT cells were stably transfected with an AP-1-luciferase plasmid in the presence or absence of stimulation with UVB (0.04 J/cm^2) for 1 h. #, $p < 0.05$ between the control group and the group exposed to UVB alone; *$p < 0.05$ and **$p < 0.01$ between groups irradiated with UVB and syringic acid and the group exposed to UVB alone.

IV-3-2. Syringic acid inhibits UVB-induced phosphorylation of MAPKs, MAPKKs, and EGFR in HaCaT cells

Since the transcription factor AP-1 is regulated by the upstream MAPK (Karin & Hawkins, 1996), I next examined the effects of syringic acid on the UVB-induced phosphorylation of MAPKs. Syringic acid inhibited the UVB-induced phosphorylation of ERK1/2/JNK1/2/p38, MEK1/2/MKK4/7/MKK3/6, B-Raf, Akt, and Src in HaCaT cells (Figure IV-2A–C). Moreover, syringic acid inhibited the UVB-induced phosphorylation of EGFR on the tyrosine 1068 and 1045 residues (Figure IV-2D).

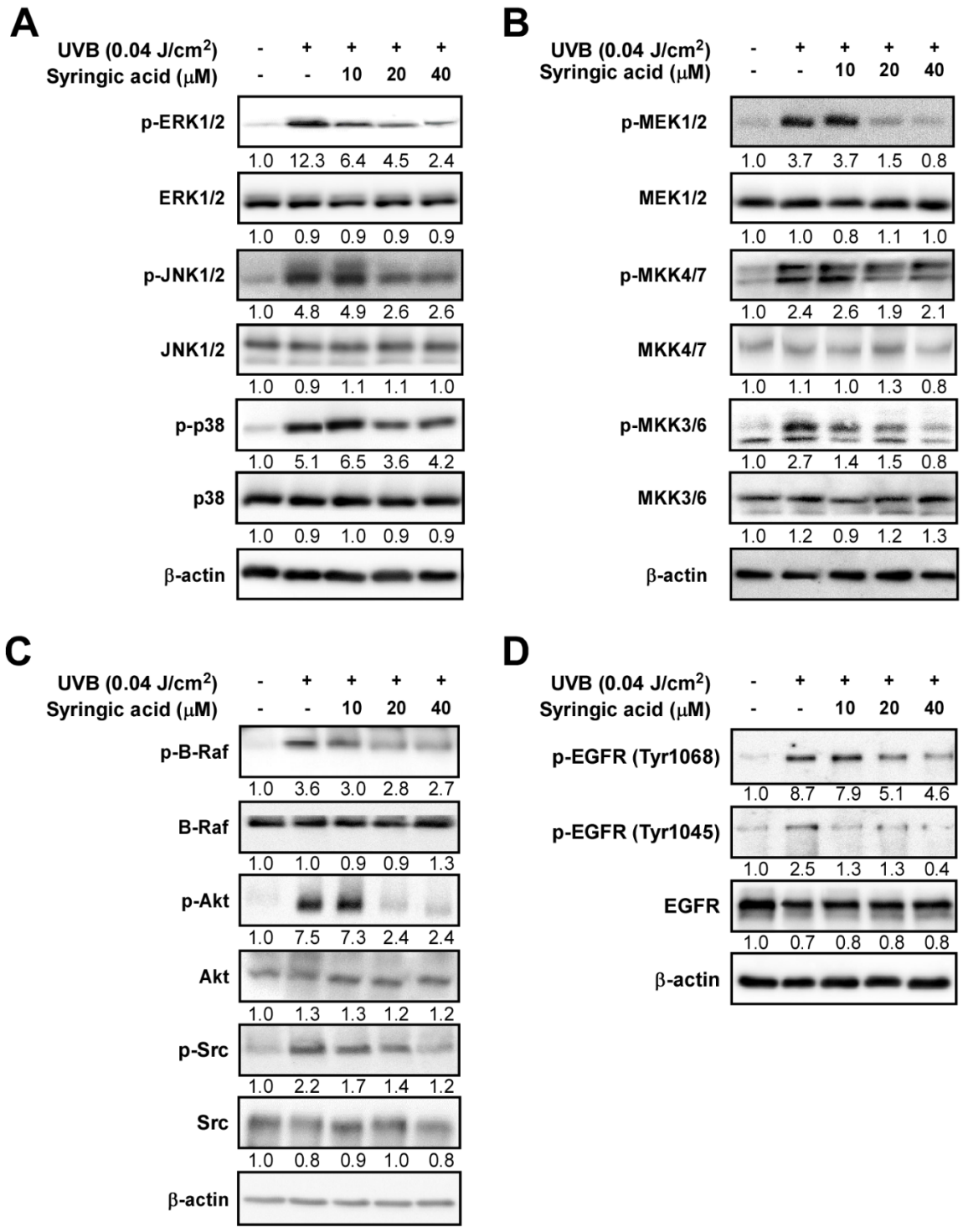

Figure IV-2. Effects of syringic acid on the UVB-induced phosphorylation of MAPKs, MAPKKs, and EGFR in HaCaT cells. (A) Syringic acid inhibits the UVB-induced phosphorylation of ERK1/2, JNK1/2, and p38 in HaCaT cells. (B) Syringic acid inhibits the UVB-induced phosphorylation of MEK1/2, MKK4/7, and MKK3/6 in HaCaT cells. (C)

Syringic acid inhibits the UVB-induced phosphorylation of B-Raf, Akt, and Src in HaCaT cells. (D) Syringic acid inhibits the UVB-induced phosphorylation of EGFR (Tyr 1068) and EGFR (Tyr 1045) in HaCaT cells. Phosphorylation and expression levels were detected by western blotting with specific antibodies. The data represent the mean ± SD of three independent experiments. Densitometry measurements, normalized to β-actin and then compared to control group, are indicated below the corresponding blot.

IV-3-3. Syringic acid inhibits the UVB-induced oxidization of PTP-κ in HaCaT cells

Given that syringic acid suppressed the phosphorylation of EGFR without affecting EGFR expression, I hypothesized that syringic acid may affect the activity of the EGFR phosphatase PTP-κ. UVB irradiation of HaCaT cells decreased PTP-κ activity, which was significantly prevented by treatment with syringic acid (Figure IV-3A). However, PTP-κ protein levels were not changed following UVB irradiation with syringic acid (Figure IV-3D). Immunoprecipitation of EGFR and PTP-κ showed that the level of oxidized PTP-κ was increased by UVB irradiation, which was prevented by syringic acid (Figure IV-3B). In addition, syringic acid inhibited the UVB-induced dissociation of binding between PTP-κ and EGFR in HaCaT cells (Figure IV-3B and C). However, syringic acid did not affect UVB-induced amphiregulin expression (Data not shown), and there was no change in the levels of the EGF-induced phosphorylation of EGFR and Src in HaCaT cells (Data not shown). These results indicated that syringic acid blocks the UVB-mediated inactivation of PTP-κ and the subsequent phosphorylation of EGFR.

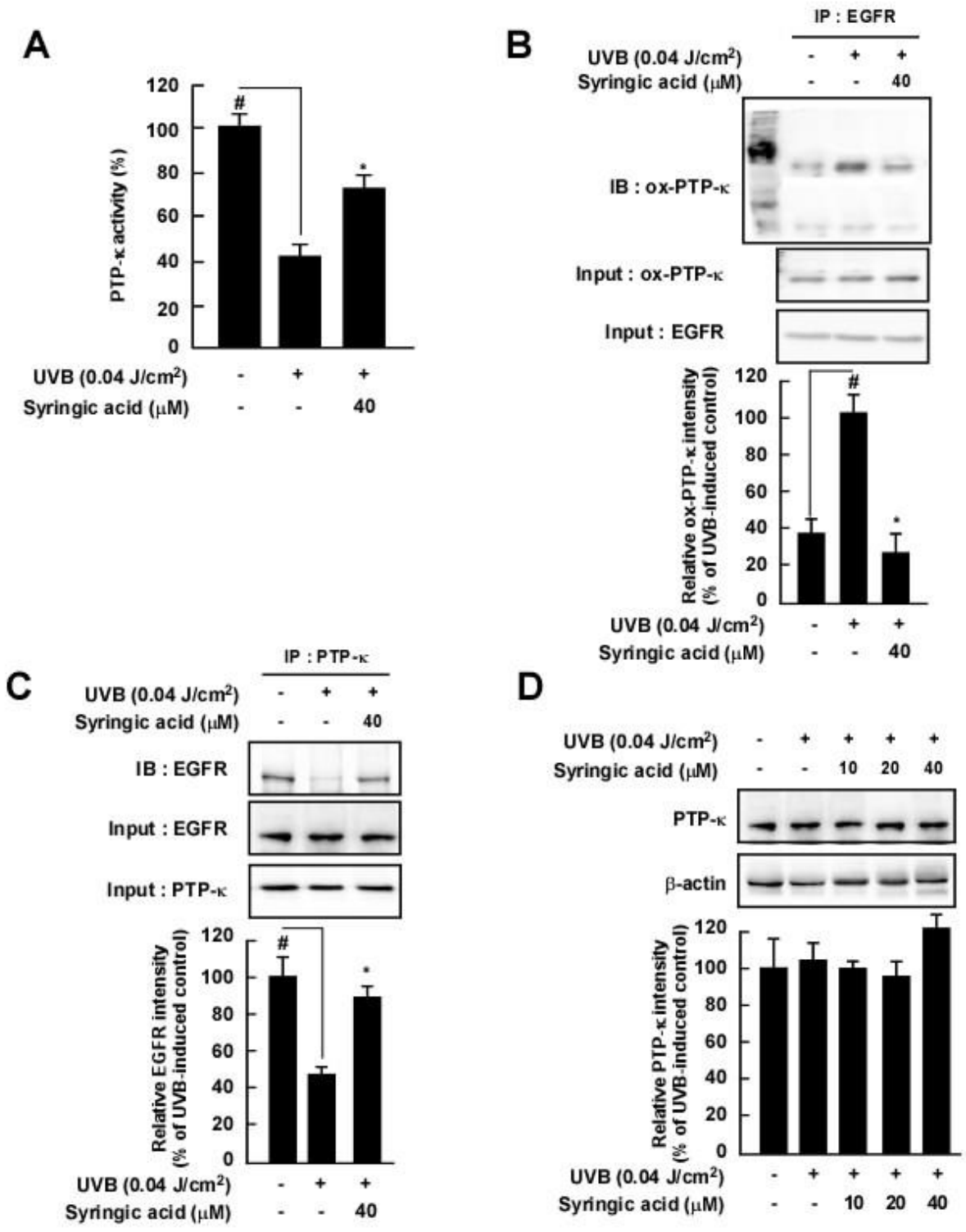

Figure IV-3. Effects of syringic acid on UVB-induced oxidative of PTP-κ in HaCaT cells. (A) Syringic acid increases UVB-induced PTP-κ activity in HaCaT cells. (B) Syringic acid inhibits UVB-induced oxidized PTP-κ in HaCaT cells. (C) Syringic acid inhibits UVB-

induced PTP-κ as a regulator of EGFR activation in HaCaT cells. (D) PTP-κ protein levels were not changed following UVB irradiation and syringic acid treatment. #, $p < 0.05$ between the control group and the group exposed to UVB alone; *$p < 0.05$ between groups irradiated with UVB and syringic acid and the group exposed to UVB alone. PTP-κ was immunoprecipitated, and phosphatase activity was determined using a phosphorylated EGFR peptide as substrate. Phosphatase activity was normalized to PTP-κ protein content in the immunoprecipitates, which was quantified by western blot analysis using chemifluorescent detection. Results are the mean ± SD of three independent experiments.

IV-3-4. Syringic acid and NAC inhibit UVB-induced intracellular ROS generation in HaCaT cells

To investigate the effect of syringic acid on UVB-induced ROS production, I evaluated several potential probes that detect specific ROS species, and found that syringic acid only affected CM-2′,7′-dichlorofluorescein diacetate (CM-H_2DCFDA), (Figure IV-4A, B, C and D), which is a hydrogen peroxide-detecting probe commonly used for the measurement of hydrogen peroxide in intact cells (Singh, Schneider, Knyazev, & Ullrich, 2009). Therefore, I assumed that syringic acid may affect NADPH oxidase activity and subsequently regulate UVB-induced $O_2 \cdot^-$ production. To compare the antioxidant effect of syringic acid, I used the established antioxidant NAC as a positive control. UVB irradiation increased intracellular ROS levels, which was decreased with treatment of syringic acid in HaCaT cells (Figure IV-4A and B). In particular, NADPH oxidase activity was markedly increased by UVB-irradiation, which was inhibited by both syringic acid and NAC (Figure IV-4E). Moreover, NAC inhibited the UVB-induced phosphorylation of EGFR, Src, and MAPKs in HaCaT cells (Figure IV-5A and B). These inhibitory effects were exactly in agreement with those of syringic acid (Figure IV-2).

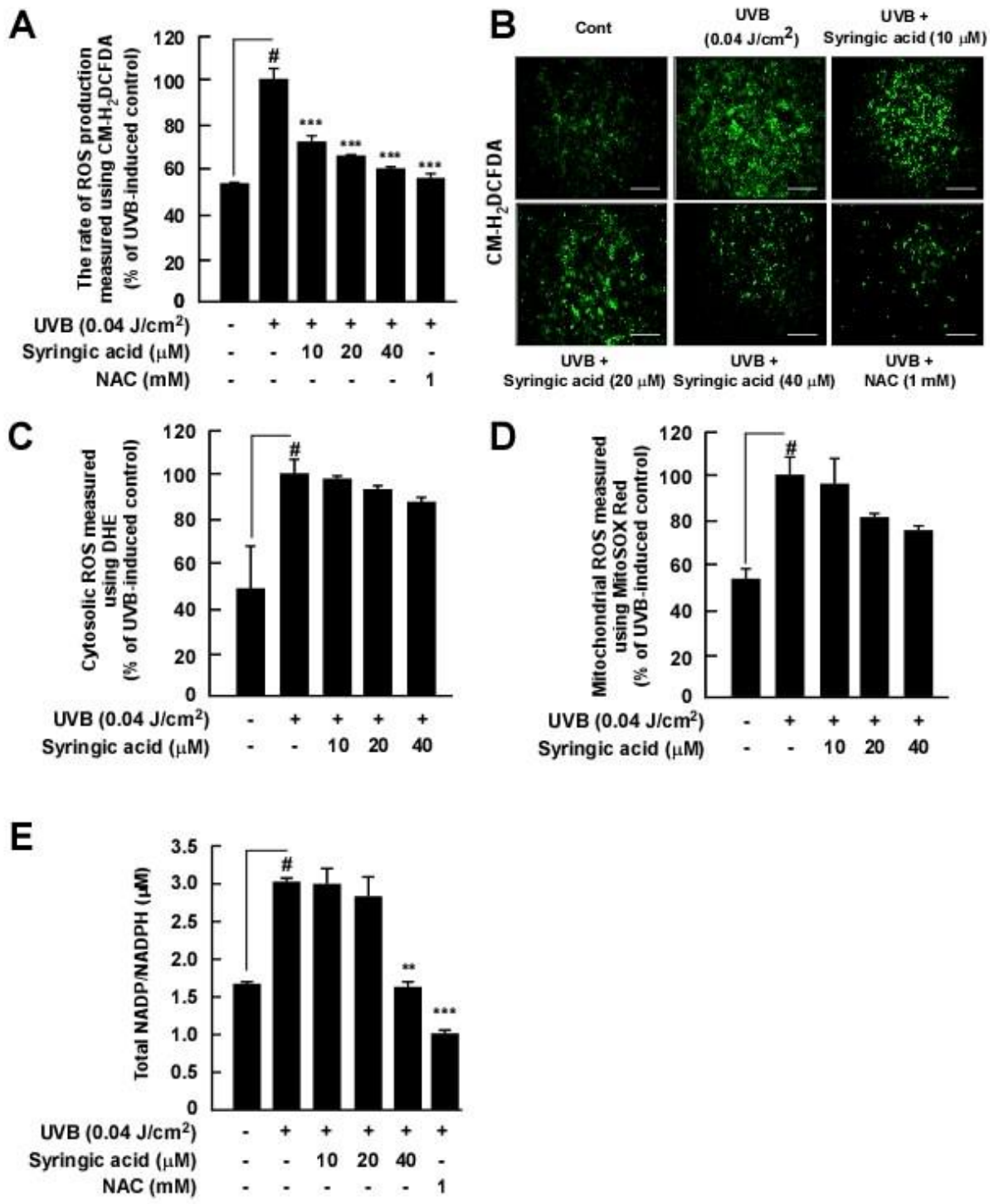

Figure IV-4. Effects of syringic acid and NAC on UVB-induced intracellular reactive oxygen species (ROS) generation in HaCaT cells. (A) Syringic acid and NAC inhibit UVB-induced intracellular ROS generation in HaCaT cells. (B) H_2DCFHDA fluorescence was visualized by fluorescence microscopy. (C) Syringic acid was not affected UVB-induced cytosolic ROS

generation in HaCaT cells. (D) Syringic acid was not affected UVB-induced mitochondrial ROS generation in HaCaT cells. (E) Syringic acid and NAC inhibit UVB-induced NADPH oxidase activity. Densitometry measurements, normalized to β-actin and then compared to control group, are indicated below the corresponding blot. The data represent the mean ± SD of three independent experiments. *#, $p < 0.05$* between the control group and the group exposed to UVB alone; ***$p < 0.01$* and ****$p < 0.001$* between groups irradiated with UVB and syringic acid and the group exposed to UVB alone.

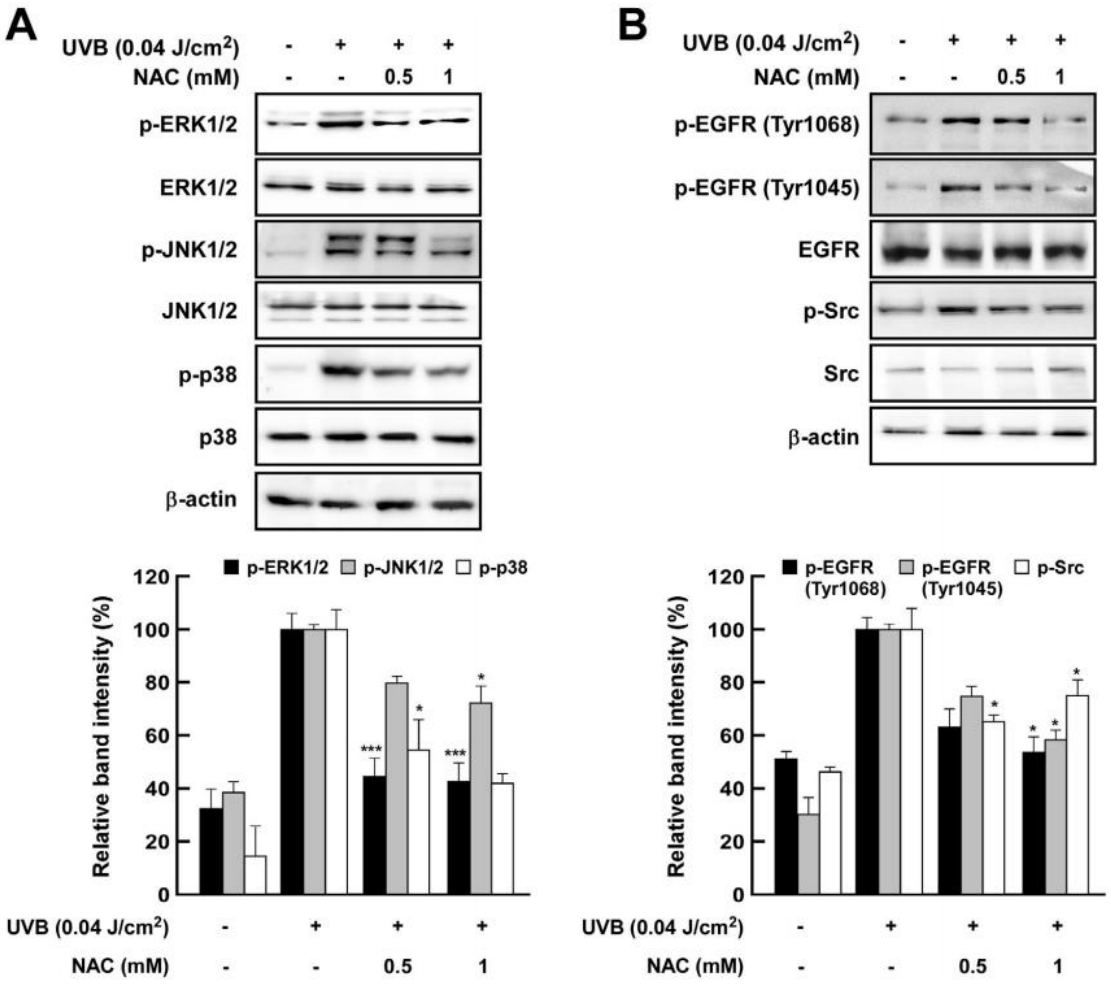

Figure IV-5. Effects of NAC on UVB-induced phosphorylation of MAPKs, EGFR, and Src in HaCaT cells. (A) NAC inhibits UVB-induced phosphorylation of ERK1/2, JNK1/2, and p38 in HaCaT cells. (B) NAC inhibits UVB-induced phosphorylation of EGFR (Tyr 1068), EGFR (Tyr 1045), and Src in HaCaT cells. Phosphorylation and expression were detected by Western blotting with specific antibodies. Densitometry measurements, normalized to β-actin and then compared to the control group, are shown below the corresponding blot. The data represent the mean ± SD of three independent experiments. #, $p < 0.05$ between the control group and the group exposed to UVB alone; **$p < 0.01$ and ***$p < 0.001$ between the groups irradiated with UVB and syringic acid and the group exposed to UVB alone.

IV-3-5. Syringic acid prevents UVB-induced skin tumorigenesis in SKH-1 hairless mice

To evaluate the direct anti-tumorigenic activity of syringic acid *in vivo*, I investigated the effect of syringic acid on UVB-induced two-stage skin tumorigenesis. Representation photographs of the tumors that developed in the mice are shown in Figure IV-5A, demonstrating that syringic acid significantly inhibited UVB-induced mouse skin cancer development compared with the UVB-only irradiated mice. Topical application of syringic acid on the mouse skin reduced the tumor number by 17.7% at 0.2 mM and by 35.7% at 1 mM compared to the UVB-only irradiated group (Figure IV-6B*).* Skin tumors developed after 10 weeks in the UVB-only-treated group, whereas tumor development in the syringic acid-treated group was delayed by 1–2 weeks in the SKH-1 mice (Figure IV-6C). Further, the syringic acid-treated mice showed a significant reduction in epidermal thickening by 48.4% compared to the UVB irradiation-only mice (Figure IV-6D).

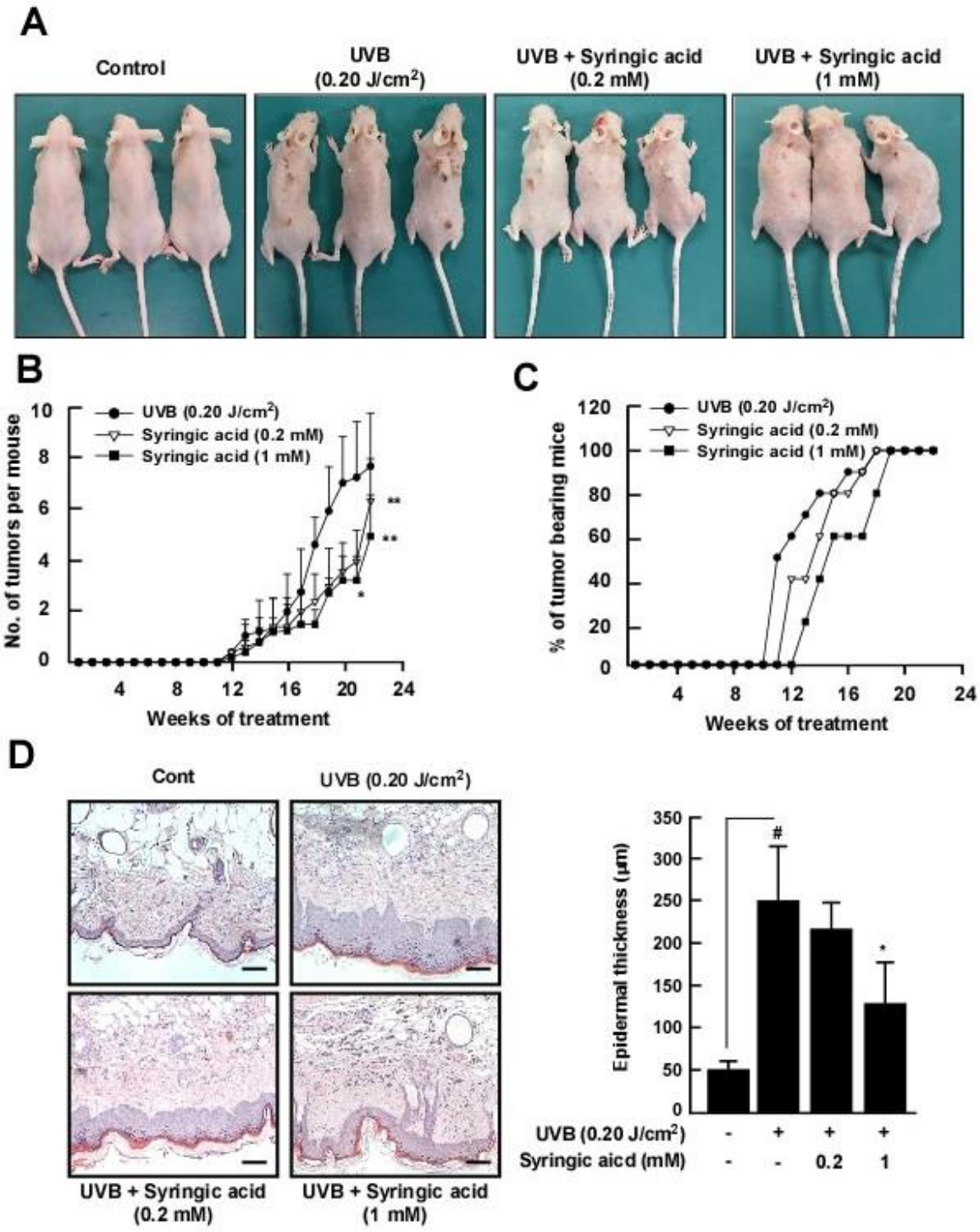

Figure IV-6. Effects of syringic acid on UVB-induced skin carcinogenesis in the SKH-1 hairless mouse. Control mice (n = 5) received topical treatment of 200 μL acetone (no UVB), and experimental mice (n = 5) were topically treated with 200 μL acetone before UVB (0.2 J/cm^2) exposure (3 days/week for 22 weeks). The mice in the third and fourth groups received topical application of syringic acid (0.2 or 1 mM, respectively, per mouse in 200 μL acetone)

on the dorsal surface 1 h before UVB (0.2 J/cm^2) irradiation 3 days/week for 22 weeks. (A) External appearance of tumors. (B) Syringic acid inhibits UVB-induced cancer incidence in the SKH-1 hairless mouse. (C) Syringic acid retarded the incidence of skin tumors compared with the UVB only-treated group. (D) Syringic acid inhibits UVB-induced increasing mouse epidermal thickness. Hematoxylin and eosin-stained images of UVB-irradiated mouse skin. Images are representative of results from 5 tissue samples. #, $p < 0.05$ between the control group and the group exposed to UVB alone; *$p < 0.05$ and **$p < 0.01$, between groups irradiated with UVB and syringic acid and the group exposed to UVB alone.

IV-3-6. Syringic acid inhibits UVB-induced COX-2 and MMP-13 expression in SKH-1 hairless mice

Similar to *in vitro* results, the western blot assay showed that syringic acid significantly inhibited UVB-induced COX-2 and MMP-13 expression in the skin of SKH-1 hairless mice (Figure IV-7A). Immunohistochemical analysis confirmed the syringic acid-dependent inhibition of UVB-induced COX-2 and MMP-13 expression (Figure IV-7B).

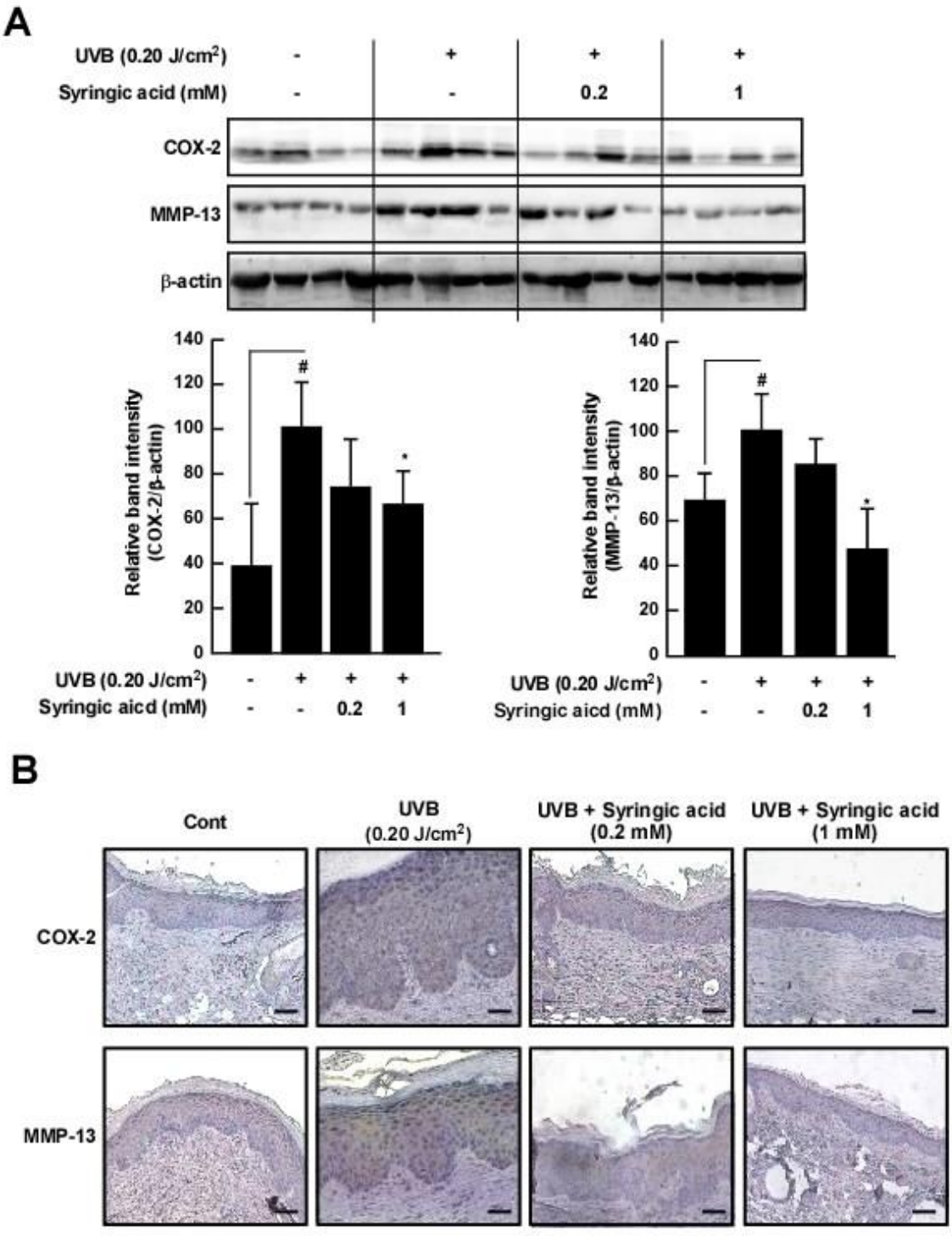

Figure IV-7. Effect of syringic acid on UVB-induced COX-2 and MMP-13 expression in SKH-1 hairless mice. (A) Syringic acid inhibits UVB-induced COX-2 and MMP-13 expression in SKH-1 hairless mice. Skin samples from mice were analyzed for COX-2 and MMP-13 expression by western blot. (B) Immunohistochemical staining for COX-2 and

MMP-13 expression in the skin (magnification 200×). Skin samples were stained for COX-2 and MMP-13 expression with a specific polyclonal antibody and analyzed by microscopy. *#*, $p < 0.05$ between the control group and the group exposed to UVB alone; *$p < 0.05$ between groups irradiated with UVB and syringic acid and the group exposed to UVB alone. The data represent the mean ± SD of five mice per group.

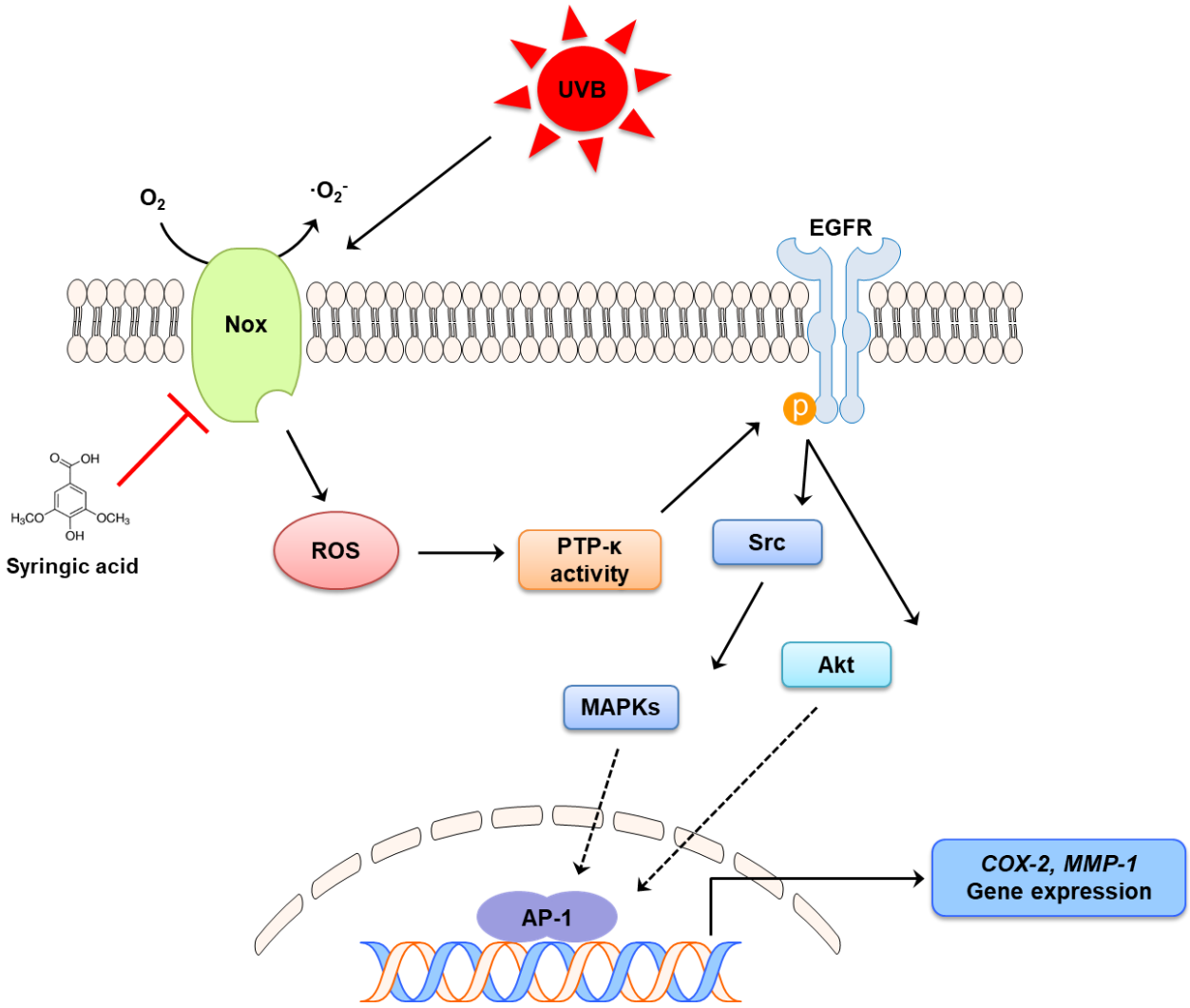

Figure IV-8. Mechanism of syringic acid prevents skin carcinogenesis via regulation of Nox and EGFR signaling.

IV-4. Discussion

Skin cancer is one of the most common forms of cancer worldwide, which is largely caused by UV exposure (Vaid, Singh, Prasad, & Katiyar, 2014). Indeed, UV irradiation is a complete carcinogen, capable of causing cell transformation and promoting tumor formation. ROS are constantly generated and eliminated in biological systems and are required to drive regulatory pathways (Oh, Kim, Park, Yi, Park, Rho, et al., 2013). Under normal physiological conditions, cells control ROS levels by balancing the generation with their elimination via scavenging system (Liou & Storz, 2010; Schafer & Werner, 2015). However, when the UV-induced generation of ROS exceeds the capacity of chemical and enzymatic redox system in cells, the oxidative damage can lead to the development of chronic diseases, including cancer (Lobo, Patil, Phatak, & Chandra, 2010).

One of the main damaging features of this response to UV is the induction of AP-1, which is mediated by numerous cytokines, COX-2, and MMPs (Rundhaug & Fischer, 2008). Fischer et al. (Fischer, Pavone, Mikulec, Langenbach, & Rundhaug, 2007) found that mice with COX-2 deficiency showed a 50–65% decrease in UV-induced tumor multiplicity compared with wild-type mice, highlighting the major role of COX-2 in UVB-induced skin cancer. Indeed, in the present study, the MMP-1 reporter gene assay and western blot assay clearly showed that syringic acid could strongly suppress UVB-induced COX-2 and MMP-1 expression, as well as PGE_2 production, by suppressing MMP-1 promoter activity. Since our previous study showed that phytochemicals from plants have strong chemopreventive effects via the suppression of AP-1/COX-2 signaling pathways, the present results strongly support the potent chemopreventive effects of syringic acid.

UV irradiation to skin activates several oncogenic signaling pathways (de Gruijl et al., 2001). Once hyperactivated by UV, EGFR up-regulates the expression of MAPKs and Akt in HaCaT cells and in the skin of SKH-1 hairless mice (Jung et al., 2010; Xu, Shao, Zhou, Voorhees, & Fisher, 2009). I observed that syringic acid could effectively suppress this UVB-induced phosphorylation of EGFR, Src, MAPKKs/ MAPKs, and Akt in HaCaT cells. EGFR plays a central role in UV-induced carcinogenesis, promoting cancer cell growth and survival. UV regulates ADAM activity and consequently cleaves amphiregulin, a ligand for EGFR (Nakayama, Fukuda, Inoue, Nishida-Fukuda, Shirakata, Hashimoto, et al., 2012; Singh, Schneider, Knyazev, & Ullrich, 2009). Therefore, among the multiple mechanisms of EGFR activation, I initially hypothesized that syringic acid would affect the ADAM and amphiregulin levels; however, syringic acid did not influence UVB-induced amphiregulin expression or the EGF-induced phosphorylation of EGFR and Src in HaCaT cells. Therefore, I excluded the possibility that syringic acid regulates EGFR activity via modulating production of the EGFR ligand.

UV-mediated EGFR activation has been reported to be closely related to the phosphor (Paulsen, Truong, Garcia, Homann, Gupta, Leonard, et al., 2012; Rittie & Fisher, 2002). PTP-κ is a phosphatase that regulates the phosphorylation/activation of the intra-cytoplasmic domain of membrane-bound EGFR (Xu, Shao, Voorhees, & Fisher, 2006), and inhibition of protein tyrosine phosphatases increases intrinsic receptor phosphorylation/activation by shifting the balance toward the phosphorylated state (Xu, Tan, Grachtchouk, Voorhees, & Fisher, 2005). In support of this mechanism, syringic acid significantly increased PTP-κ activity, as a regulator of EGFR activation in HaCaT cells. Zorov et al (Zorov, Juhaszova, & Sollott, 2014) indicated that UV-induced ROS production impaired PTP-κ activity. Indeed, our immunoprecipitation and western blot assay results clearly showed that syringic acid strongly blocks the UV-induced oxidation of PTP-κ;

however, syringic acid did not affect PTP-κ or EGFR expression. Collectively, these results indicate that syringic acid suppresses UVB-induced EGFR phosphorylation via inhibition of the oxidation of PTP-κ.

Moreover, both syringic acid and the known antioxidant NAC inhibited UVB-induced intracellular ROS generation in HaCaT cells. NAC also inhibited the UVB-induced phosphorylation of EGFR, Src, and MAPKs in HaCaT cells, showing a similar role to syringic acid. NADPH oxidase (Nox) is the key enzyme responsible for ROS production, and its inhibition thus represents an attractive therapeutic target for the treatment of many diseases related to oxidative stress (Jaquet, Scapozza, Clark, Krause, & Lambeth, 2009). Although UVB radiation enhanced NADPH oxidase activity, both syringic acid and NAC inhibited these effects. Interestingly, although NAC had a higher inhibitory effect on UVB-induced NADPH oxidase activity, the concentration of syringic acid (40 μM) was 10 times lower than that of NAC. Currently, several antioxidants that targets NADPH oxidase are commonly used as pharmaceuticals or in research (Williams & Griendling, 2007). However, because of their lack of specificity and isoform selectivity, effective novel inhibitors are still desired. These results suggest that syringic acid acts as an inhibitor of Nox to reduce ROS. However, prior to the application of syringic acid as a pharmaceutical inhibitor of Nox, the binding affinity between syringic acid and Nox should be investigated and the specific binding site should be further elucidated.

The SKH-1 mouse line is a common model used in research on UV carcinogenesis (Jung et al., 2010). Chronic exposure of these mice to UVB irradiation leads to the development of benign epidermal tumors. I further confirmed that syringic acid suppresses chronic UV-irradiation induced skin cancer in the skin of SKH-1 hairless mice. As expected, topical application of syringic acid prevented chronic UV-induced tumor incidence and the

up-regulated expression of COX-2 and MMP-13 in the mouse skin.

IV-5. Conclusions

Overall, my study demonstrates that syringic acid exerted excellent inhibitory effects on UV-induced skin carcinogenesis by targeting the Nox/ROS/PTP-κ/EGFR axis. Thus, syringic acid is expected to have highly beneficial effects in the prevention of skin carcinogenesis. Syringic acid is a naturally derived compound with antioxidative, anti-inflammatory, and anti-carcinogenesis effects. However, its inhibitory mechanisms remain unclear, and its effects on UV-induced oxidative damage to the skin have not been examined. Here, I demonstrate that syringic acid suppressed the UVB-induced activation of AP-1/COX-2 signaling pathways in human keratinocytes, and reduced tumor formation in the skin of UV-irradiated hairless mice, strongly supporting its potent chemopreventive activity. Syringic acid can serve as a pharmaceutical inhibitor of NADPH oxidase to inhibit UV-induced reactive oxygen species production and prevent skin cancer development, highlighting its potential as a natural therapeutic agent.

IV-6. References

Buckman, S., Gresham, A., Hale, P., Hruza, G., Anast, J., Masferrer, J., & Pentland, A. P. (1998). COX-2 expression is induced by UVB exposure in human skin: implications for the development of skin cancer. *Carcinogenesis, 19*(5), 723-729.

D'Orazio, J., Jarrett, S., Amaro-Ortiz, A., & Scott, T. (2013). UV radiation and the skin. *International Journal of Molecular Sciences, 14*(6), 12222-12248.

de Gruijl, F. R., van Kranen, H. J., & Mullenders, L. H. (2001). UV-induced DNA damage, repair, mutations and oncogenic pathways in skin cancer. *Journal of Photochemistry and Photobiology B: Biology, 63*(1-3), 19-27.

Elmets, C. A., Ledet, J. J., & Athar, M. (2014). Cyclooxygenases: mediators of UV-induced skin cancer and potential targets for prevention. *Journal of Investigative Dermatology, 134*(10), 2497-2502.

Fischer, S. M., Pavone, A., Mikulec, C., Langenbach, R., & Rundhaug, J. E. (2007). Cyclooxygenase-2 expression is critical for chronic UV-induced murine skin carcinogenesis. *Molecular Carcinogenesis, 46*(5), 363-371.

Ha, S. J., Lee, J., Kim, H., Song, K.-M., Lee, N. H., Kim, Y. E., Lee, H., Kim, Y. H., & Jung, S. K. (2016). Preventive effect of Rhus javanica extract on UVB-induced skin inflammation and photoaging. *Journal of Functional Foods, 27*, 589-599.

Herrlich, P., Karin, M., & Weiss, C. (2008). Supreme EnLIGHTenment: damage recognition and signaling in the mammalian UV response. *Molecular Cell, 29*(3), 279-290.

Jaquet, V., Scapozza, L., Clark, R. A., Krause, K.-H., & Lambeth, J. D. (2009). Small-molecule Nox inhibitors: ROS-generating NADPH oxidases as therapeutic targets. *Antioxidants & Redox Signaling, 11*(10), 2535-2552.

Jemal, A., Siegel, R., Xu, J., & Ward, E. (2010). Cancer statistics, 2010. *CA: A Cancer Journal for Clinicians, 60*(5), 277-300.

Jung, S. K., Ha, S. J., Jung, C. H., Kim, Y. T., Lee, H. K., Kim, M. O., Lee, M. H., Mottamal, M., Bode, A. M., & Lee, K. W. (2016). Naringenin targets ERK 2 and suppresses UVB-induced photoaging. *Journal of Cellular and Molecular Medicine, 20*(5), 909-919.

Jung, S. K., Ha, S. J., Jung, C. H., Kim, Y. T., Lee, H. K., Kim, M. O., Lee, M. H., Mottamal, M., Bode, A. M., & Lee, K. W. (2010). Myricetin inhibits UVB-induced angiogenesis by regulating PI-3 kinase in vivo. *Carcinogenesis, 31*(5), 911-917.

Jung, S. K., Lee, K. W., Kim, H. Y., Oh, M. H., Byun, S., Lim, S. H., Heo, Y.-S., Kang, N. J., Bode, A. M., & Dong, Z. (2010). Myricetin suppresses UVB-induced wrinkle formation and MMP-9 expression by inhibiting Raf. *Biochemical Pharmacology, 79*(10), 1455-1461.

Karin, M., & Marshall, C. J. (1996). The regulation of AP-1 activity by mitogen-activated protein kinases. *Philosophical Transactions of the Royal Society of London. Series B: Biological Sciences, 351*(1336), 127-134.

Lee, C.-W., Lin, Z.-C., Hu, S. C.-S., Chiang, Y.-C., Hsu, L.-F., Lin, Y.-C., Lee, I.-T., Tsai, M.-H., & Fang, J.-Y. (2016). Urban particulate matter down-regulates filaggrin via COX2 expression/PGE2 production leading to skin barrier dysfunction. *Scientific Reports, 6*(1), 1-16.

Lim, T. G., Jung, S. K., Kim, J. e., Kim, Y., Lee, H. J., Jang, T. S., & Lee, K. W. (2013). NADPH oxidase is a novel target of delphinidin for the inhibition of UVB-induced MMP-1 expression in human dermal fibroblasts. *Experimental Dermatology, 22*(6), 428-430.

Liou, G.-Y., & Storz, P. (2010). Reactive oxygen species in cancer. *Free Radical Research,*

44(5), 479-496.

Lobo, V., Patil, A., Phatak, A., & Chandra, N. (2010). Free radicals, antioxidants and functional foods: Impact on human health. *Pharmacognosy Reviews, 4*(8), 118.

Muthukumaran, J., Srinivasan, S., Venkatesan, R. S., Ramachandran, V., & Muruganathan, U. (2013). Syringic acid, a novel natural phenolic acid, normalizes hyperglycemia with special reference to glycoprotein components in experimental diabetic rats. *Journal of Acute Disease, 2*(4), 304-309.

Nakayama, H., Fukuda, S., Inoue, H., Nishida-Fukuda, H., Shirakata, Y., Hashimoto, K., & Higashiyama, S. (2012). Cell surface annexins regulate ADAM-mediated ectodomain shedding of proamphiregulin. *Molecular Biology of the Cell, 23*(10), 1964-1975.

Oh, J., Kim, J. H., Park, J. G., Yi, Y.-S., Park, K. W., Rho, H. S., Lee, M.-S., Yoo, J. W., Kang, S.-H., & Hong, Y. D. (2013). Radical scavenging activity-based and AP-1-targeted anti-inflammatory effects of lutein in macrophage-like and skin keratinocytic cells. *Mediators of Inflammation, 2013*.

Pacheco-Palencia, L. A., Mertens-Talcott, S., & Talcott, S. T. (2008). Chemical composition, antioxidant properties, and thermal stability of a phytochemical enriched oil from Acai (Euterpe oleracea Mart.). *Journal of Agricultural and Food Chemistry, 56*(12), 4631-4636.

Park, W. H. (2013). The effects of exogenous H2O2 on cell death, reactive oxygen species and glutathione levels in calf pulmonary artery and human umbilical vein endothelial cells. *International Journal of Molecular Medicine, 31*(2), 471-476.

Paulsen, C. E., Truong, T. H., Garcia, F. J., Homann, A., Gupta, V., Leonard, S. E., & Carroll, K. S. (2012). Peroxide-dependent sulfenylation of the EGFR catalytic site enhances kinase activity. *Nature Chemical Biology, 8*(1), 57.

Ricciotti, E., & FitzGerald, G. A. (2011). Prostaglandins and inflammation. *Arteriosclerosis,*

Thrombosis, and Vascular Biology, 31(5), 986-1000.

Rittié, L., & Fisher, G. J. (2002). UV-light-induced signal cascades and skin aging. *Ageing Research Reviews, 1*(4), 705-720.

Rogers, H. W., Weinstock, M. A., Feldman, S. R., & Coldiron, B. M. (2015). Incidence estimate of nonmelanoma skin cancer (keratinocyte carcinomas) in the US population, 2012. *JAMA Dermatology, 151*(10), 1081-1086.

Rundhaug, J. E., & Fischer, S. M. (2008). Cyclo-oxygenase-2 plays a critical role in UV-induced skin carcinogenesis. *Photochemistry and Photobiology, 84*(2), 322-329.

Ryu, J. Y., & Na, E. J. (2018). MMP expression alteration and MMP-1 production control by syringic acid via AP-1 mechanism. *Biomedical Dermatology*, 2(1), 1-10.

Schäfer, M., & Werner, S. (2015). Nrf2—A regulator of keratinocyte redox signaling. *Free Radical Biology and Medicine, 88*, 243-252.

Schieber, M., & Chandel, N. S. (2014). ROS function in redox signaling and oxidative stress. *Current Biology, 24*(10), R453-R462.

Siegel, R., Ma, J., Zou, Z., & Jemal, A. (2014). Cancer statistics, 2014. *CA: A Cancer Journal for Clinicians, 64*(1), 9-29.

Siegel, R. L., Miller, K. D., & Jemal, A. (2016). Cancer statistics, 2016. *CA: A Cancer Journal for Clinicians, 66*(1), 7-30.

Singh, B., Schneider, M., Knyazev, P., & Ullrich, A. (2009). UV-induced EGFR signal transactivation is dependent on proligand shedding by activated metalloproteases in skin cancer cell lines. *International Journal of Cancer, 124*(3), 531-539.

Sun, Z., Park, S. Y., Hwang, E., Zhang, M., Seo, S. A., Lin, P., & Yi, T. H. (2017). Thymus vulgaris alleviates UVB irradiation induced skin damage via inhibition of MAPK/AP-1 and activation of Nrf2-ARE antioxidant system. *Journal of Cellular and Molecular Medicine, 21*(2), 336-348.

Svobodova, A., Walterova, D., & Vostalova, J. (2006). Ultraviolet light induced alteration to the skin. *Biomedical Papers-Palacky University in Olomouc, 150*(1), 25.

Vaid, M., Singh, T., Prasad, R., & Katiyar, S. K. (2014). Intake of high-fat diet stimulates the risk of ultraviolet radiation-induced skin tumors and malignant progression of papillomas to carcinoma in SKH-1 hairless mice. *Toxicology and Applied Pharmacology, 274*(1), 147-155.

Williams, H. C., & Griendling, K. K. (2007). NADPH oxidase inhibitors: new antihypertensive agents? *Journal of Cardiovascular Pharmacology, 50*(1), 9-16.

Wojtala, A., Bonora, M., Malinska, D., Pinton, P., Duszynski, J., & Wieckowski, M. R. (2014). Methods to monitor ROS production by fluorescence microscopy and fluorometry. *Methods in Enzymology, 542*, 243-262.

Wu, W., Silbajoris, R. A., Whang, Y. E., Graves, L. M., Bromberg, P. A., & Samet, J. M. (2005). p38 and EGF receptor kinase-mediated activation of the phosphatidylinositol 3-kinase/Akt pathway is required for Zn2+-induced cyclooxygenase-2 expression. *American Journal of Physiology-Lung Cellular and Molecular Physiology, 289*(5), L883-L889.

Xu, Y., Baker, D., Quan, T., Baldassare, J. J., Voorhees, J. J., & Fisher, G. J. (2010). Receptor type protein tyrosine phosphatase-kappa mediates cross-talk between transforming growth factor-beta and epidermal growth factor receptor signaling pathways in human keratinocytes. *Molecular Biology of the Cell, 21*(1), 29-35.

Xu, Y., Shao, Y., Voorhees, J. J., & Fisher, G. J. (2006). Oxidative inhibition of receptor-type protein-tyrosine phosphatase κ by ultraviolet irradiation activates epidermal growth factor receptor in human keratinocytes. *Journal of Biological Chemistry, 281*(37), 27389-27397.

Xu, Y., Shao, Y., Zhou, J., Voorhees, J. J., & Fisher, G. J. (2009). Ultraviolet irradiation-

induces epidermal growth factor receptor (EGFR) nuclear translocation in human keratinocytes. *Journal of Cellular Biochemistry, 107*(5), 873-880.

Xu, Y., Tan, L.-J., Grachtchouk, V., Voorhees, J. J., & Fisher, G. J. (2005). Receptor-type protein-tyrosine phosphatase-κ regulates epidermal growth factor receptor function. *Journal of Biological Chemistry, 280*(52), 42694-42700.

Zorov, D. B., Juhaszova, M., & Sollott, S. J. (2014). Mitochondrial reactive oxygen species (ROS) and ROS-induced ROS release. *Physiological Reviews, 94*(3), 909-950.

국문 초록

과도한 자외선(UV)의 노출은 피부 염증 및 피부암 발생의 주요 원인 중 하나이다. 유전적 요인과 생활습관에 따라 그 경향은 다르게 나타날 수 있지만, 반복적으로 자외선에 노출된 피부는 불규칙한 갈색 반점과 주름 형성이 나타나며, 이를 총칭하여 광노화(photoaging)라고 한다. 전사 인자 AP-1은 *mmp-1*과 *cox-2* 유전자의 발현 조절을 통해 광노화, 피부염증, 피부암의 발생에 주요한 역할을 한다. AP-1이 자외선에 의한 광노화 및 염증의 중심 매개체이기 때문에, AP-1 활성을 억제할 수 있는 화합물을 효율적으로 선별 가능한 분석 도구의 개발은 새로운 항 광노화 및 항 염증 제를 개발하기 위한 효과적인 전략이 될 것이다.

새로운 항 광노화 및 항염증 제를 선별하기 위해, MMP-1 프로모터를 인간 각질세포인 HaCaT 세포에서 안정적으로 발현되는 형질전환 세포를 구축하였으며, 항생제 선별을 통해 MMP-1 프로모터가 포함된 pGF1 벡터로 HaCaT 세포에 성공적으로 형질전환 된 것을 확인하였다. MMP-1 luciferase 분석 조건을 확립하고 infection 된 세포의 자외선에 대한 반응을 분석하기 위하여 자외선 강도와 시간에 따른 luciferase 활성을 확인하였다. 실험결과 0.04 J/cm^2, 5시간에서 가장 높은 luciferase 활성을 나타내어, 향후 luciferase assay 조건으로 고정하였다. 이 세포를 이용하여, 식물 추출물 9개를 선별하였다. 그 결과, 오배자 추출물(RJE)과 봉출 추출믈이 UVB에 의하여 유도된 MMP-1 프로모터 결합 활성을 각각 80.9%, 75.8%로 억제하여 가장 우수한 광노화 억제 소재로 선별하였다. 또한, 25-100 μg/mL의 농도에서 HaCaT 세포에서 독성이 나타나지 않았다.

UVB에 의하여 유도된 MMP-1 프로모터 결합 활성 및 세포 독성에 대한 다양한 RJE의 농도 별로 평가한 결과 RJE는 UVB에 의하여 유도된 MMP-1 프로모터 결합 활성을 농도 의존적으로 억제하는 것으로 나타났다. UVB에 의하여 COX-2와 MMP-1의 발현이 증가하였으며, RJE의 농도 의존적으로 COX-2와 MMP-1의 발현을 현저하게 저해하였다. 또한, RJE가 HaCaT 세포에서 UVB에 의하여 유도된 MAPKs/MAPKKs/Akt 인산화를 모든 농도에서 현저하게 억제하였다. SKH-1 무모 쥐 모델을 사용한 실험 결과에서 RJE의 경구 투여가 UVB에 의하여 생성된 주름의 형성과 마우스 피부조직에서 COX-2 및 MMP-13 발현을 유의적으로 억제하였다. 이러한 결과는 RJE가 COX-2 및 MMP-1 발현을 억제하는 강력한 항염증 및 광노화 억제제로 개발 가능성을 제시하고 있다.

또 다른 소재로, 봉출 추출물(CZE)이 HaCaT 세포에서 UVB에 의하여 유도된 COX-2 및 MMP-13 발현을 유의하게 억제하는 것을 확인하였다. Western blot 분석 결과에서 MPAKKs/MAPKs의 인산화가 CZE에 의해 억제되었다. 또한, CZE는 HaCaT 세포에서 UVB에 의하여 유도된 Akt 인산화와 EGFR 및 Src의 인산화를 유의적으로 억제하였다. SKH-1 무모 쥐 모델을 사용한 실험 결과에서는 CZE의 경구 투여는 UVB에 의하여 유도된 주름 형성과 마우스 피부조직에서 COX-2 및 MMP-13 발현을 유의하게 억제하였다. CZE에 존재하는 특정 화합물 중 커큐민은 UVB에 의하여 유도된 MMP-1 프로모터 결합 활성을 가장 높게 억제하는 효과를 나타내었다.

RJE 화합물 중 syringic acid은 MMP-1 프로모터 결합 저해 활성이 가장 높게 나타났다. 따라서 syringic acid가 UVB에 의하여 유도된 피부암의 형성에 미치는 영향을 분석하였다. HaCaT세포에서 syringic acid으로 처리한 뒤, 유전자와 단백질 발현 수준을 측정하였으며, 이를 통해 syringic acid에 인한 ROS의 생

성이 조절됨을 확인하였고, FDA에서 승인된 항산화제인 N-acetyl-L-systein(NAC)의 효과와 비교한 결과 유사한 저해 효과가 있음을 밝혔다. NADPH 산화 효소에 syringic acid의 영향을 평가한 결과 syringic acid가 NADPH 산화 효소의 활성을 저해함을 확인하였다. Syringic acid의 피부암 예방 가능성을 평가하기 위해 동물실험을 실시하였다. 그 결과, 만성적인 UVB 처리에 의하여 무모 쥐의 피부 종양 발생과 그와 관련된 분자의 발현을 억제하였다. Syringic acid는 NADPH 산화 효소의 억제제로 작용하여 자외선에 의한 ROS 생산을 억제하고 피부암 발생을 방지하여, 천연 치료제로서의 가능성을 제시하고 있다.

주제어: 오배자 추출물, 봉출 추출물, 시린산, 광노화, 피부암, 싸이클로옥시게나제-2, 기질금속단백분해효소-1, 표피성장인자수용체, 활성산소

학번: 2017-33697